

A Novel Approach for Shock Capturing in Unstructured High-Order Methods

Abhishek Sheshadri

Department of Aeronautics
and Astronautics, Stanford
University

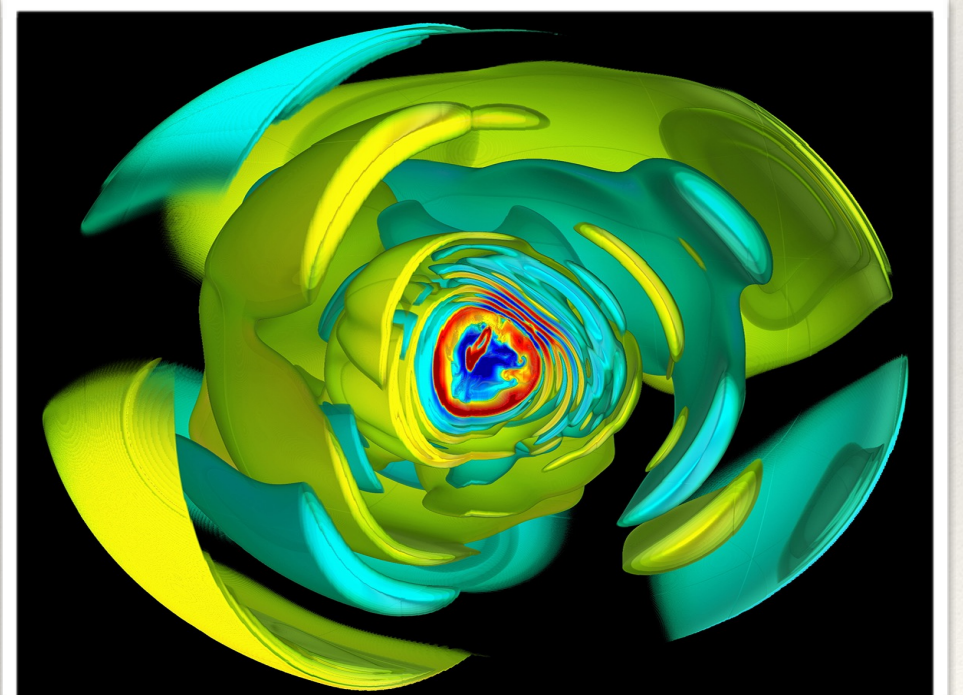
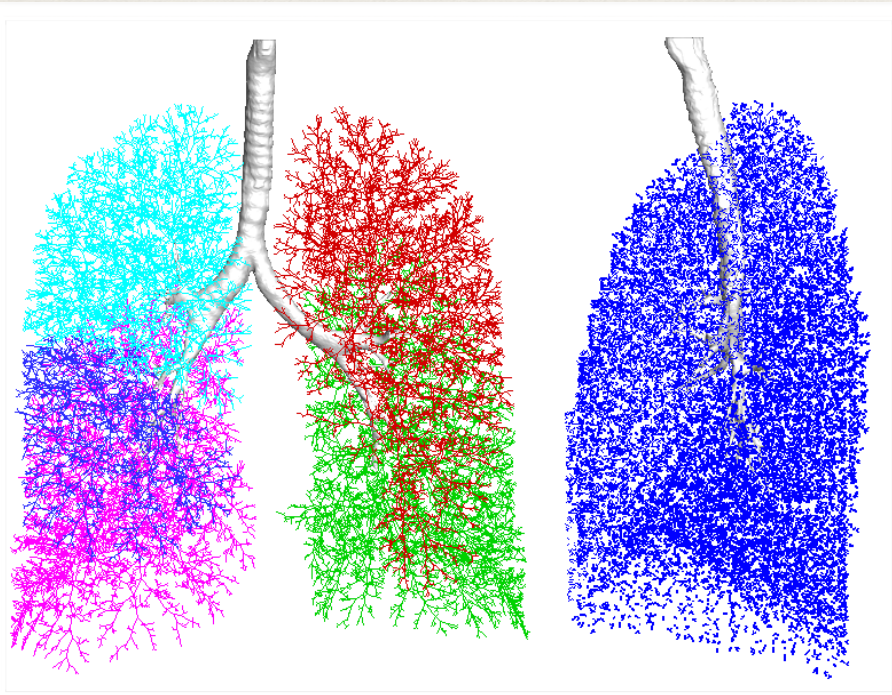
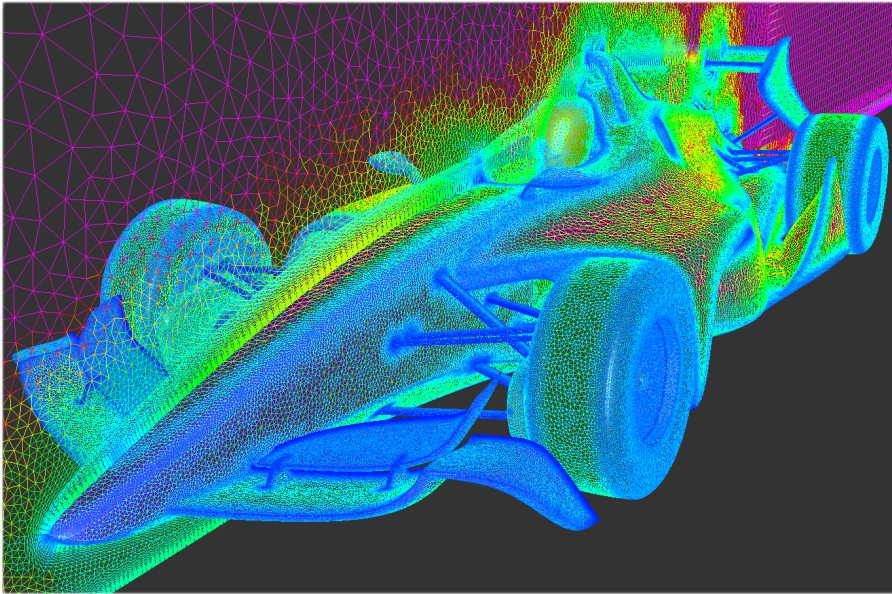
AMS Seminar Series

NASA Ames Research Center, July 7th, 2016

Low-Order Methods

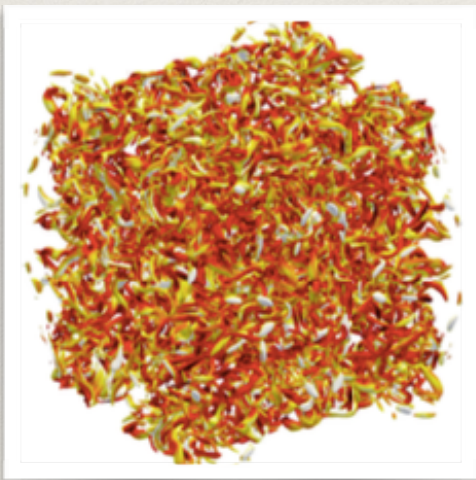
- ❖ Shape Optimization
- ❖ Steady flows

*Image Courtesy: Car: Pointwise; Lungs: Youbin Ying;
Planet: Vriesema Jess*



High vs. Low

- ❖ Dissipation
- ❖ Computational Efficiency



pyFR vs. STARCCM+

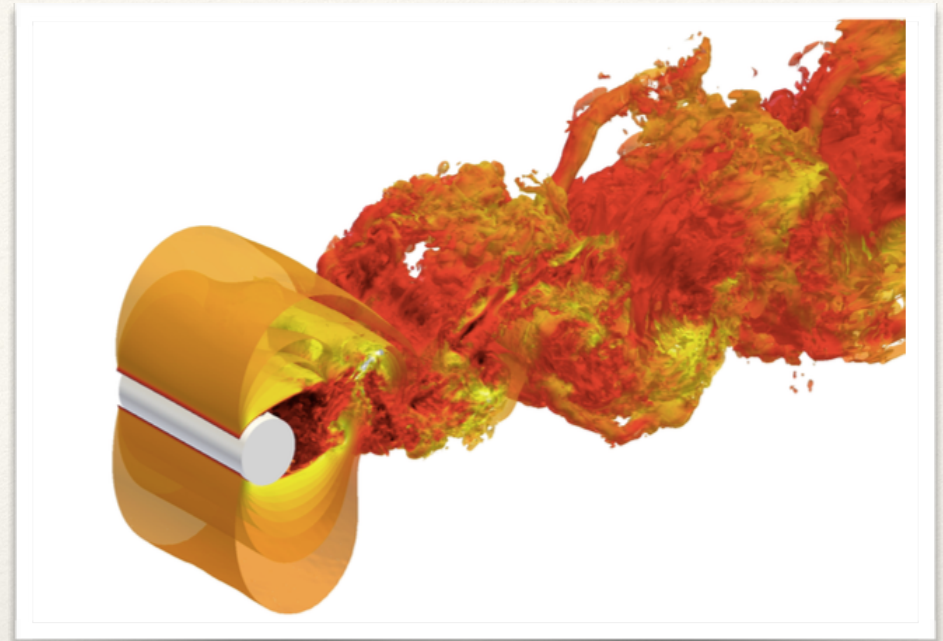


Image Courtesy: Vermiere et al.

High-Order Methods

- ❖ Vortex Dominated Flows
- ❖ Aeroacoustics

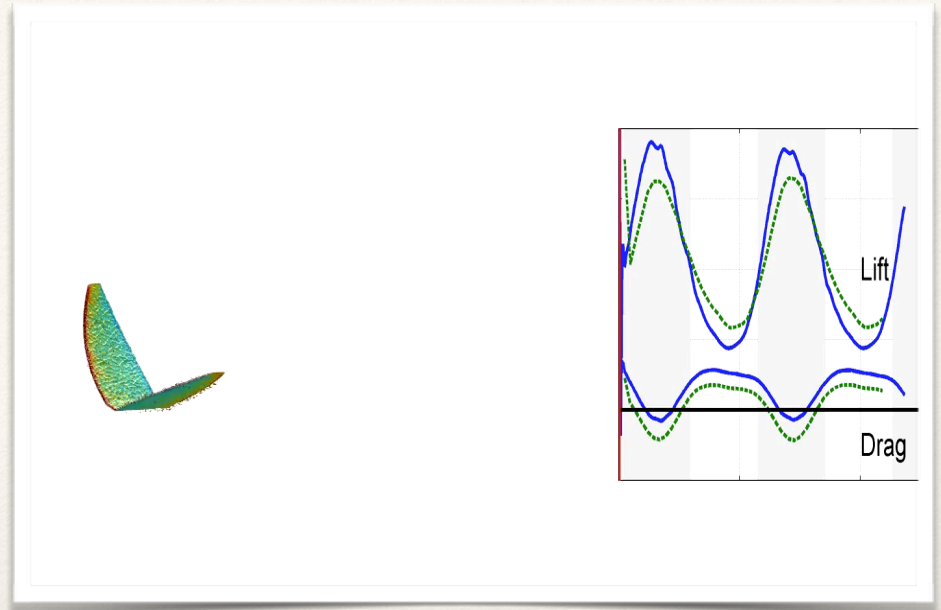


Image Courtesy: Wings: Persson and Peraire; Landing Gear: Hoffman et al.(Unicorn)

High-Order Methods

- ❖ Why are they not adopted in the industry?
- ❖ Lack of Robustness
- ❖ High-Order Mesh Generation
- ❖ BCs, Time-stepping

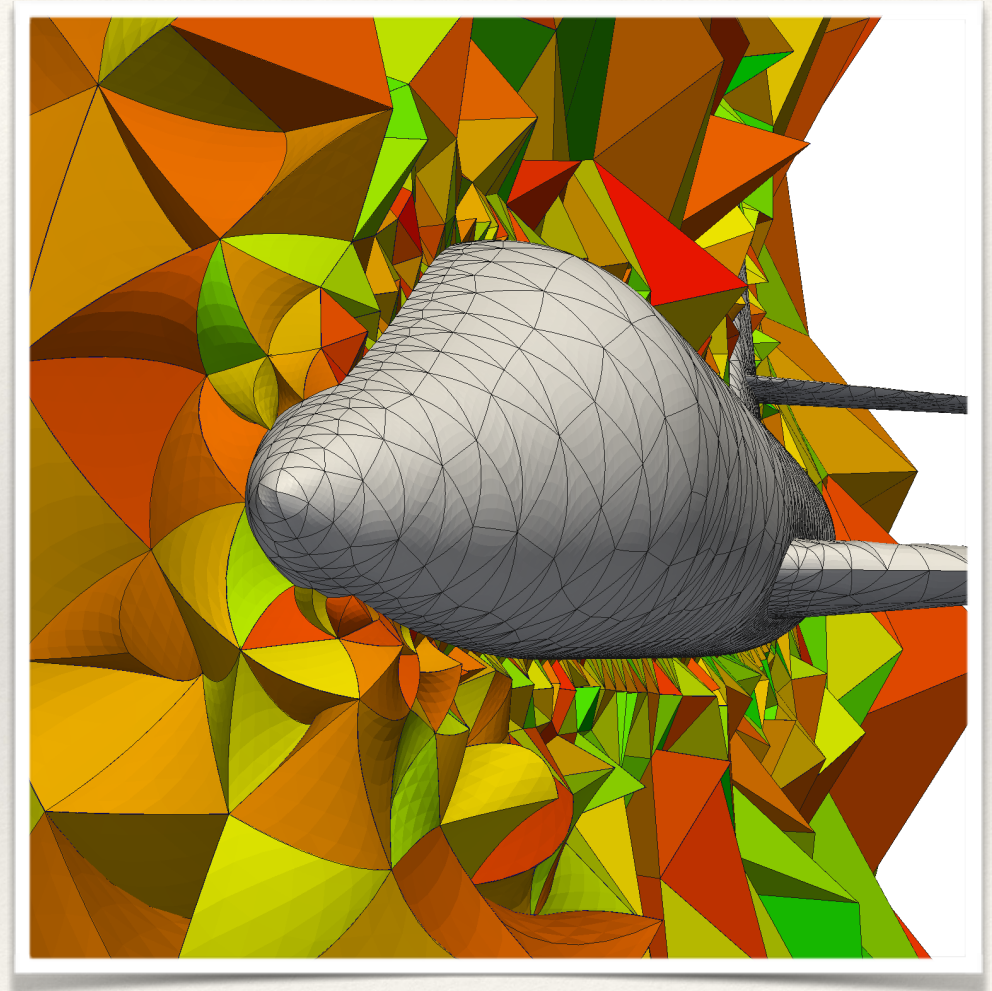


Image Courtesy: Josep Sarrate Ramos

Outline

Introduction

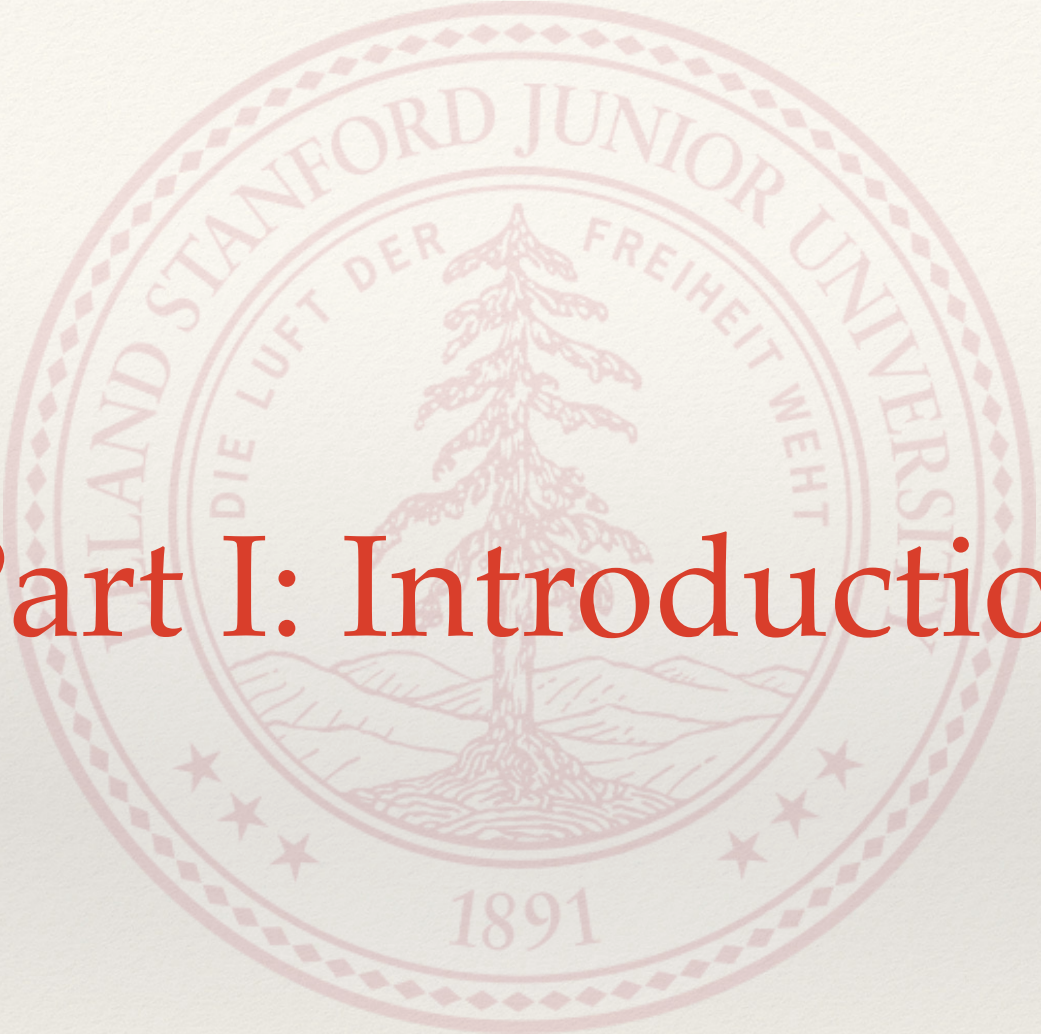
- ❖ Unstructured High Order Methods
- ❖ FR Formulation
- ❖ Motivation

Linear Stability Theory

- ❖ Tensor Product Elements
- ❖ Advection Equation
- ❖ Advection-Diffusion Equation

Compressible Flow Simulation

- ❖ Shock Capturing Strategy
- ❖ Shock Detection
- ❖ Numerical Results

The image features a large, faint watermark of the Stanford University seal in the background. The seal is circular and contains a redwood tree in the center, with the text "Leland Stanford Junior University" around the top, "Die Luft der Freiheit weht" on the sides, and "1891" at the bottom. The main title "Part I: Introduction" is overlaid on the seal in a large, bold, red serif font.

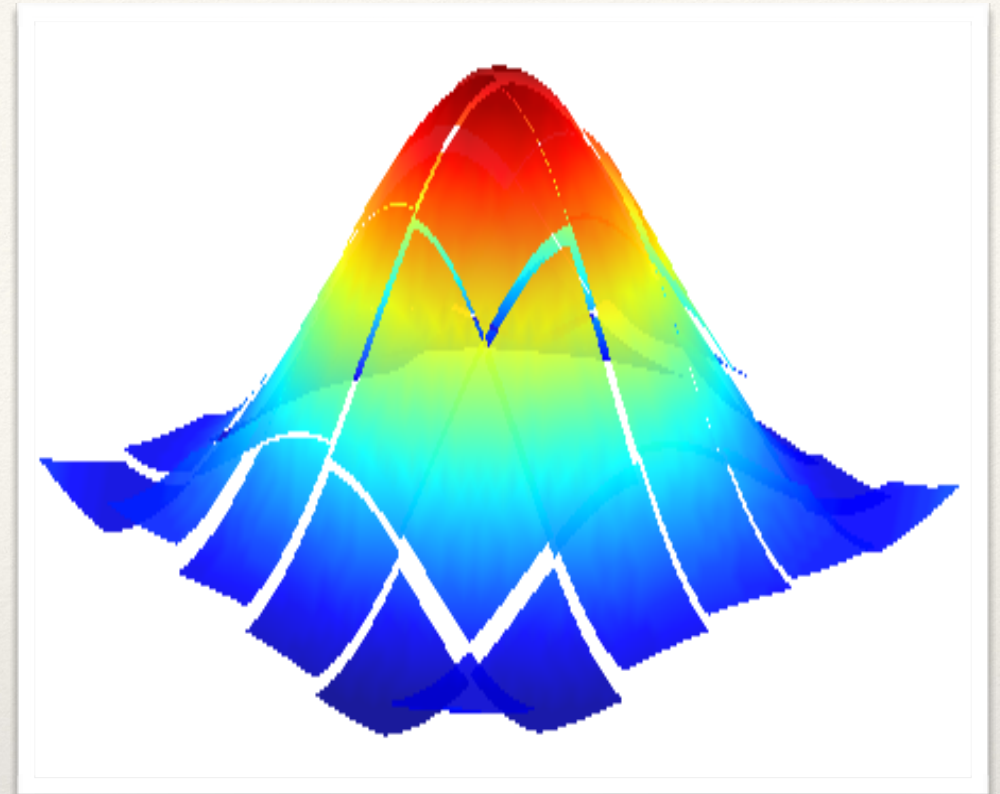
Part I: Introduction

High-Order Extensions

	Methodology	Examples	+/-
Finite Difference	<ul style="list-style-type: none"> • Stencil Widening • Compact forms 	<ul style="list-style-type: none"> • Compact FD 	<ul style="list-style-type: none"> + Efficient - Only Structured
Spectral Methods	<ul style="list-style-type: none"> • Sinusoids 	<ul style="list-style-type: none"> • Spectral • Spectral Element 	<ul style="list-style-type: none"> + Efficient - Structured
Finite Volume	<ul style="list-style-type: none"> • High-order interpolation 	<ul style="list-style-type: none"> • ENO • WENO 	<ul style="list-style-type: none"> + Unstructured - Non-Compact - Limited order
Finite Element	<ul style="list-style-type: none"> • High-order polynomial 	<ul style="list-style-type: none"> • CG-FEM • DG-FEM • SD, FR 	<ul style="list-style-type: none"> + Unstructured + Compact + Arbitrary order

Discontinuous Galerkin FEM

- ❖ Integral or Weak Form of PDE
- ❖ Solution discontinuous across elements
- ❖ Suitable for hyperbolic PDEs
- ❖ High-order polynomials



CG vs. DG

Image Courtesy: Bottom: Kauffman et al., ETH Zurich

Flux Reconstruction

- ❖ Unifying Framework - can recover DG and SD schemes
- ❖ Parametrized Family
 - ❖ Time-step
 - ❖ Dispersion and Dissipation
- ❖ Differential or Strong Form
- ❖ Explicit Time-stepping: GPUs

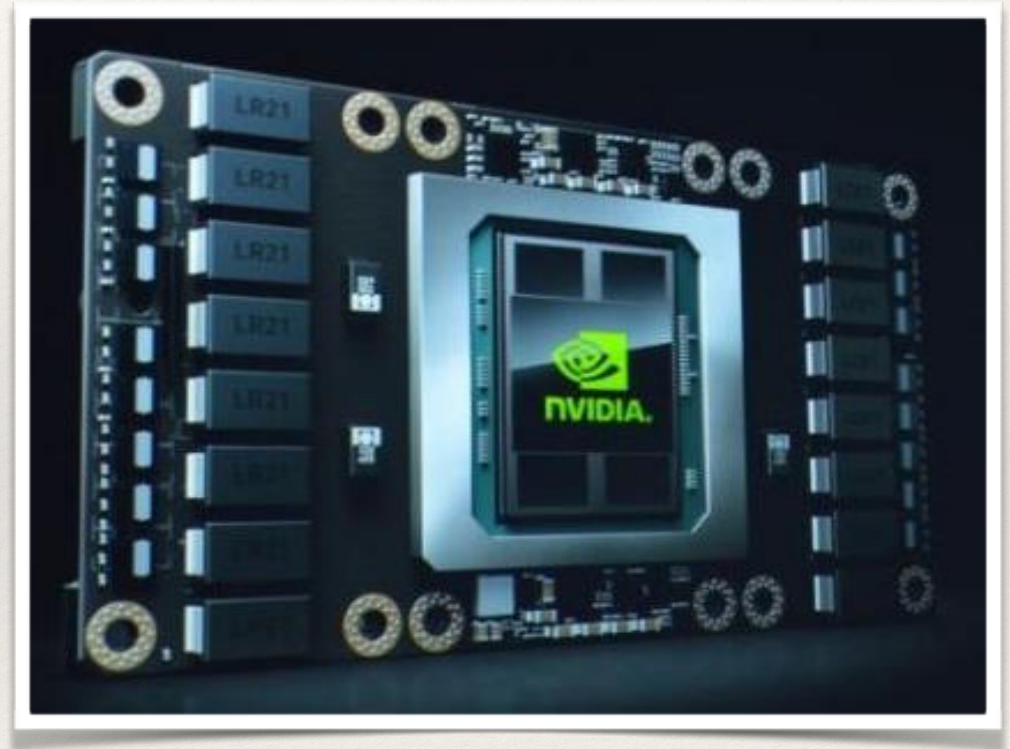


Image Courtesy: NVIDIA

FR Formulation in 1D

- Consider the 1D Conservation Law

$$\frac{\partial u}{\partial t} + \frac{\partial f}{\partial x} = 0 \quad \text{where} \quad f = f(u)$$

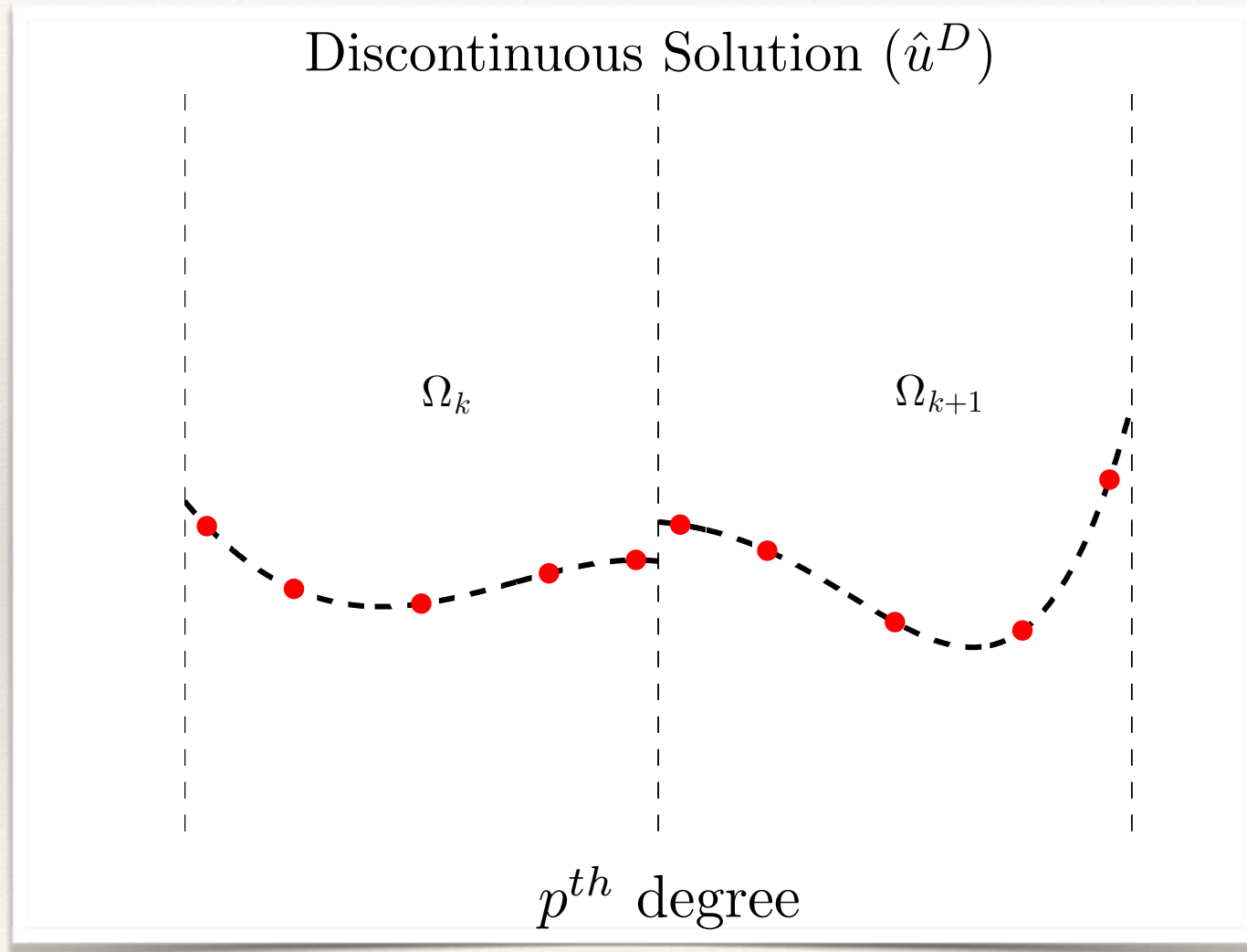
- Discretize the domain into elements



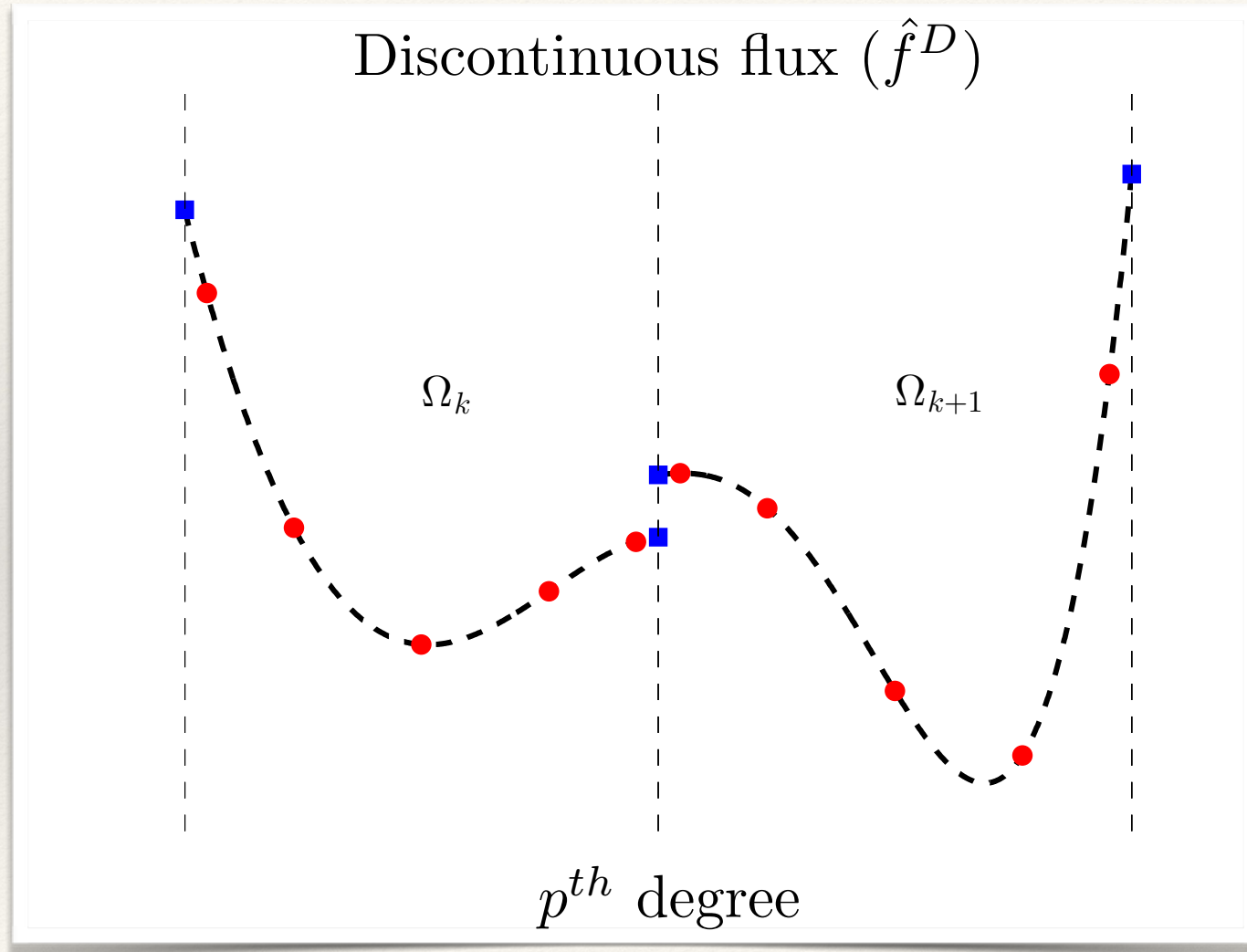
FR Formulation in 1D

- Transform quantities and equation inside each element to a reference domain $\Omega_S : [-1, 1]$
- Suppose we have the (discontinuous) solution \hat{u}^D at a time-step and we want to compute the solution at next time-step

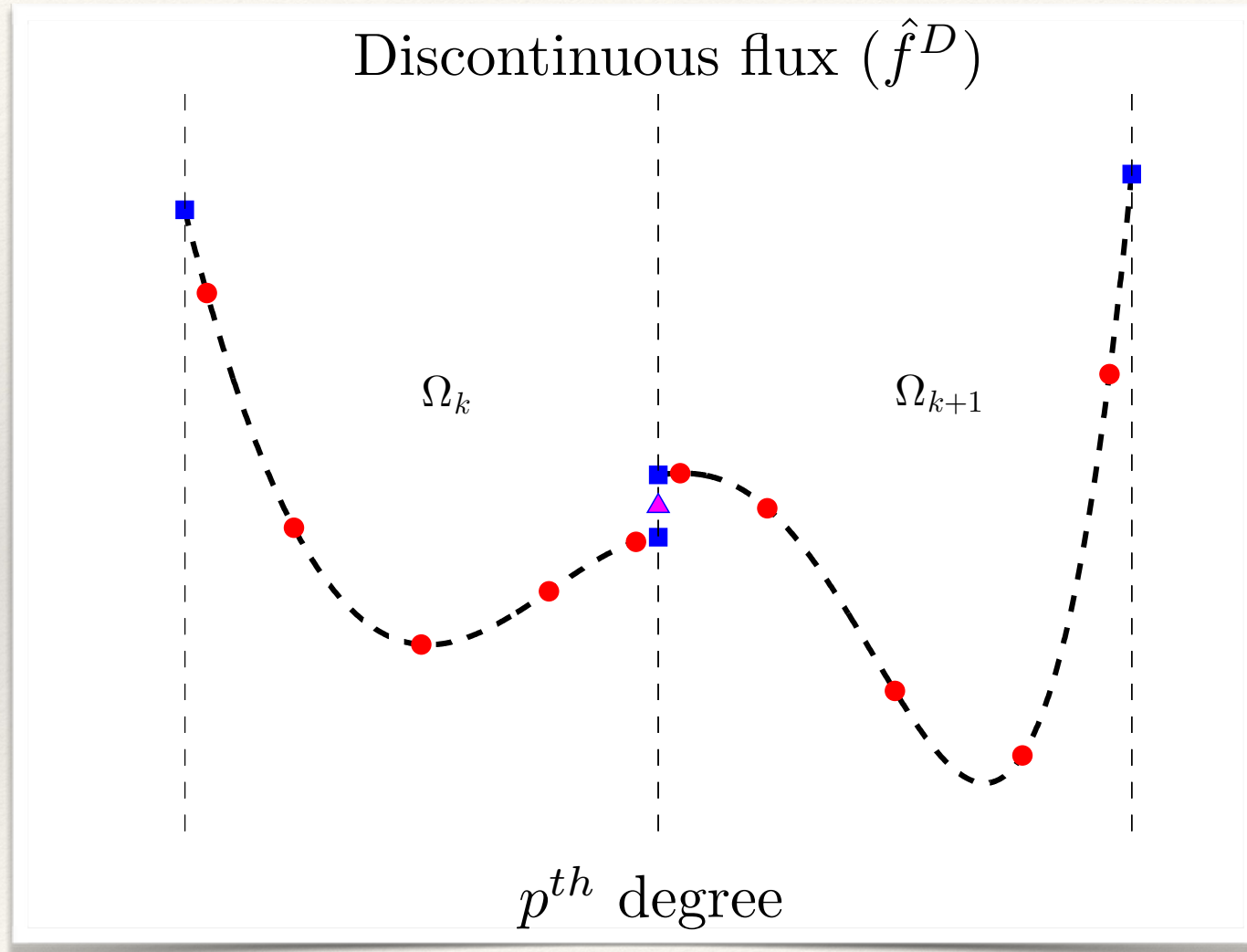
FR Formulation in 1D



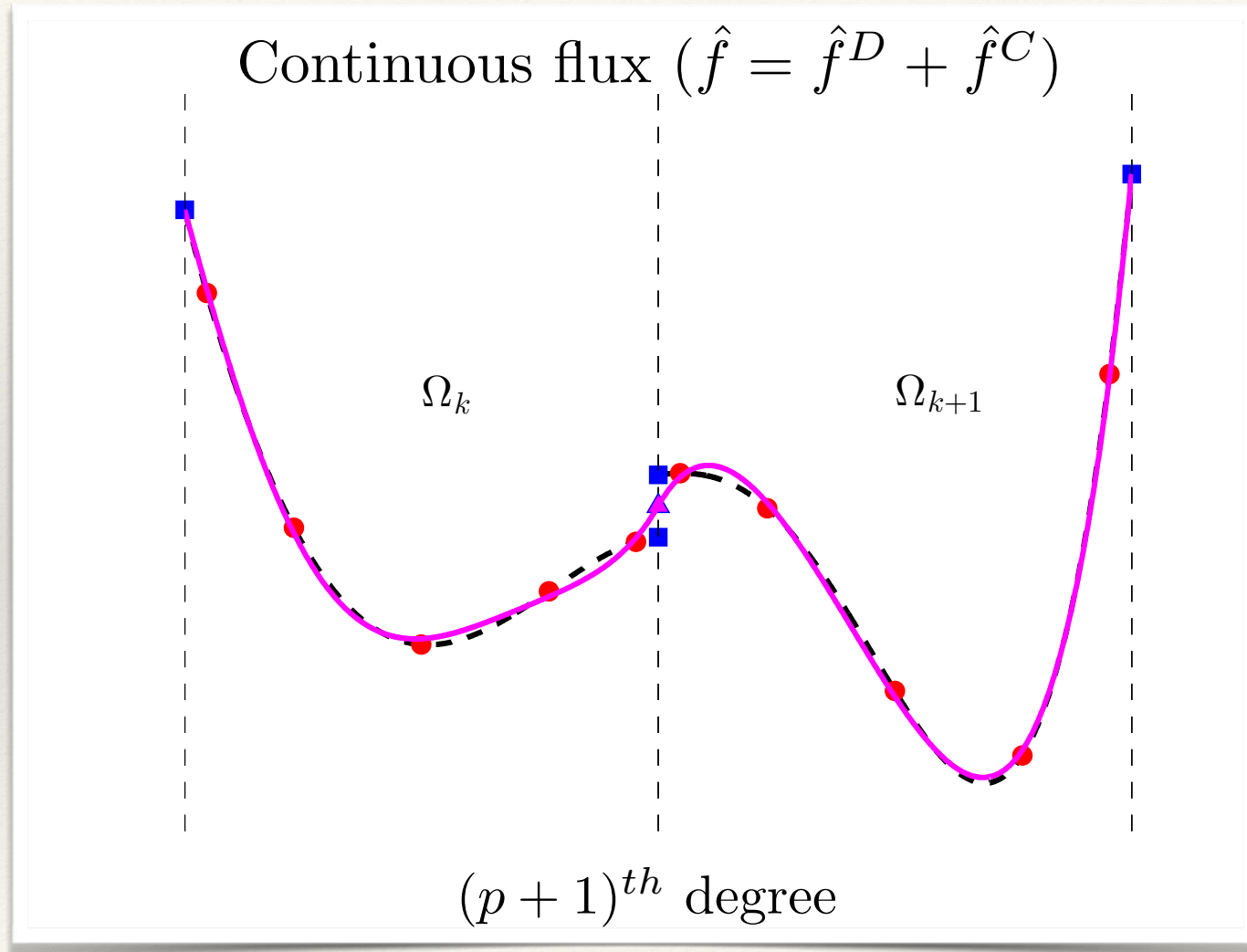
FR Formulation in 1D



FR Formulation in 1D



FR Formulation in 1D



FR Formulation in 1D

- Calculate the derivative of the flux and time-advance to get \hat{u}^D at next time-step

$$\frac{d\hat{u}_k^D}{dt} = -D^h \hat{f}_k^D - D \hat{f}_k^C$$

- For second order PDEs (diffusive fluxes), split into first-order PDEs and perform similar procedure for each

FR Formulation in 1D

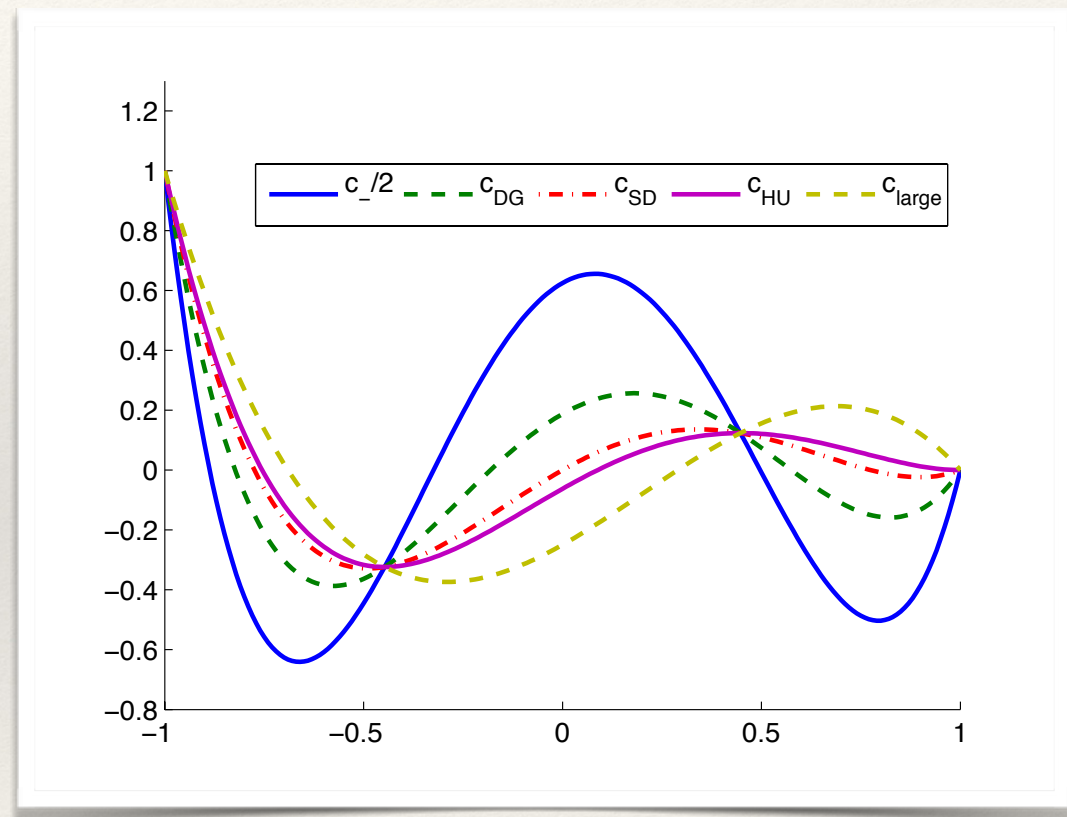
$$\frac{\partial u}{\partial t} + \frac{\partial f}{\partial x} = 0 \quad \text{in } \Omega; \quad \text{where } f = f\left(u, \frac{\partial u}{\partial x}\right)$$

↓ Split

$$\begin{aligned} \frac{\partial u}{\partial t} + \frac{\partial f(u, q)}{\partial x} &= 0 \\ q - \frac{\partial u}{\partial x} &= 0 \end{aligned}$$

VCJH Correction Functions

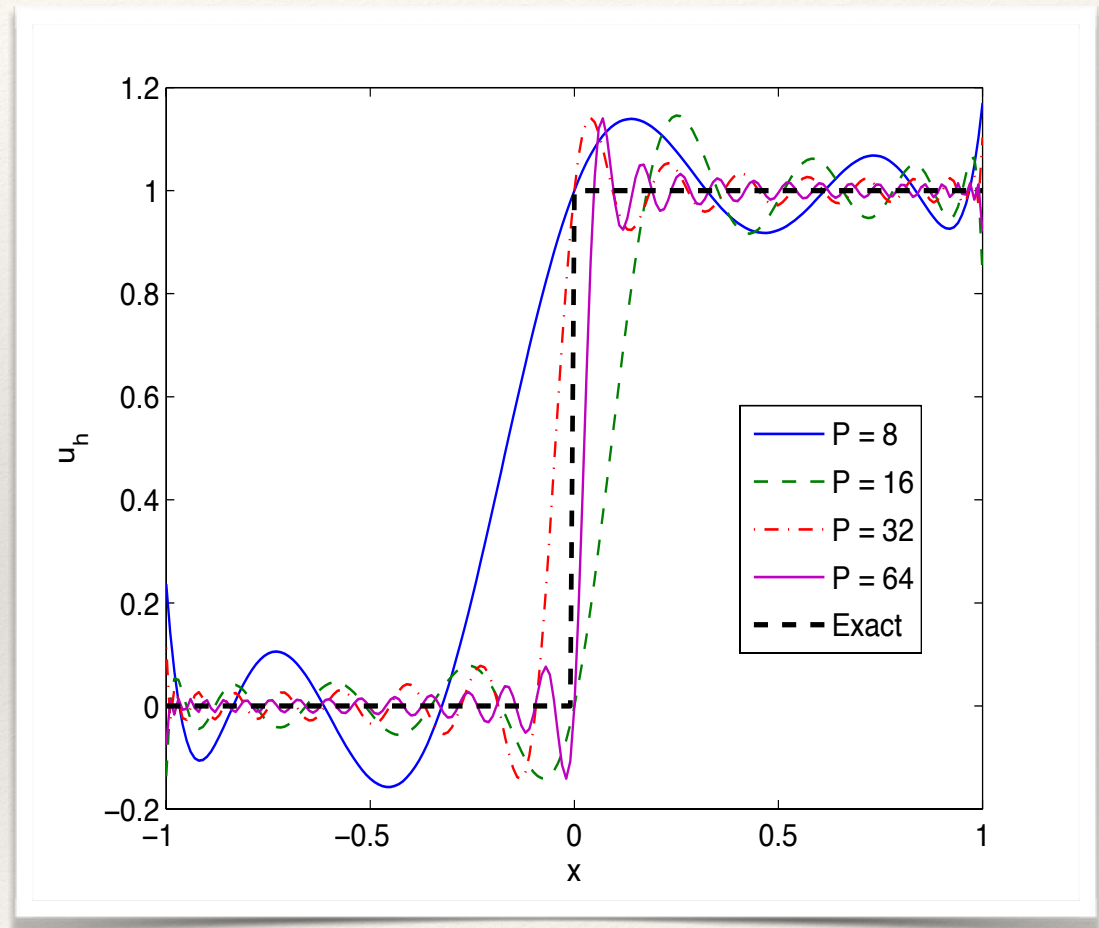
- ❖ Single-parameter (denoted c) family - can recover DG, SD, G2 schemes by varying this parameter
- ❖ Built to get energy stable schemes for linear problems
- ❖ Can vary c to get different dissipation, dispersion and time-step limits.

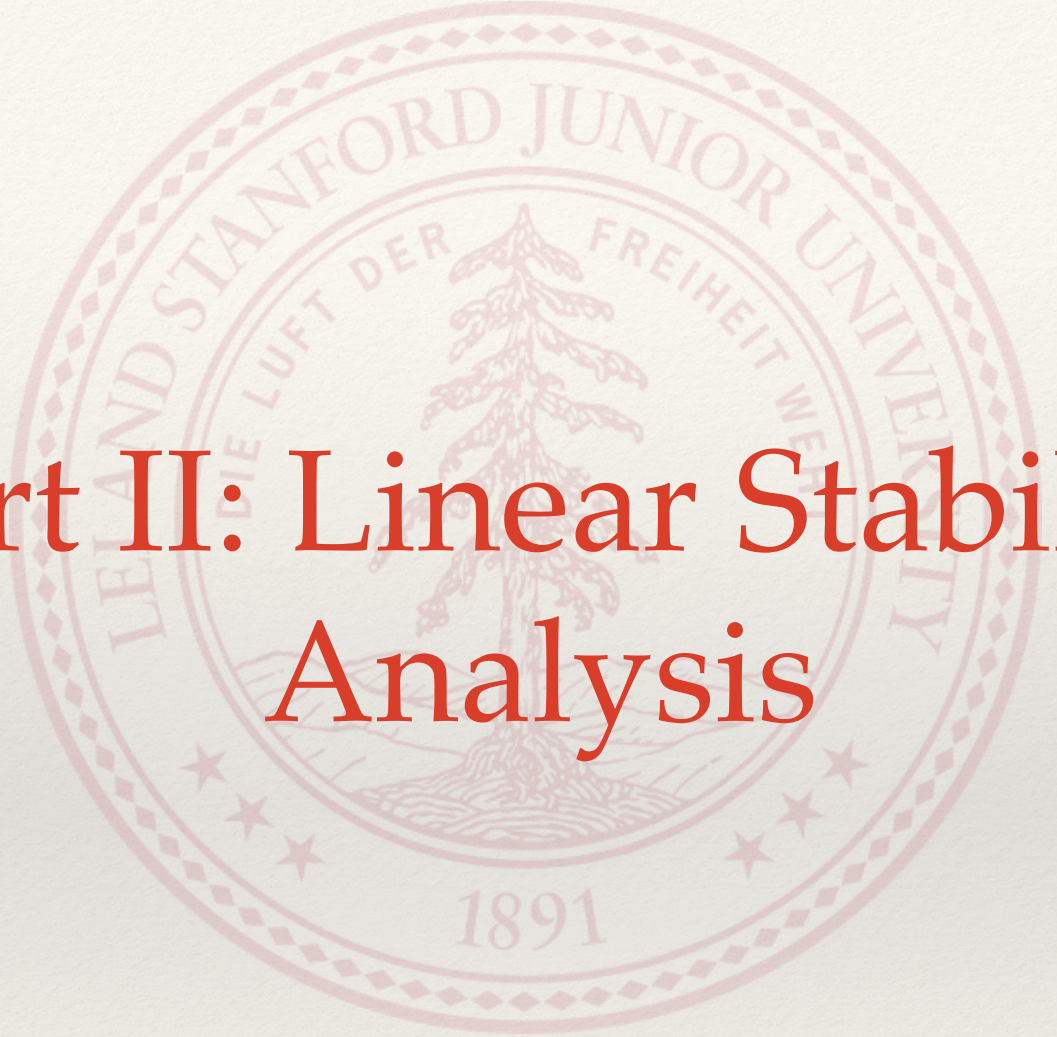


Scheme with $P = 3$

Motivation

- ❖ Lower Dissipation: More prone to nonlinear instabilities
- ❖ Discontinuities / Shocks: Gibbs Phenomena
- ❖ Loss of hyperbolicity / unphysical solutions
- ❖ Accuracy affected



The background features a large, faint watermark of the Stanford University seal. The seal is circular and contains the text "LELAND STANFORD JUNIOR UNIVERSITY" around the top edge. Inside the seal, there is a tree and the motto "DIE LUFT DER FREIHEIT WEHT". The year "1891" is at the bottom. The seal is surrounded by a decorative border of small diamonds.

Part II: Linear Stability Analysis

The background features a large, faint watermark of the Stanford University seal. The seal is circular and contains a redwood tree in the center. The text around the tree reads "Leland Stanford Junior University" at the top, "Die Luft der Freiheit weht" on the sides, and "1891" at the bottom. There are also several stars around the inner circle.

Part III: Compressible Flow Simulation

Design Considerations

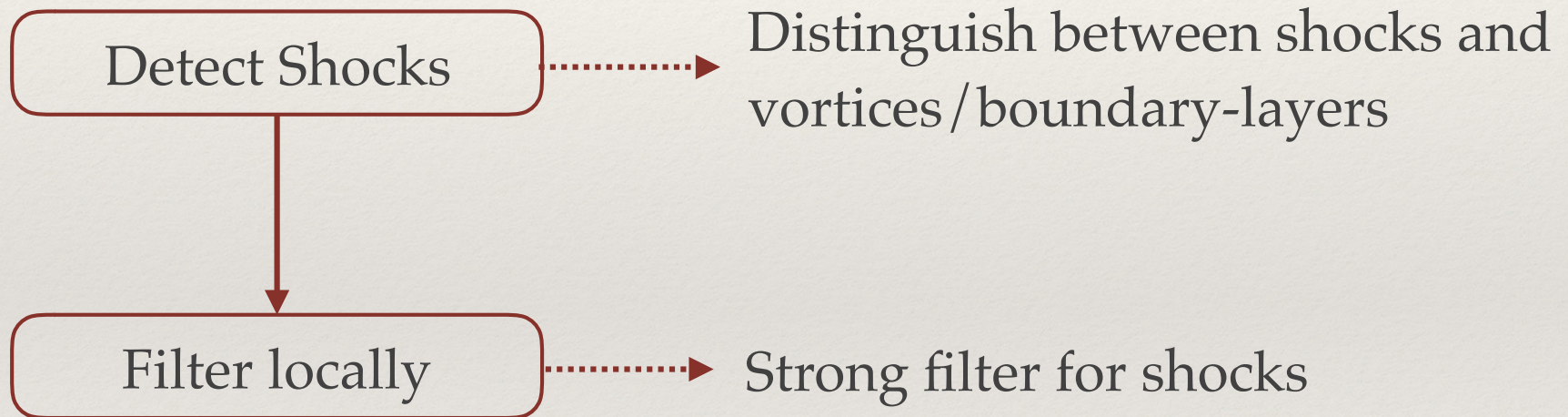
- ❖ Sub-cell shock capturing
- ❖ Suitable for explicit time-stepping schemes; GPUs
- ❖ Suitable for unstructured grids
- ❖ Not problem / physics / scheme specific

Current Methods

Method	Advantages	Disadvantages
Limiting	<ul style="list-style-type: none">• Eliminates oscillations• Robust	<ul style="list-style-type: none">• Smearred over elements• Expensive
Artificial Viscosity	<ul style="list-style-type: none">• Sub-cell shock capturing• Smoothly varying viscosity	<ul style="list-style-type: none">• High-order derivatives• Time-step restrictions• Too many parameters
Filtering	<ul style="list-style-type: none">• Sub-cell shock capturing• Very Inexpensive	<ul style="list-style-type: none">• Varying dissipation not easy• Needs a good sensor

Shock Capturing Strategy

Two-step approach



Minimize parameter fine-tuning

Filtering

- Consider a conservation law of the form

$$\frac{\partial u}{\partial t} + \frac{\partial f(u)}{\partial x} = 0$$

- Suppose we add an artificial dissipation term to stabilize

$$\frac{\partial u}{\partial t} + \frac{\partial f(u)}{\partial x} = \epsilon(-1)^{s+1} \left[\frac{\partial}{\partial x} (1 - x^2) \frac{\partial}{\partial x} \right]^s u$$

Filtering

- The time-step limit now scales as

$$\Delta t \sim \frac{1}{\lambda_{max} P^2 / h + \|\epsilon\|_{L^\infty} P^4 / h^2}$$

- Needs space-local time-stepping or time-adaptivity to somewhat alleviate the problem

Filtering

We can solve this approximately in a time-splitting fashion

- First, we solve the original ODE

$$\frac{\partial u}{\partial t} + \frac{\partial f(u)}{\partial x} = 0$$

- Then we do a Forward Euler time-step of the dissipation term

$$\frac{\partial u}{\partial t} = \epsilon(-1)^{s+1} \left[\frac{\partial}{\partial x} (1 - x^2) \frac{\partial}{\partial x} \right]^s u$$

Filtering

- Note that the solution can be represented by a hierarchical Legendre polynomial basis

$$u^h = \sum_{n=0}^P \hat{u}_n \tilde{P}_n(x)$$

- Using this, the artificial dissipation equation approximately reduces to

$$u^{h,*}(x, t) \simeq \sum_{n=0}^P \sigma\left(\frac{n}{P}\right) \hat{u}_n \tilde{P}_n(x)$$

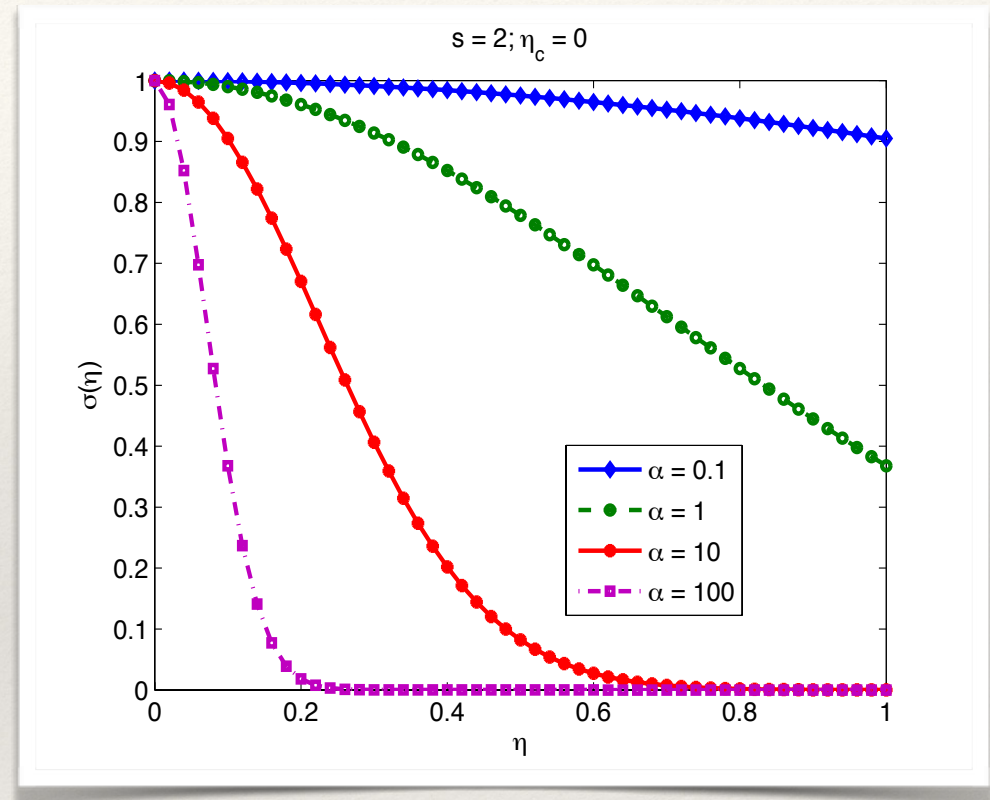
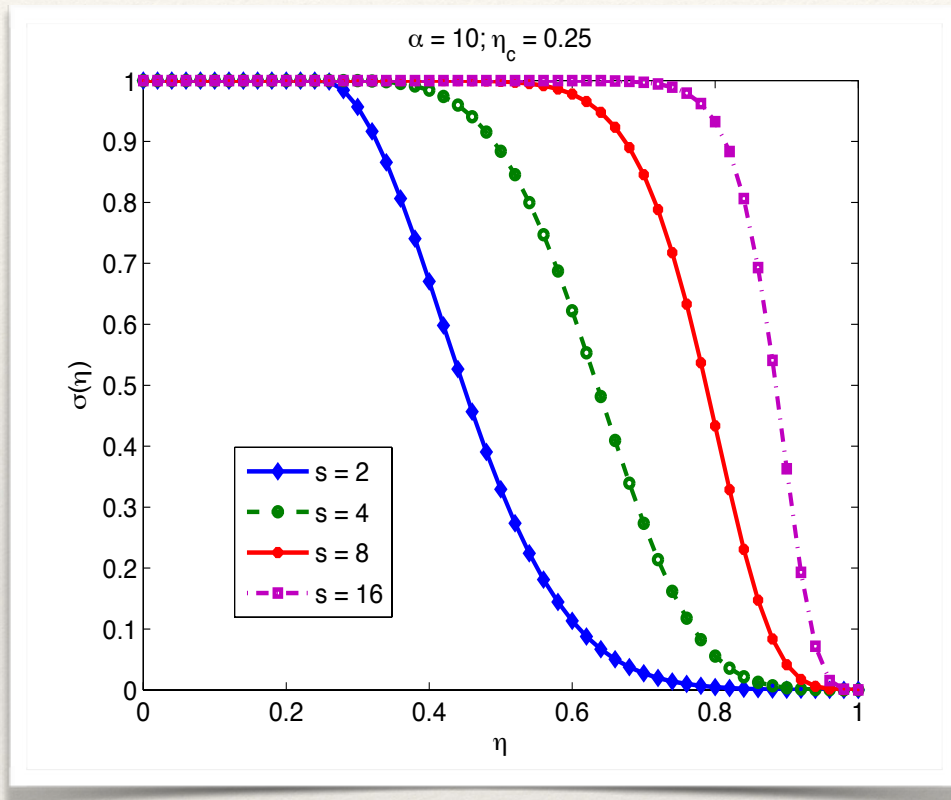
- Filtering is equivalent to approximately implementing artificial dissipation

Polynomial Modal Filtering

- Starting from \mathbf{u} , compute the modal coefficients: $\hat{\mathbf{u}} = \mathcal{V}^{-1}\mathbf{u}$
- Filter modal coefficients: $\tilde{\hat{\mathbf{u}}} = \Sigma\hat{\mathbf{u}}$
- Convert back to nodal: $\tilde{\mathbf{u}} = \mathcal{V}\tilde{\hat{\mathbf{u}}}$
- Can be cast as one matrix-vector multiplication:

$$\tilde{\mathbf{u}} = \mathcal{F}\mathbf{u} \quad \text{where} \quad \mathcal{F} = \mathcal{V}\Sigma\mathcal{V}^{-1}$$

Exponential Modal Filters



$$\sigma(\eta) = \begin{cases} 1, & 0 \leq \eta \leq \eta_c = \frac{N_c}{P} \\ \exp\left(-\alpha \left(\frac{\eta - \eta_c}{1 - \eta_c}\right)^s\right), & \eta_c \leq \eta \leq 1 \end{cases}$$

Implementation

- Execute a full time-step of original PDE
- Sense shocks and apply filter where necessary (post-processing operation)

- Fix

$$\eta_c = 0 \quad s = 2 \quad \alpha = 1$$

Vary only filter strength α based on shock strength

Shock Detection

- ❖ Suitable for unstructured high-order methods
 - ❖ Sub-cell shock capturing
- ❖ Inexpensive
- ❖ Separation of Scales: Distinguish between shocks and vortices / boundary layers
- ❖ General: Physics / Scheme independent

Current Methods

- ❖ Physics based
 - ❖ Specific to problem or type of discontinuity
 - ❖ Need derivatives: expensive
 - ❖ Hard to extend to unstructured
- ❖ Smoothness based
 - ❖ Used successfully in low-order schemes
 - ❖ Persson and Peraire - high order unstructured methods

Persson and Perraire's Method

- Based on (lack of) decay of the modal coefficients

$$\text{Sensor} \sim \frac{E_{\text{highestdegreemodes}}}{E_{\text{overall}}}$$

- Asymptotic property: Not reliable at 'low' orders
- Threshold selection and clear distinction between shocks and other gradient regions is hard

Concentration Method



- ❖ Used for image/MRI edge detection
- ❖ Works directly on Fourier spectral information

Concentration Property

- Suppose you have the spectral projection of a function:

$$S_N(f) = - \sum_{k=-N}^N \hat{f}_k e^{ikx}$$

- If f has a discontinuity, then:

$$\hat{f}_k = [f](c) \frac{e^{-ikc}}{2\pi ik} + \mathcal{O}\left(\frac{1}{k^2}\right)$$

Concentration Property

- There exist special Kernels s/t

$$K_\epsilon * S_N(f) = [f](x) + \mathcal{O}(\epsilon)$$

- Kernel action is of the form

$$K_N^\sigma * S_N(f) = i\pi \sum_{k=-N}^N \operatorname{sgn}(k) \sigma\left(\frac{|k|}{N}\right) \hat{f}_k e^{ikx}$$

- σ - concentration factors

Jacobi Polynomials

- Eigenfunctions of the Sturm-Liouville problem:

$$((1 - x^2)\omega(x)P'_k(x))' = -\lambda_k\omega(x)P_k(x) \quad -1 \leq x \leq 1$$

with weight $\omega(x) = (1 - x^2)^\alpha$

- The polynomial modal coefficients also show a lowered decay rate:

$$\hat{f}_k = \frac{1}{\lambda_k} [f](x)(1 - x^2)\omega(c)P'_k(x) + \mathcal{O}\left(\frac{1}{\lambda_k^2}\right)$$

where $\lambda_k = k(k + 2\alpha + 1)$

Jacobi Polynomials

- Concentration property for Jacobi polynomials with $-1 \leq \alpha \leq 0$:

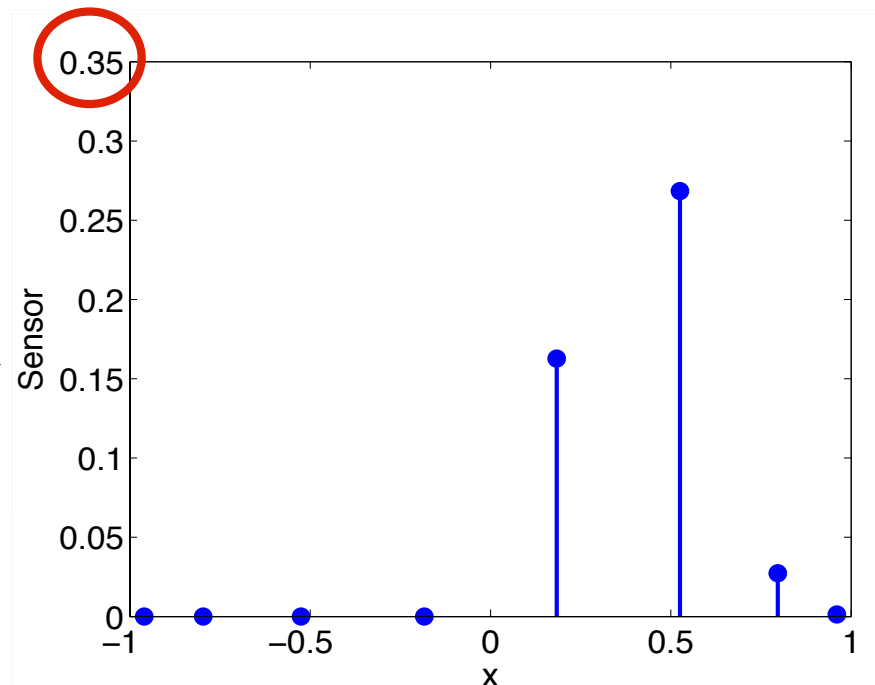
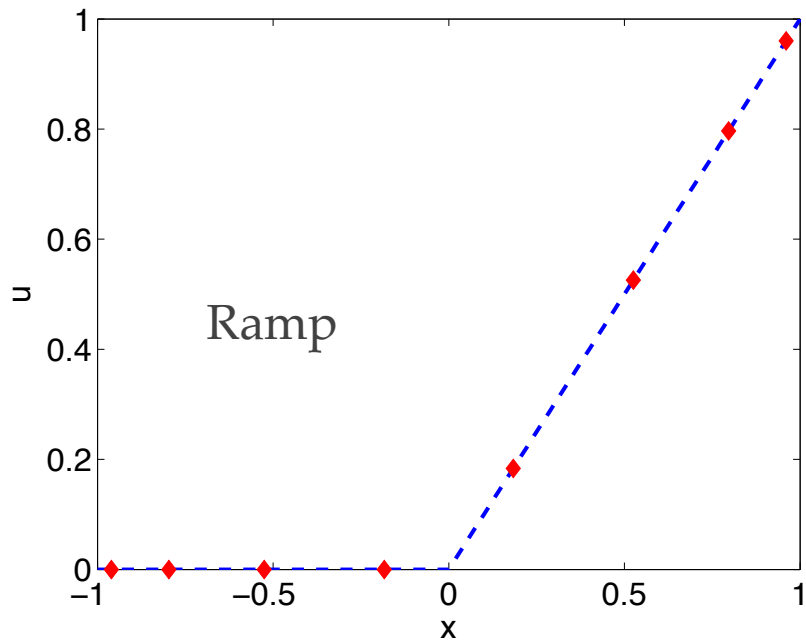
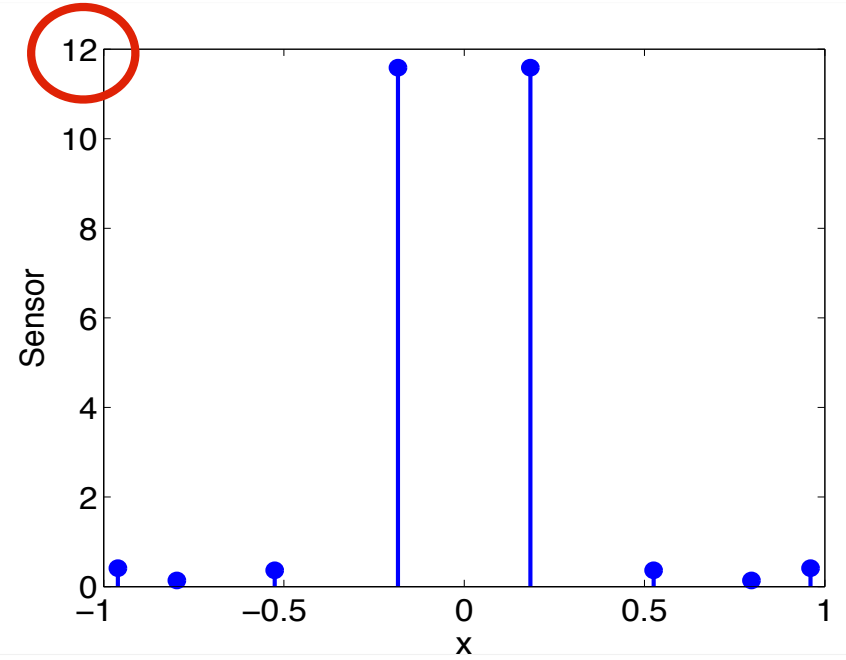
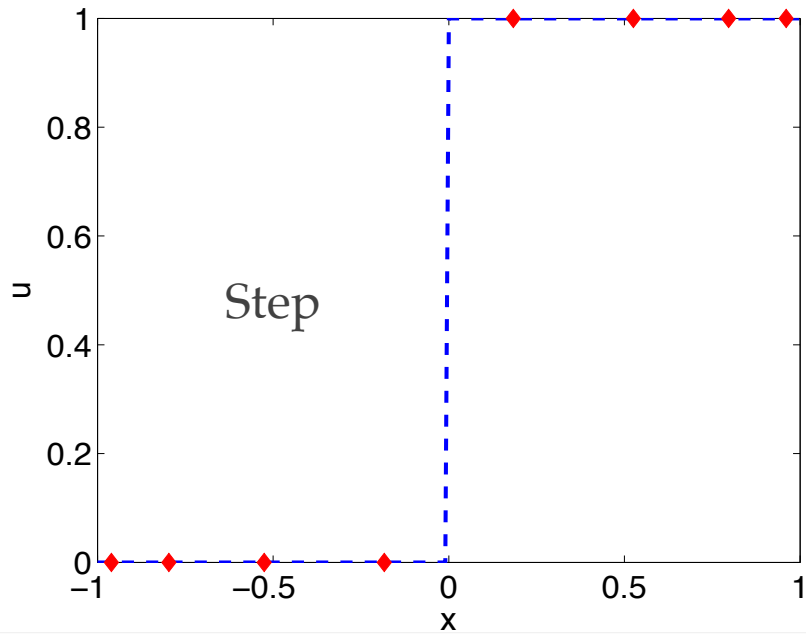
$$\left| \frac{\pi \sqrt{1-x^2}}{N} S_N(f)'(x) - [f](x) \right| \leq \frac{\text{Const}}{(1-x^2)^{\alpha/2+1/4}} \cdot \frac{\log N}{N}$$

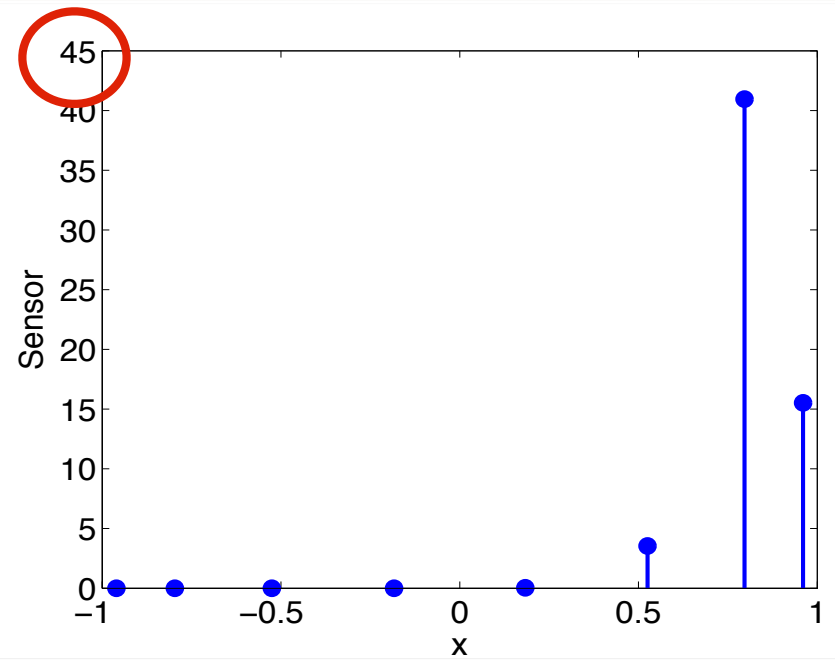
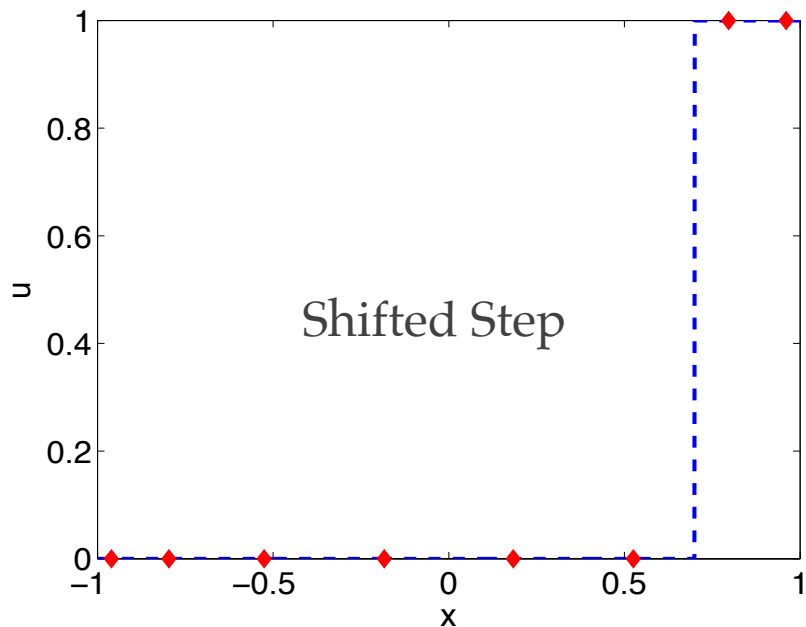
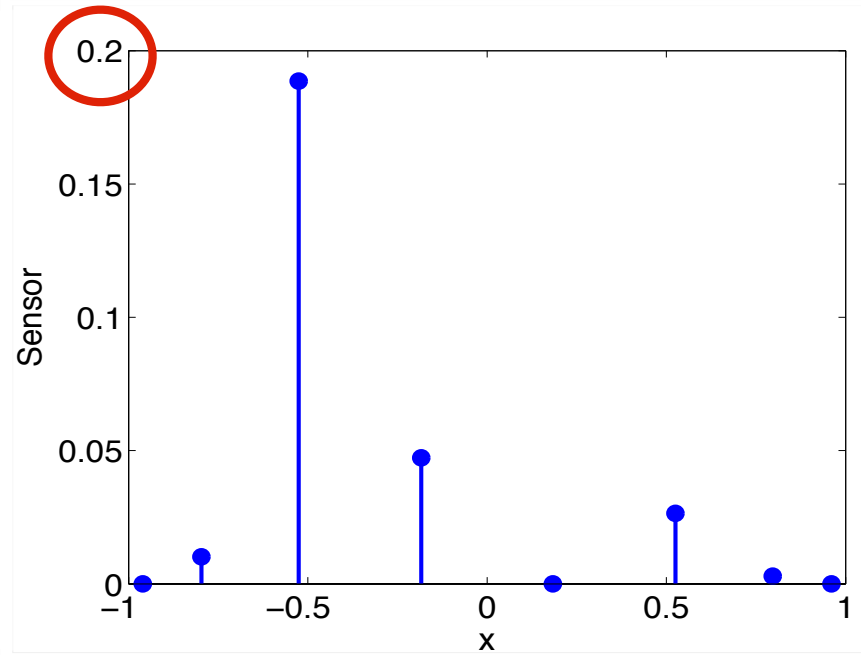
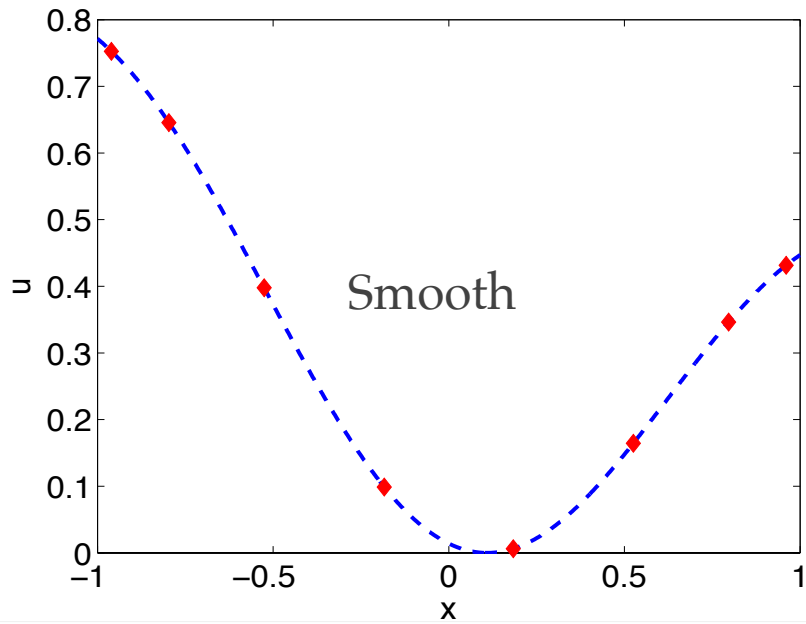
- Legendre Polynomials are special cases ($\alpha = 0$) of Jacobi Polynomials
- Can be applied on the modal coefficients similar to filter

Nonlinear Enhancement

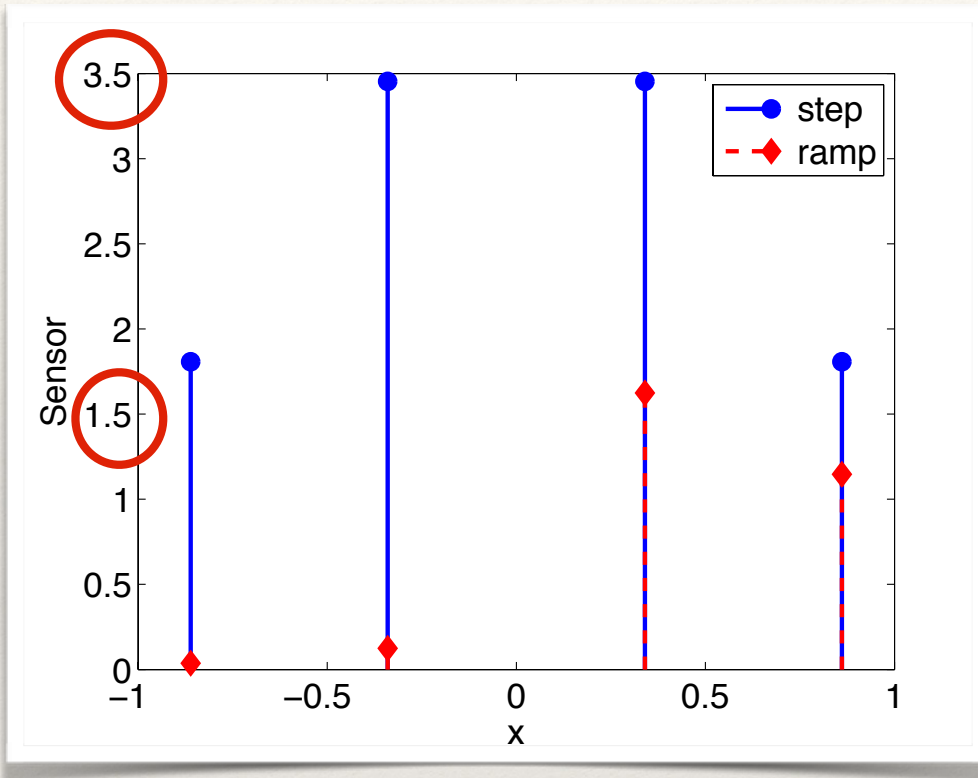
- As $N \uparrow$, this separation increases
- However, we generally have small N . We need further separation of scales.

$$\epsilon^{-p/2} (K_\epsilon \star f(x))^p \sim \begin{cases} \epsilon^{p/2}, & \text{at a smooth point } x \neq c \\ ([f](c))^p \epsilon^{-p/2}, & \text{at a discontinuity } x = c \end{cases}$$

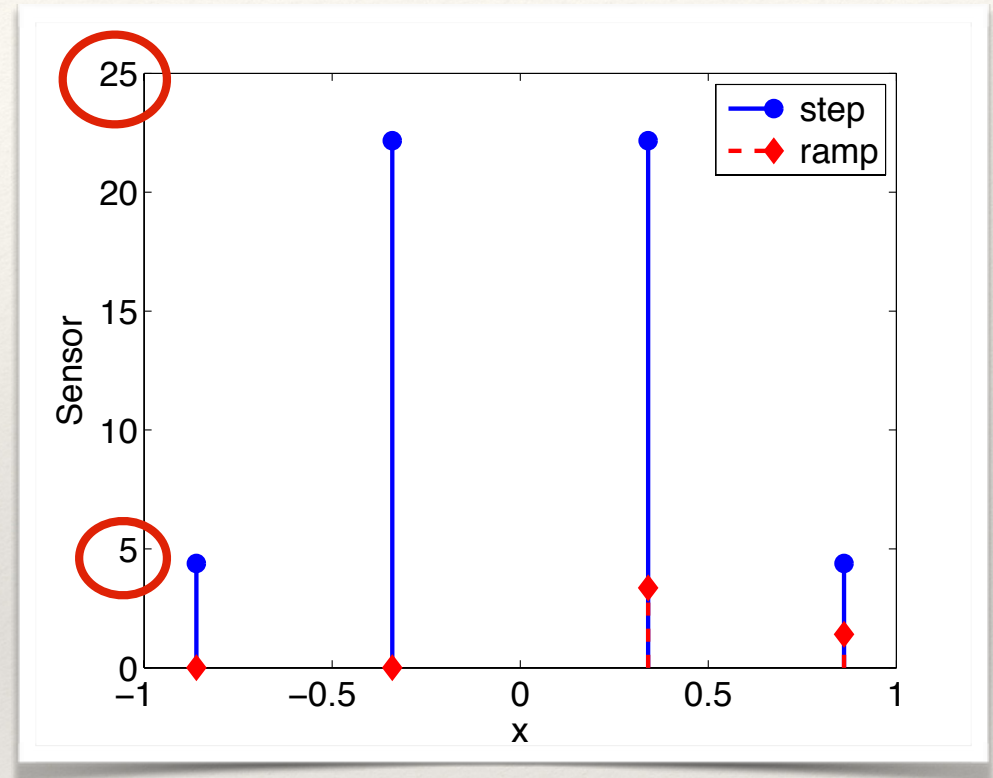




Performance at low orders



Nonlin. Exponent = 2



Nonlin. Exponent = 5

- ❖ Good separation of scales even at “low” orders

Implementation in 1D

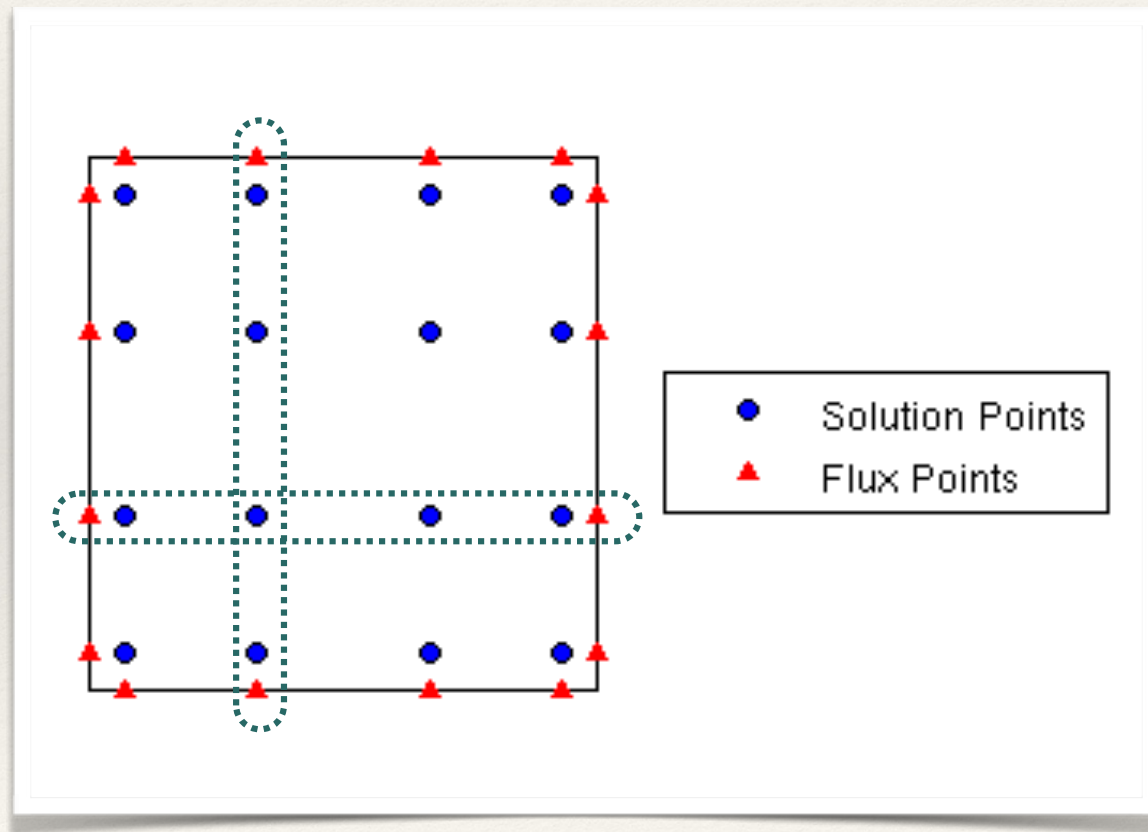
- ❖ Pre-compute the Concentration matrix C
- ❖ Choose a quantity: E.g. Density and normalize the elemental solution to $[0,1]$
- ❖ Compute the kernel by pre-multiplying by C

Implementation in 1D

- ❖ Perform Nonlinear Enhancement
- ❖ If any point in the element has this value greater than threshold, mark element for filtering
- ❖ Threshold: In between max. kernel values for step and ramp

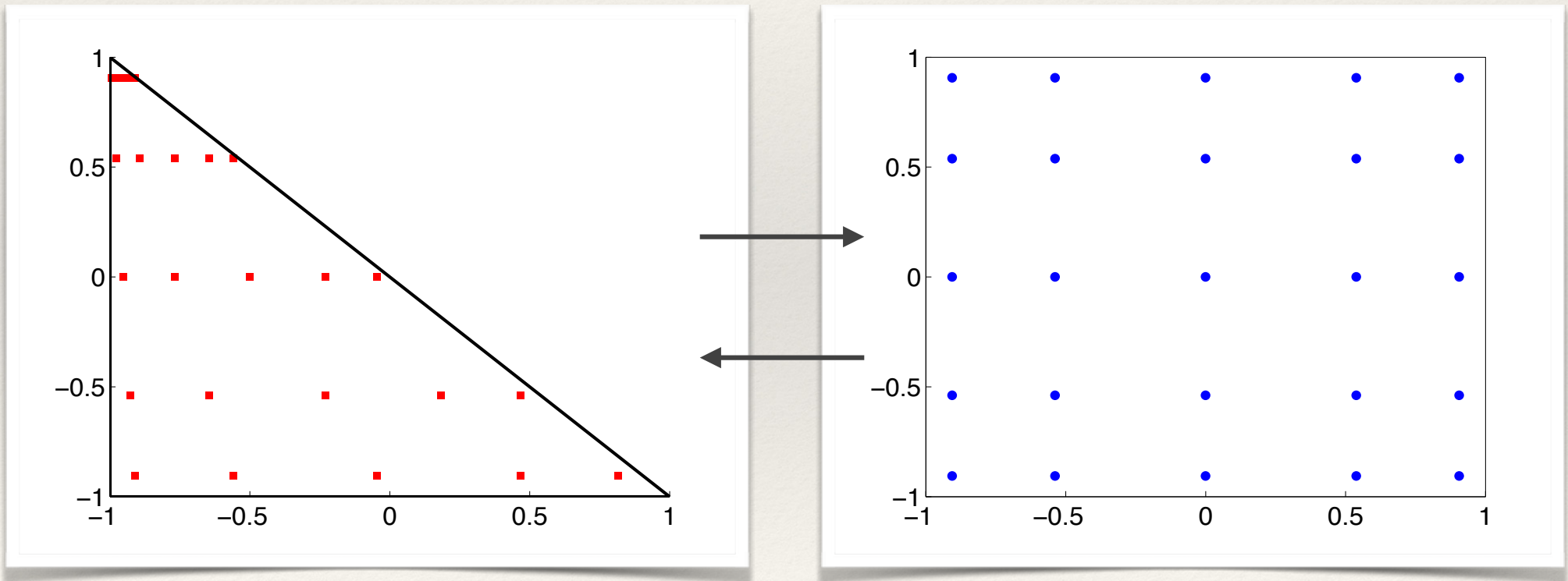
Extension to 2D and 3D

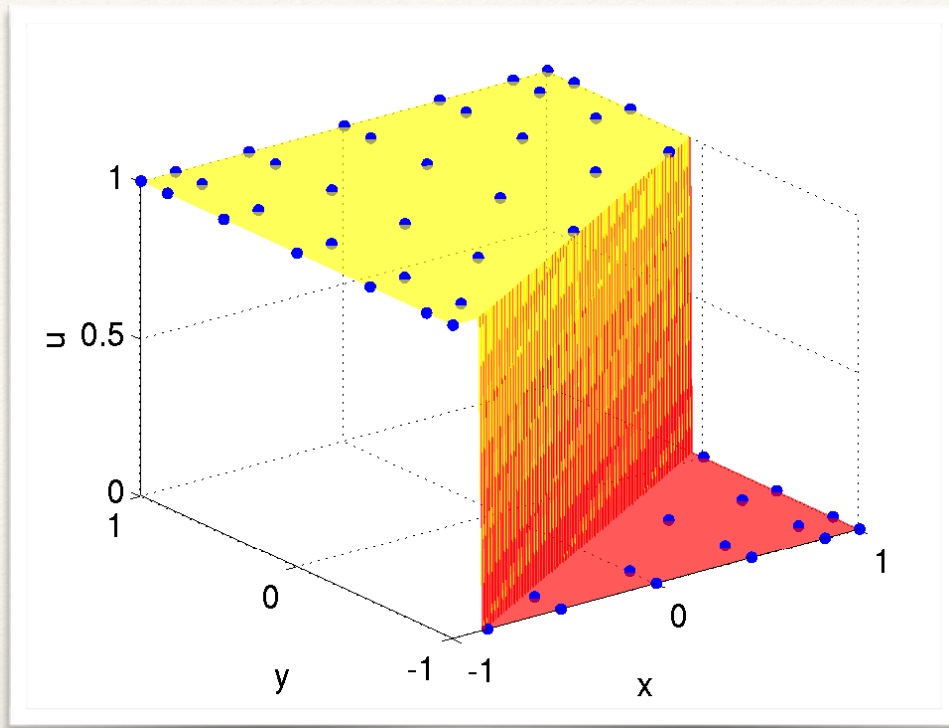
- ❖ For tensor product elements, use 1D method along x and y (and z) slices



Extension to 2D and 3D

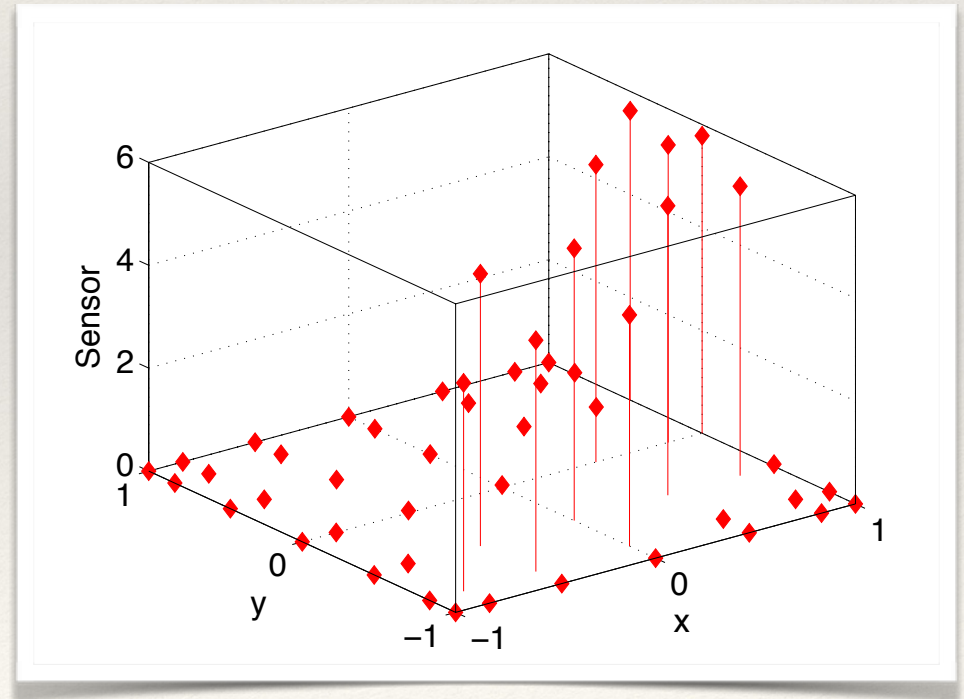
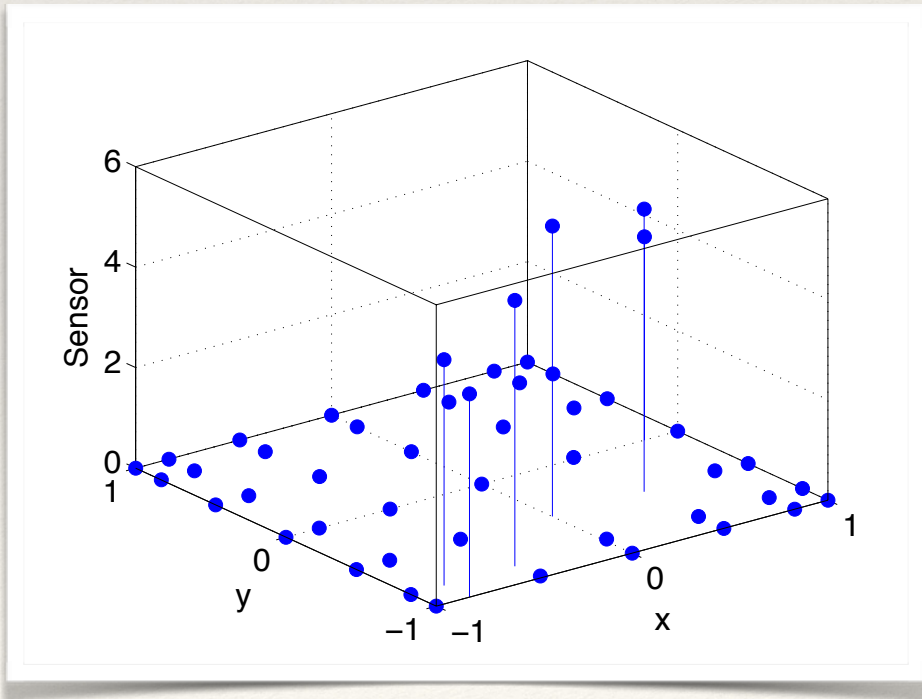
- ❖ For triangles and tetrahedra, transform to equivalent tensor product elements by un-collapsing

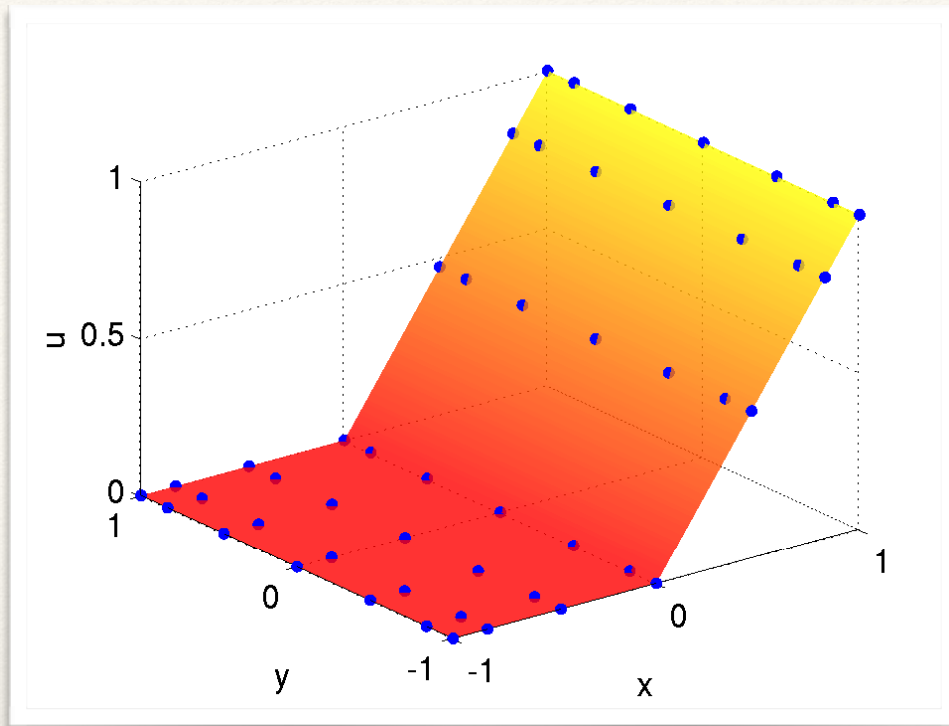




x-slices

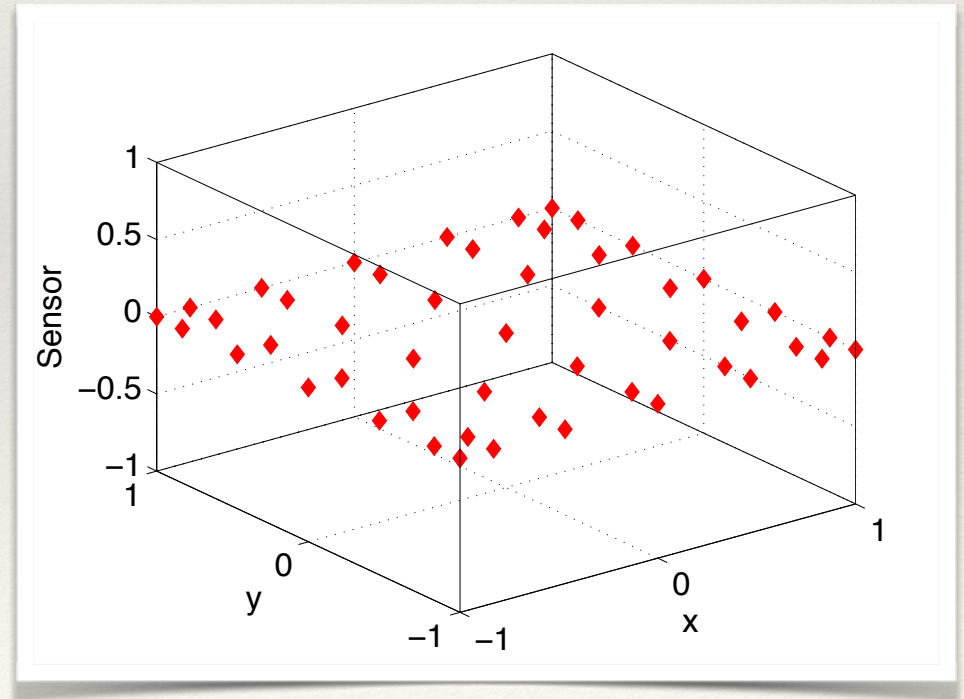
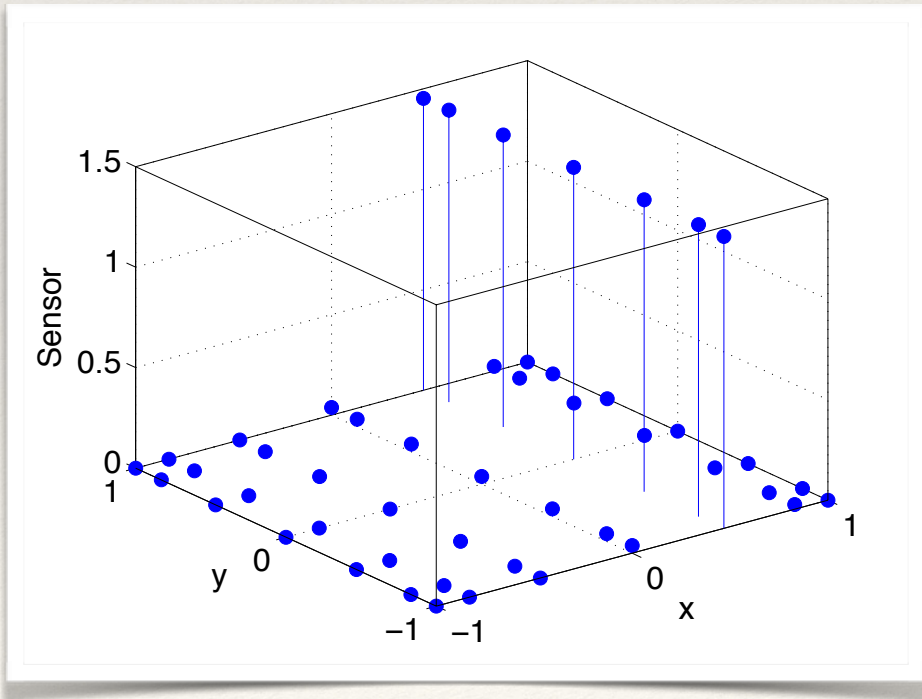
y-slices

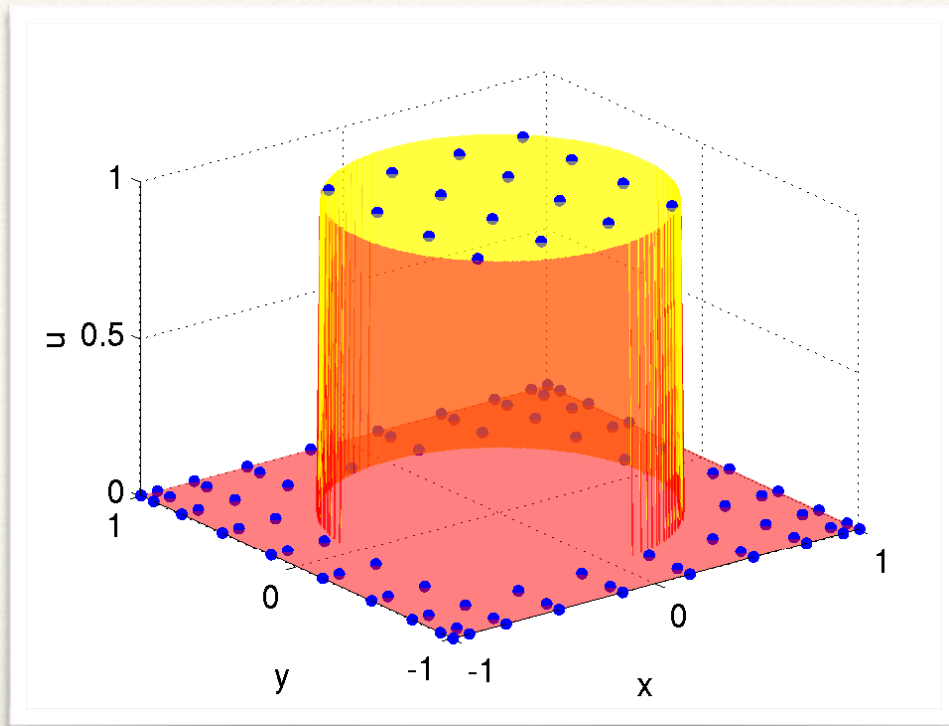




x-slices

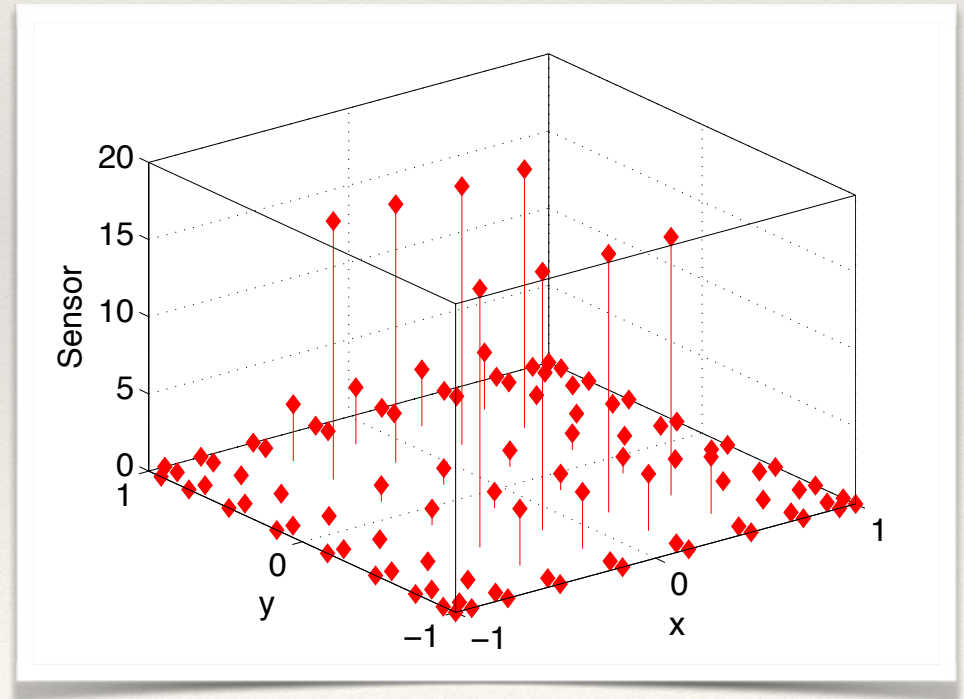
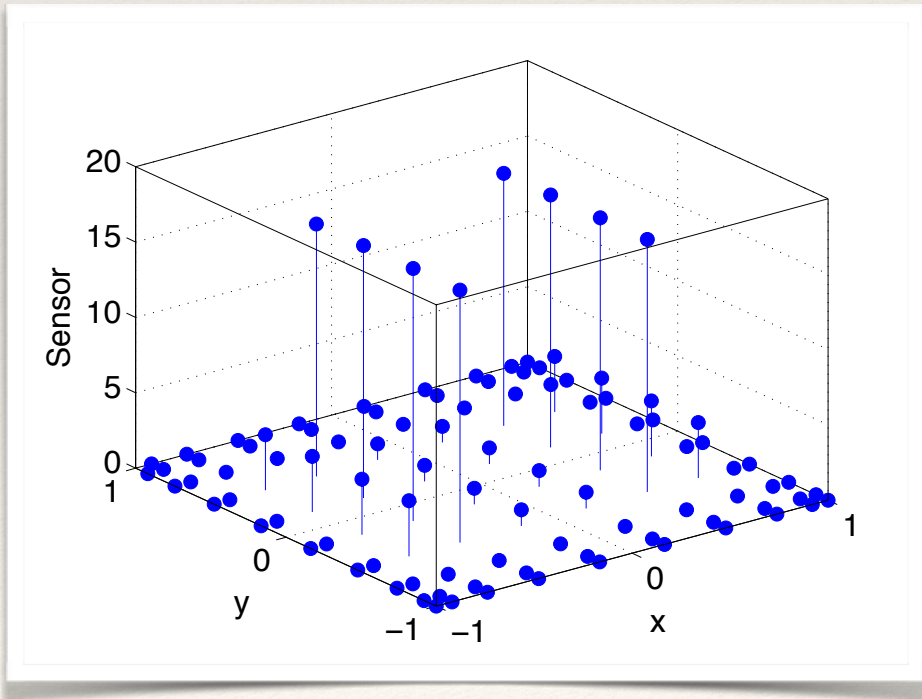
y-slices

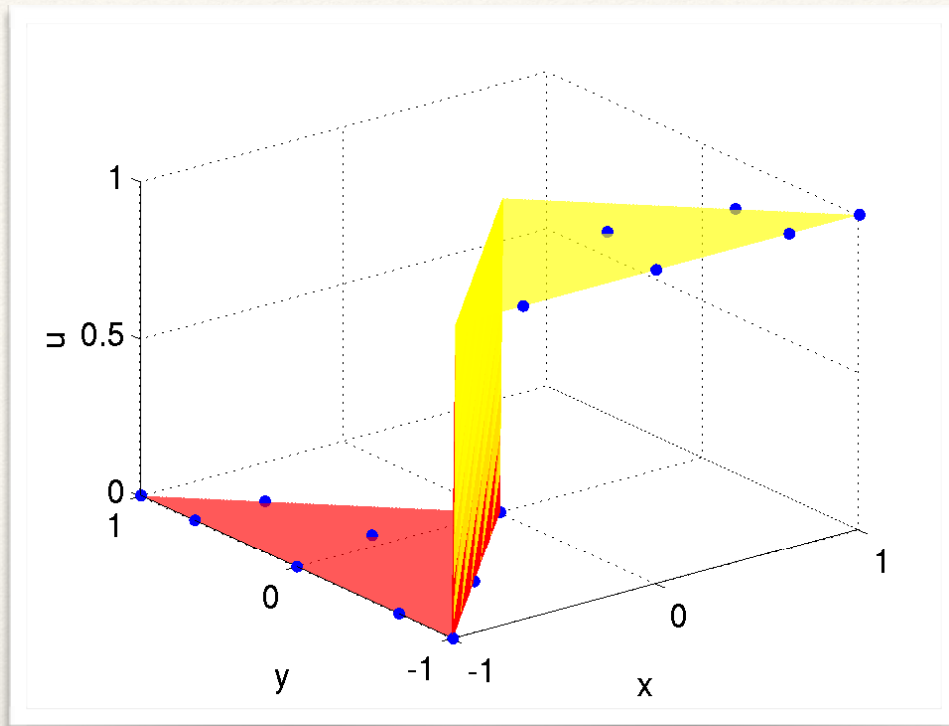




x-slices

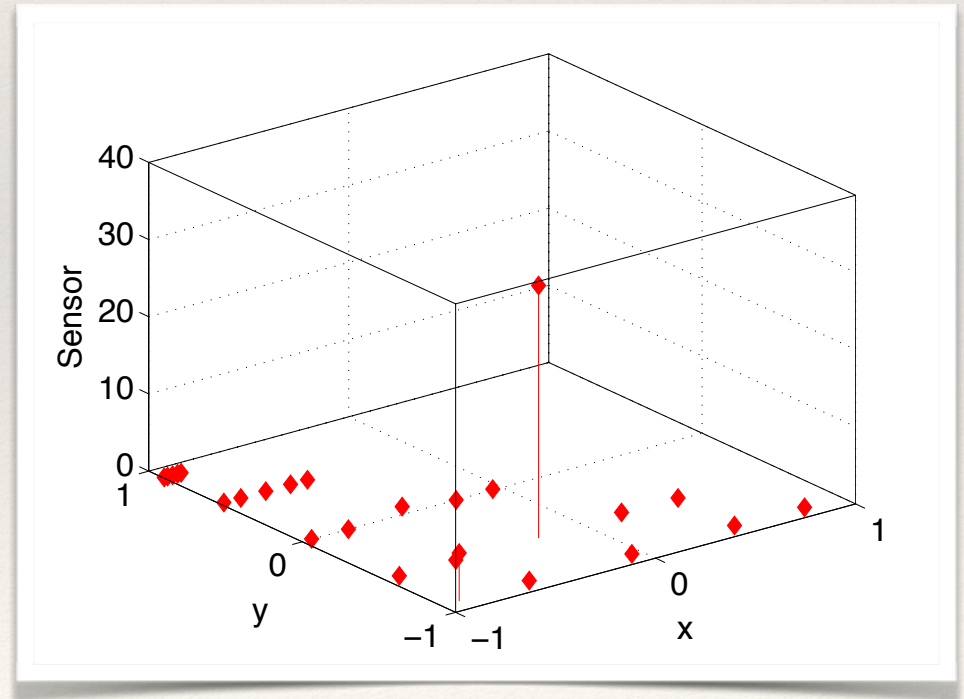
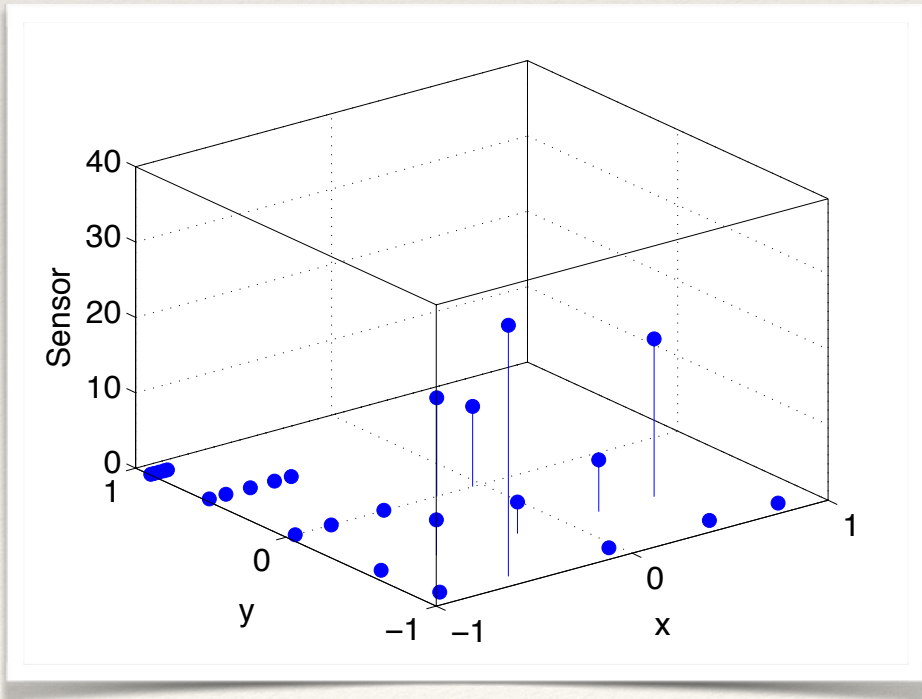
y-slices





x-slices

y-slices



Positivity Preservation

- ❖ Entropy-based limiter proposed by Zhang & Shu, improved by Lv and Ihme.
- ❖ Two step process:
 - ❖ Limit Density at all quadrature points to stay positive
 - ❖ Limit Pressure to satisfy entropy bound

Positivity Preservation

- ❖ High-order accurate in smooth regions; first order near discontinuities
- ❖ Preserves positivity of cell average at next time-step if you follow a CFL condition
- ❖ Use TVD RK3 scheme or SSP scheme

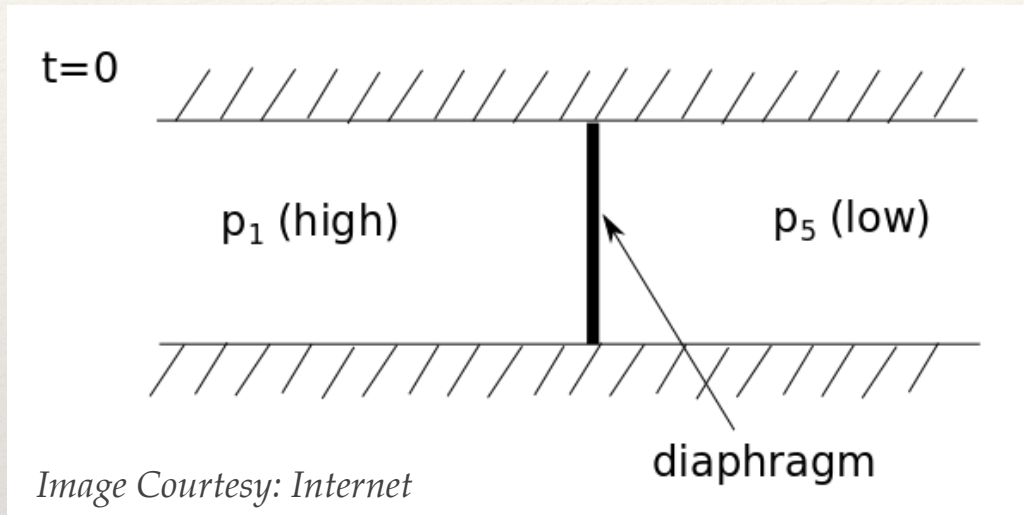
The background features a large, faint watermark of the Stanford University seal. The seal is circular and contains a redwood tree in the center. The text around the tree reads "Leland Stanford Junior University" at the top, "Die Luft der Freiheit weht" on the sides, and "1891" at the bottom. There are also several stars around the inner circle.

Numerical Experiments

Numerical Experiments

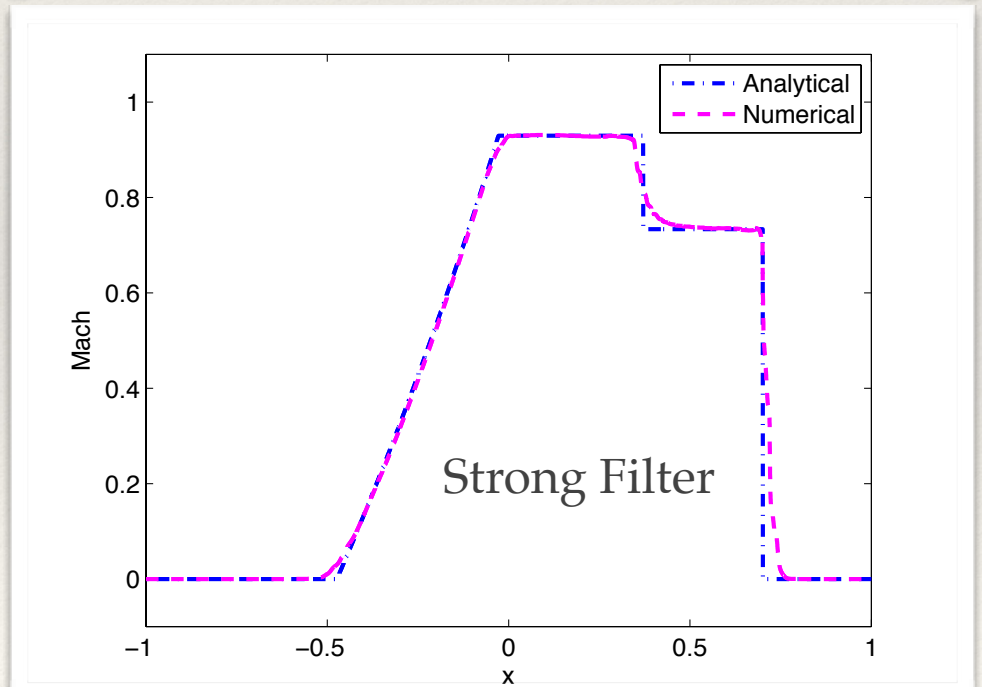
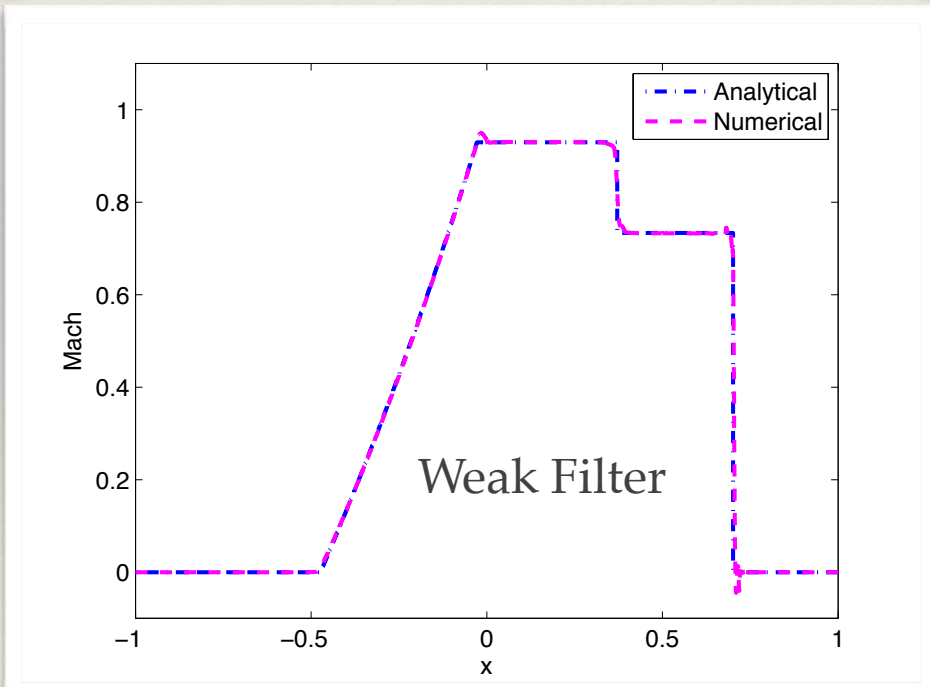
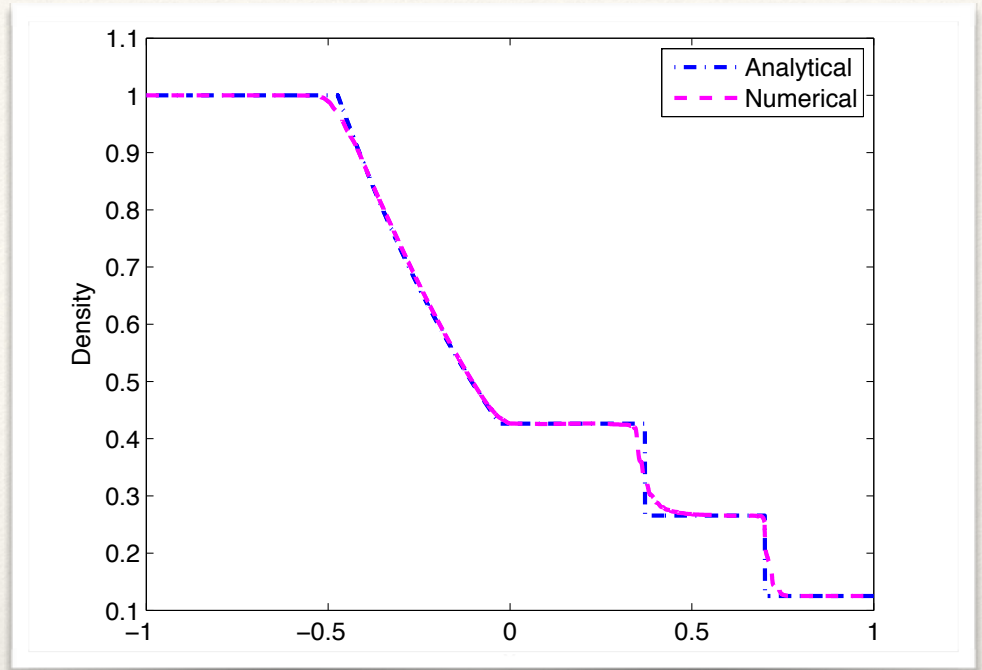
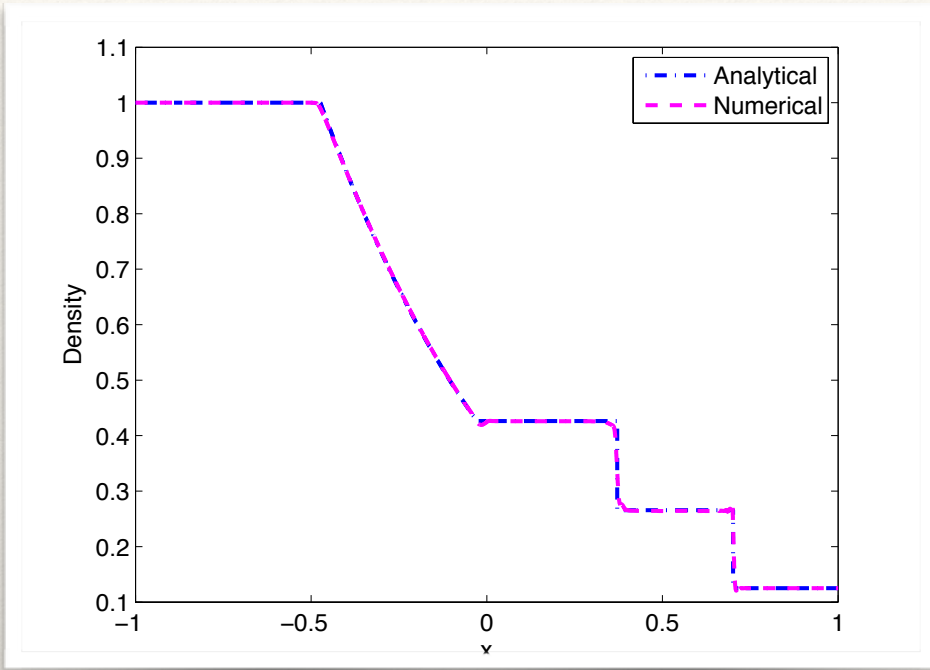
- ❖ 2D and 3D simulations run using an in-house code ZEFR developed by Josh Romero, ACL.
- ❖ Uses DFR (Direct Flux Reconstruction) - Triangles and Tets using a collapsed-edge tensor product formulation
- ❖ Run on GPU clusters - ICME GPU Cluster, XStream cluster

1D Shock Tube



$$\rho(x, 0) = \begin{cases} 1 & \text{for } x < \frac{1}{2}, \\ 0.125 & \text{for } x \geq \frac{1}{2} \end{cases}$$
$$p(x, 0) = \begin{cases} 1 & \text{for } x < \frac{1}{2}, \\ 0.1 & \text{for } x \geq \frac{1}{2} \end{cases}$$
$$u(x, 0) = 0$$

Num Elements	Order	Filter Order	Final Time
100	6	2	0.4s

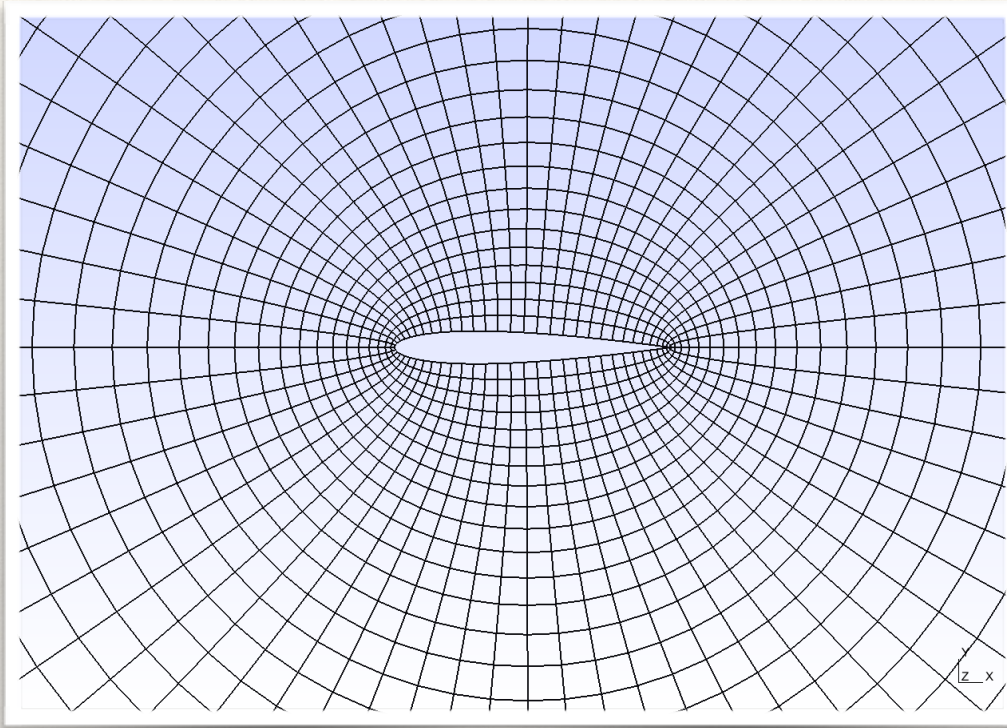


1D Shock Tube

Variable	Weak Filter		Strong Filter	
	Error in L^2	Error in L^∞	Error in L^2	Error in L^∞
ρ	0.007615	0.059184	0.017483	0.094786
u	0.037212	0.512378	0.074807	0.613601
p	0.006965	0.085243	0.015243	0.110720
M	0.031808	0.431799	0.065749	0.510206

Table 1: Norms of the difference between the numerical and analytical solutions at $t = 0.4$ for the two testcases.

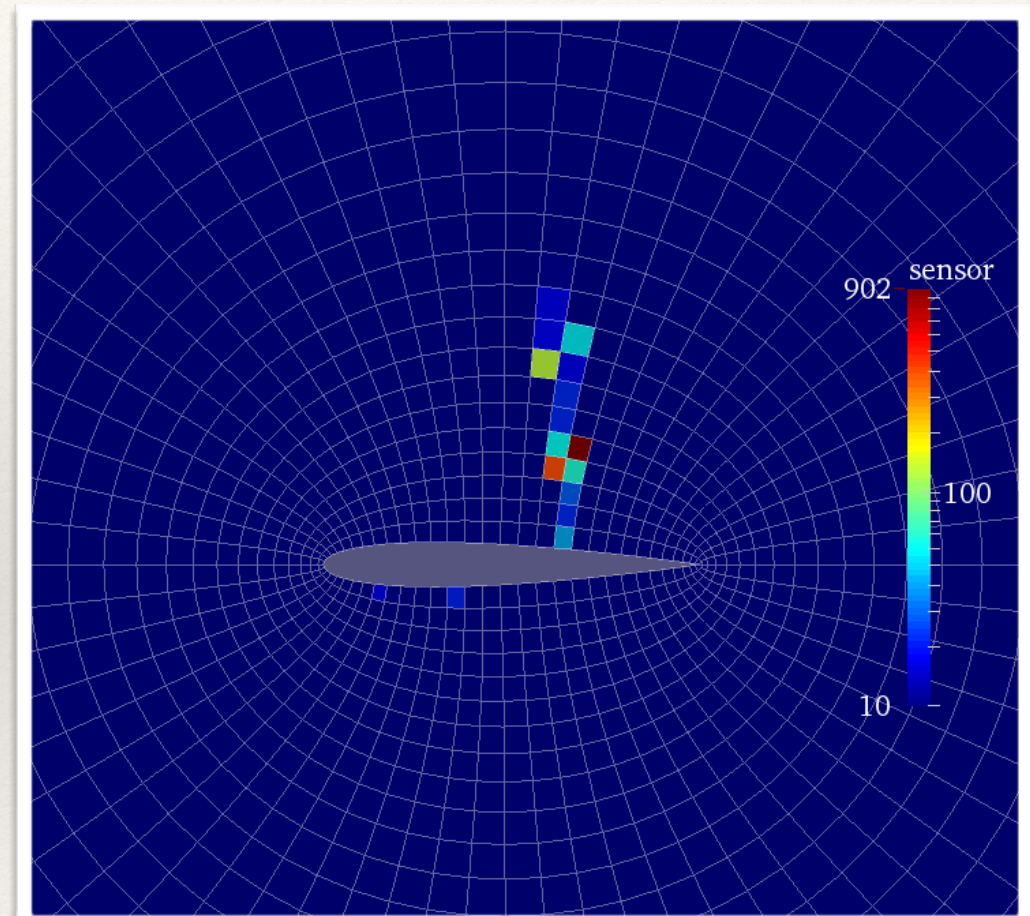
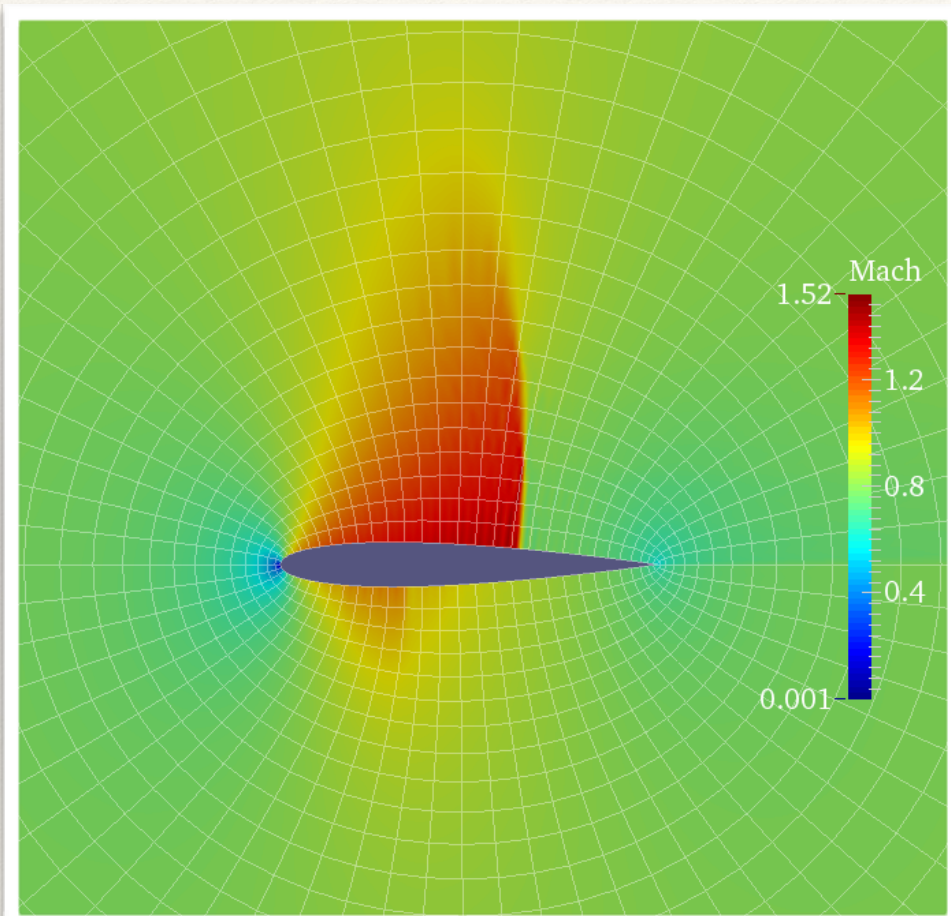
2D Transonic Flow: Quads



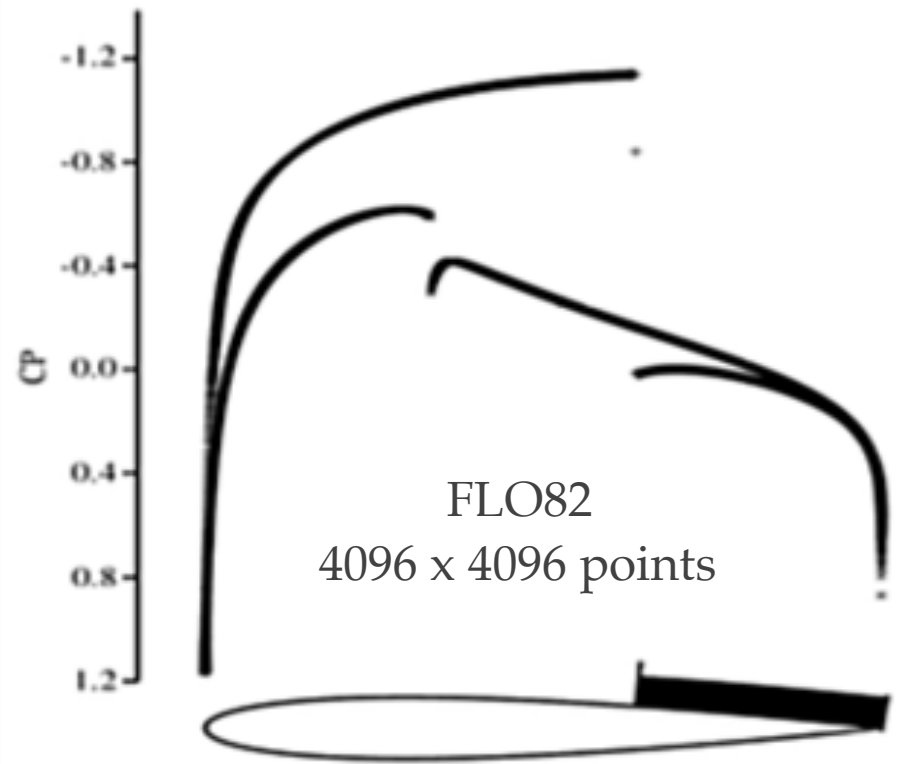
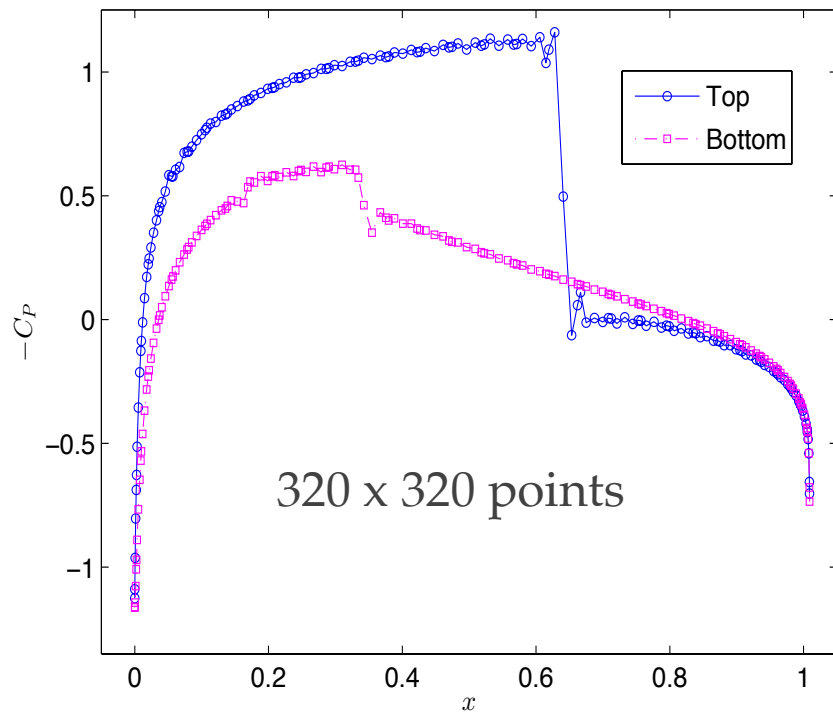
- ❖ Euler Equations
- ❖ NACA 0012 airfoil
- ❖ Steady State; p-Multigrid
- ❖ 64 x 64 O-mesh

Mach	AoA	Num Elem	Order	Filter Order	Filt Strength
0.8	1.25°	4096	5	2	1

2D Transonic Flow: Quads

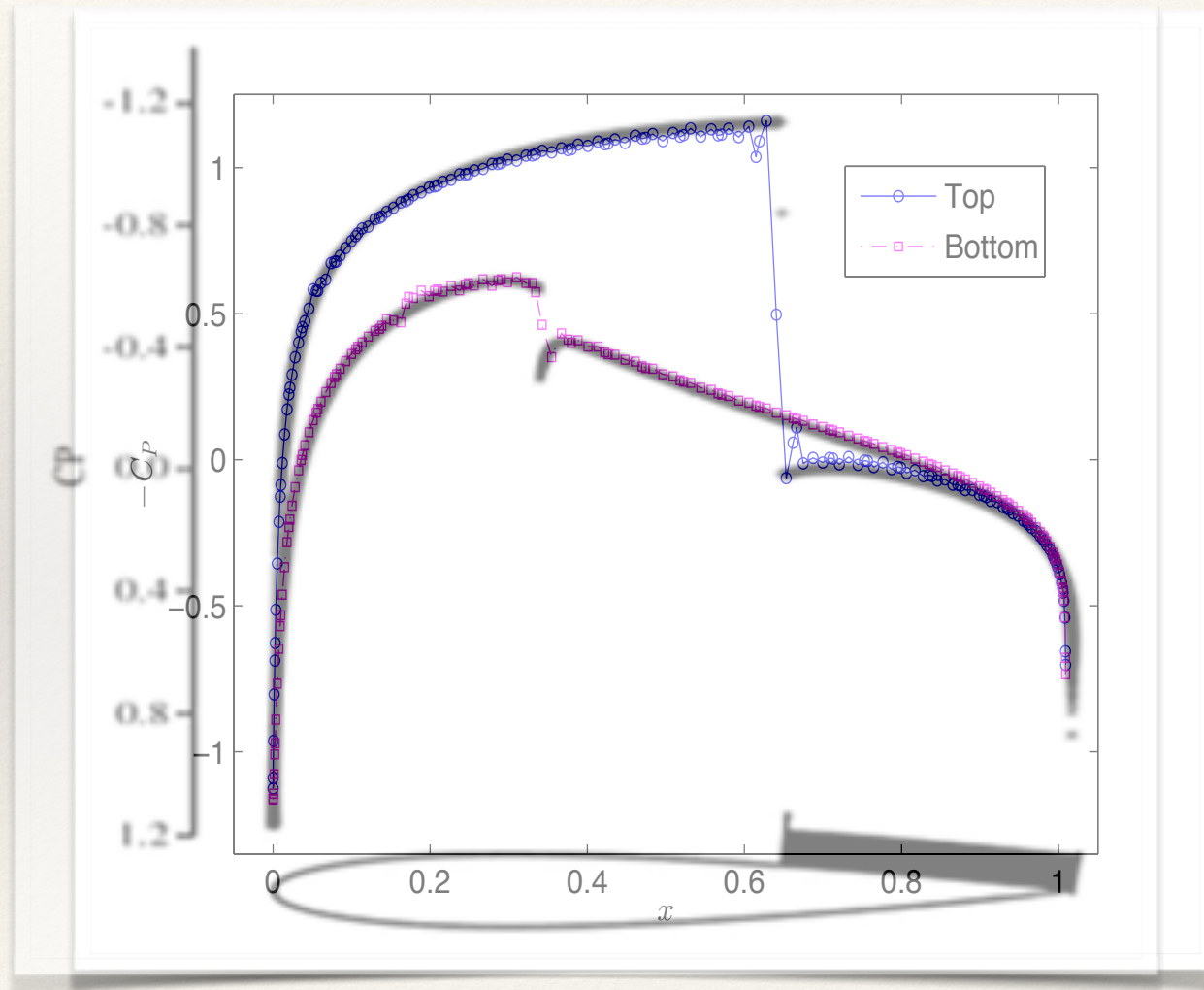


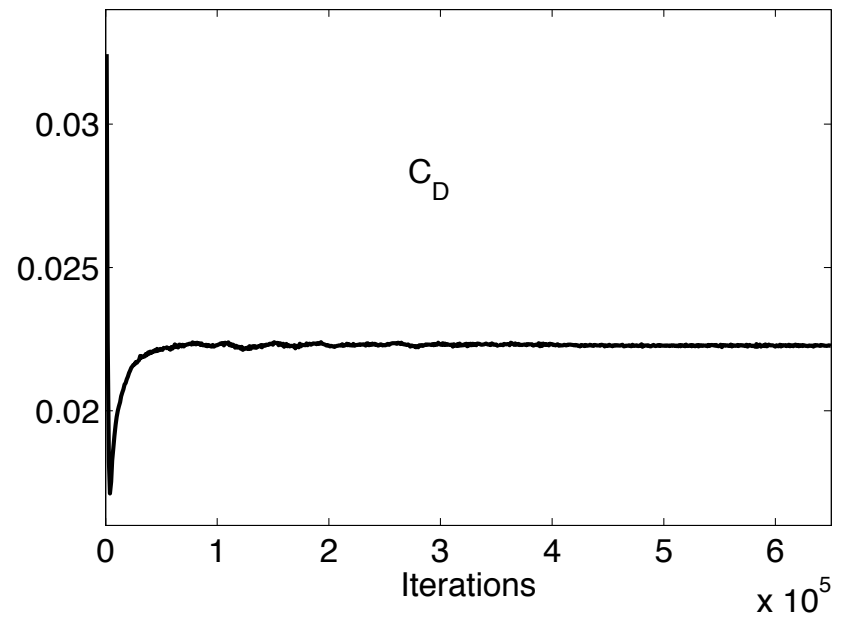
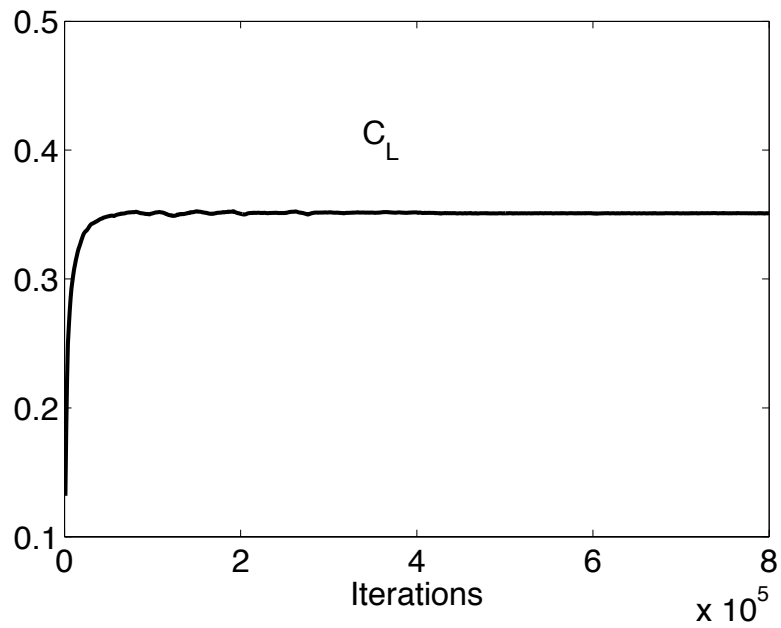
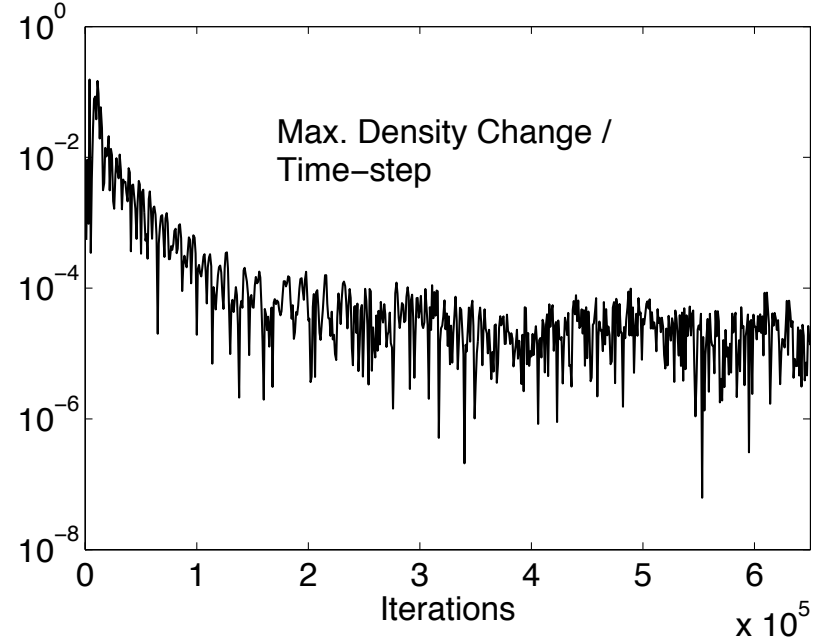
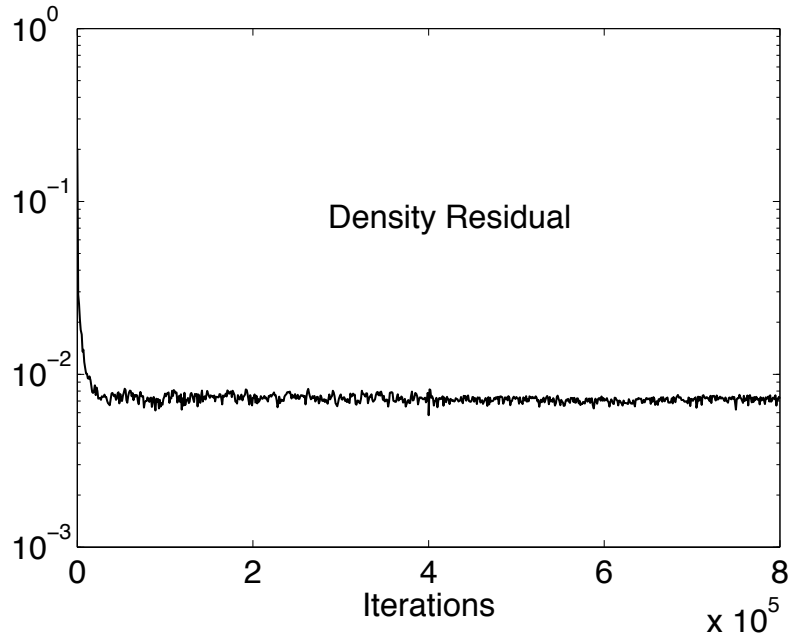
2D Transonic Flow: Quads



Reference: Vassberg and Jameson, *Journal of Aircraft*, 2010

2D Transonic Flow: Quads





2D Transonic Flow: Quads

Table 5 OVERFLOW-central transonic data at $M = 0.8$

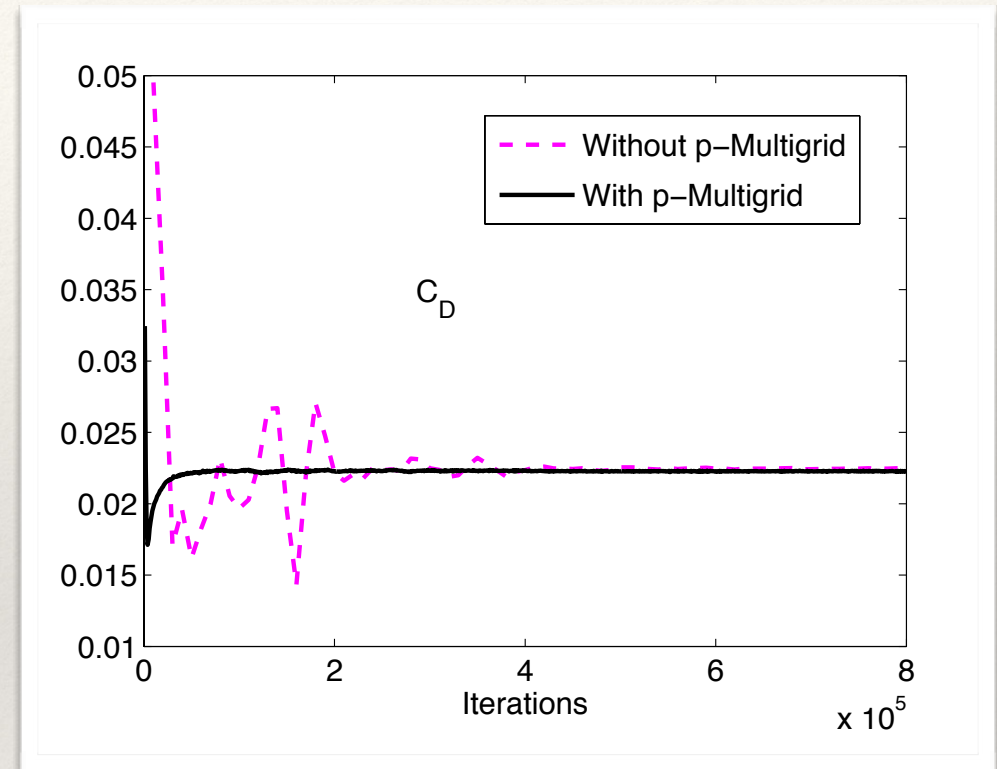
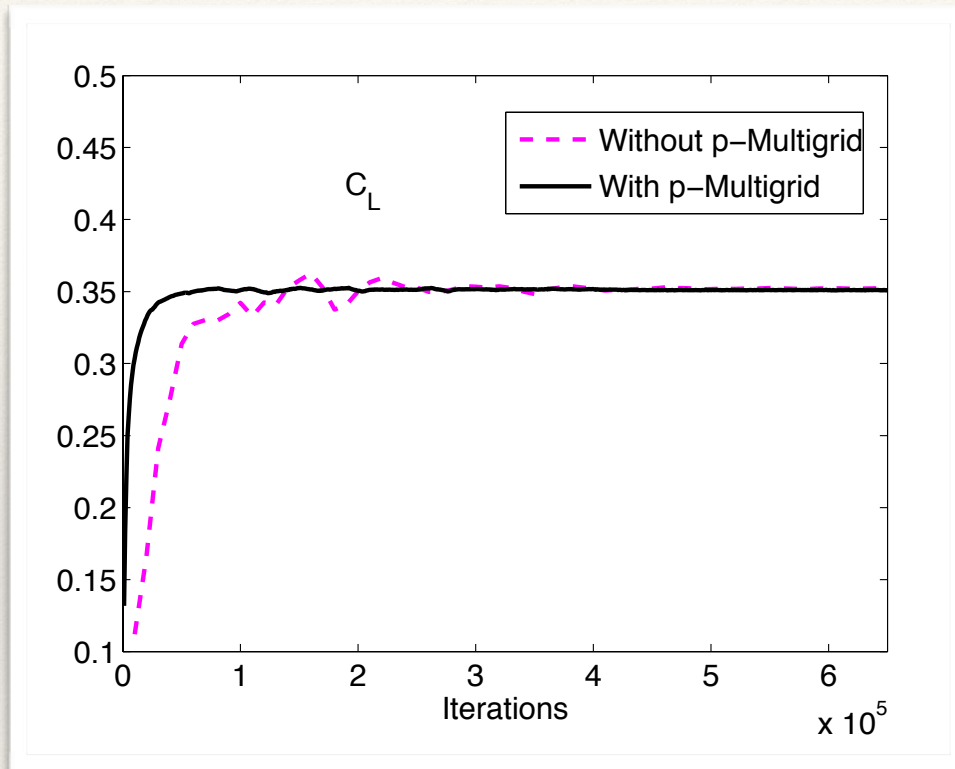
Mesh		$\alpha = 0$ deg		$\alpha = 1.25$ deg	
NC	NC^2	C_d	C_l	C_d	C_m
256	65,536	+0.008734038	+0.353909135	+0.022964252	-0.038987812
512	262,144	+0.008493959	+0.353798330	+0.022706732	-0.038656831
1,024	1,048,576	+0.008412129	+0.353241712	+0.022593342	-0.038402691
2,048	4,194,304	+0.008376064	+0.352827907	+0.022534646	-0.038251571
4,096	16,777,216	+0.008358591	+0.352522552	+0.022500576	-0.038150471
Continuum		+0.008342171	+0.351662793	+0.022453440	-0.037946129
Order p		1.046	0.438	0.785	0.580

$NDOF = 102,400$

	C_L	C_D
Mean	0.352052	0.022468
Std	0.000178	0.000039

Reference: Vassberg and Jameson, *Journal of Aircraft*, 2010

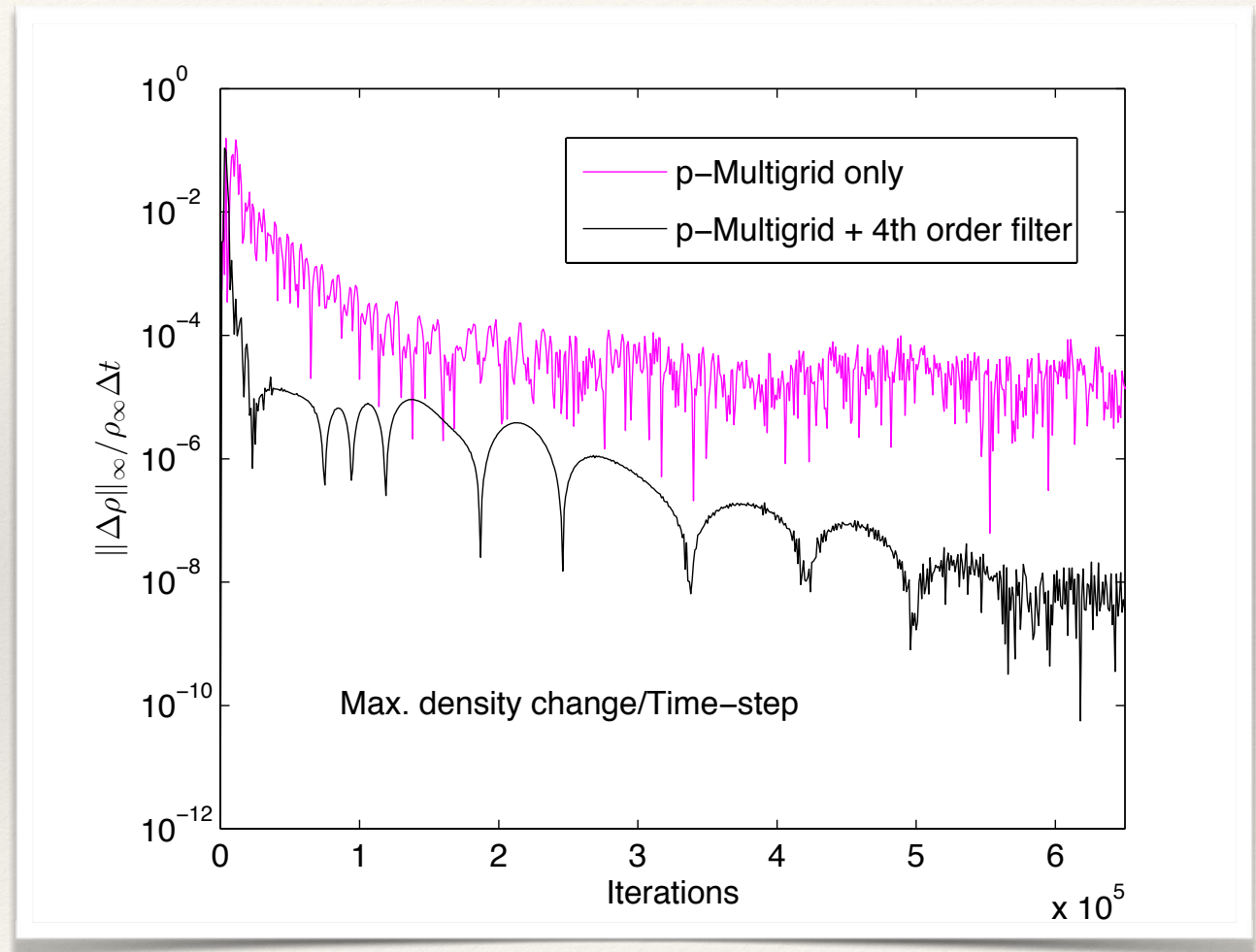
2D Transonic Flow: Quads



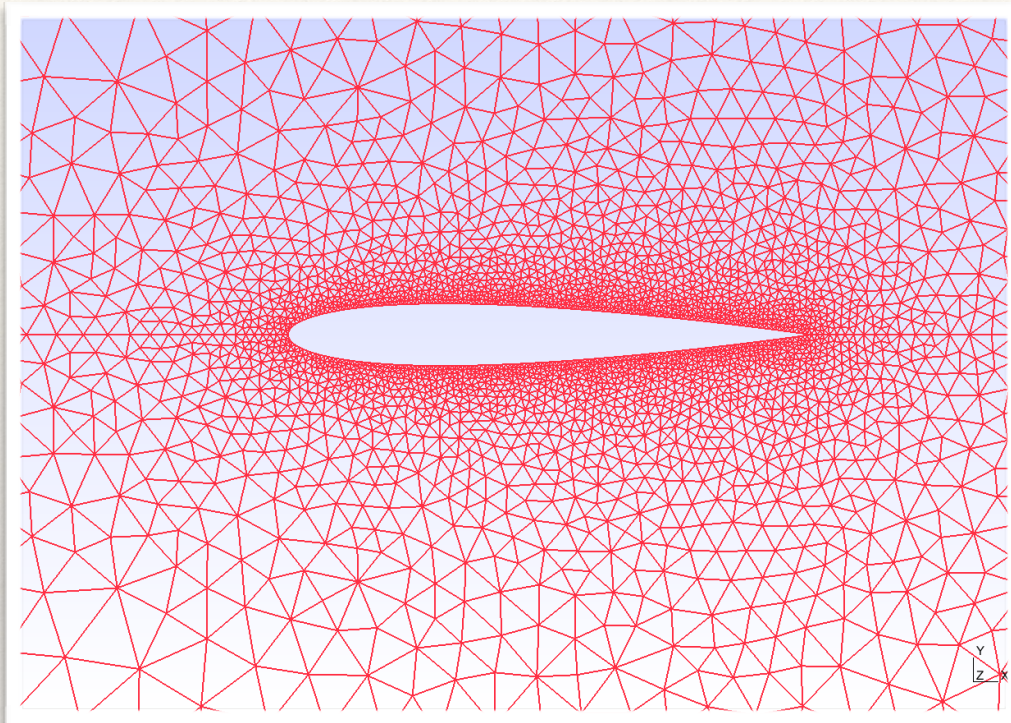
- ❖ 6-8x iteration; 2-3x wall-clock time speedup
- ❖ Can we do better?

2D Transonic Flow: Quads

- ❖ Take a cue from JST
- ❖ Add a 4th order filter in smooth regions!
- ❖ Can be switched off after initial speed-up for order of accuracy



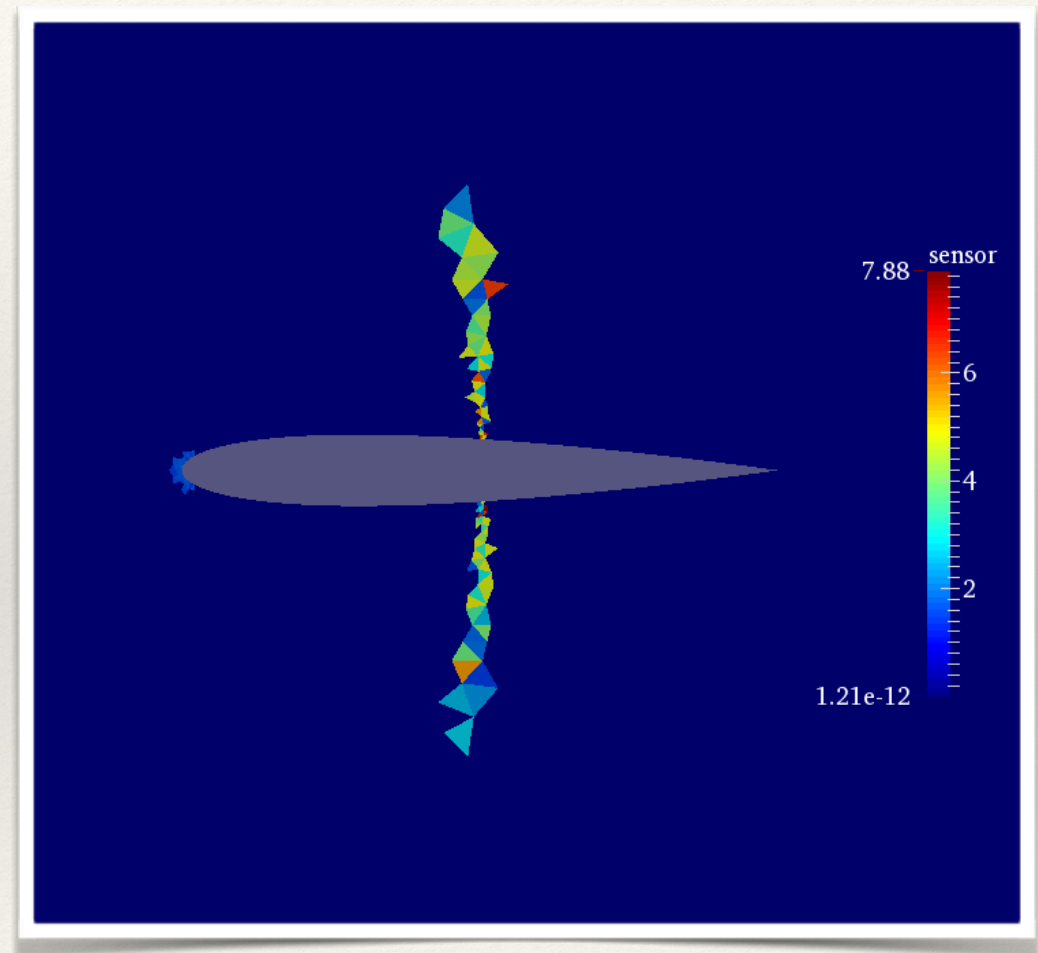
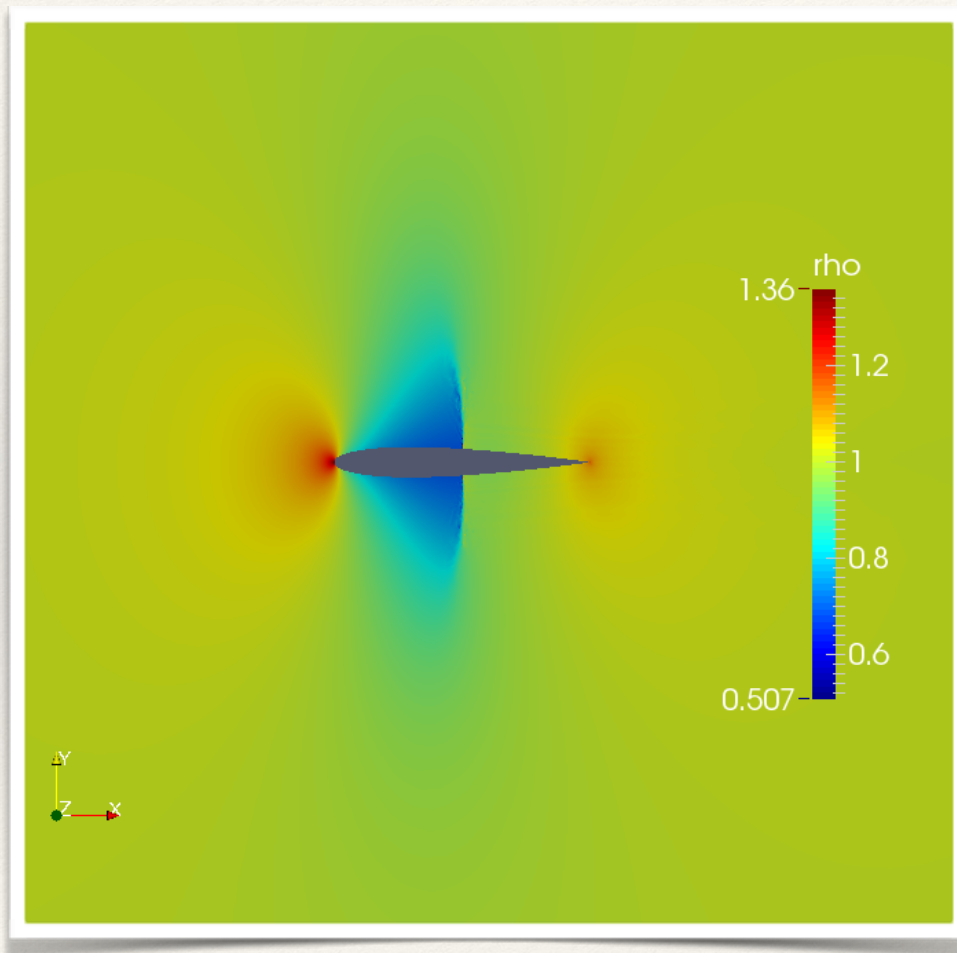
2D Transonic Flow: Triangles



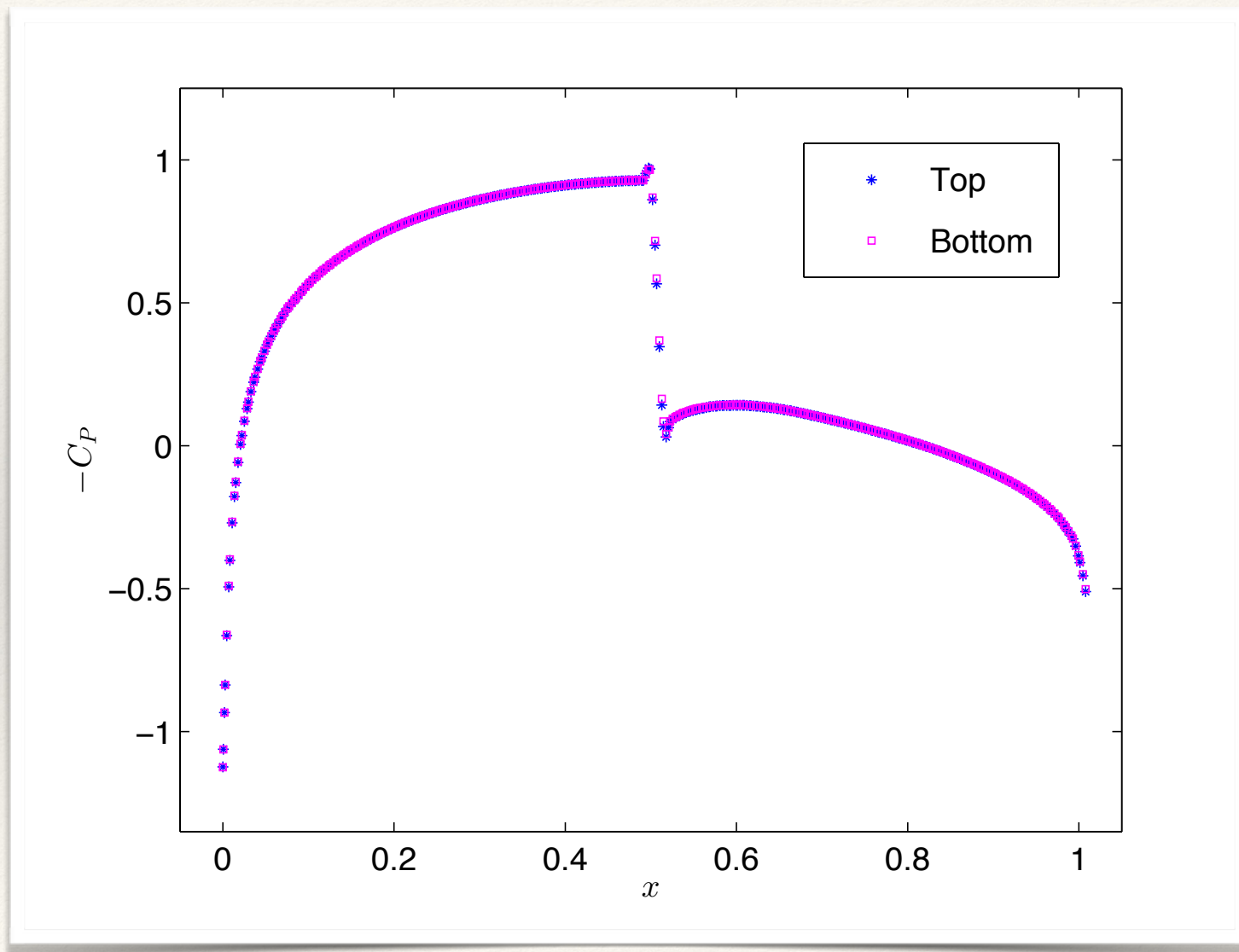
- ❖ Euler Equations
- ❖ NACA 0012 airfoil
- ❖ Steady State
- ❖ Unstructured Tri mesh

Mach	AoA	Num Elem	Order	Filter Order	Filt Strength
0.8	0°	11464	4	2	1

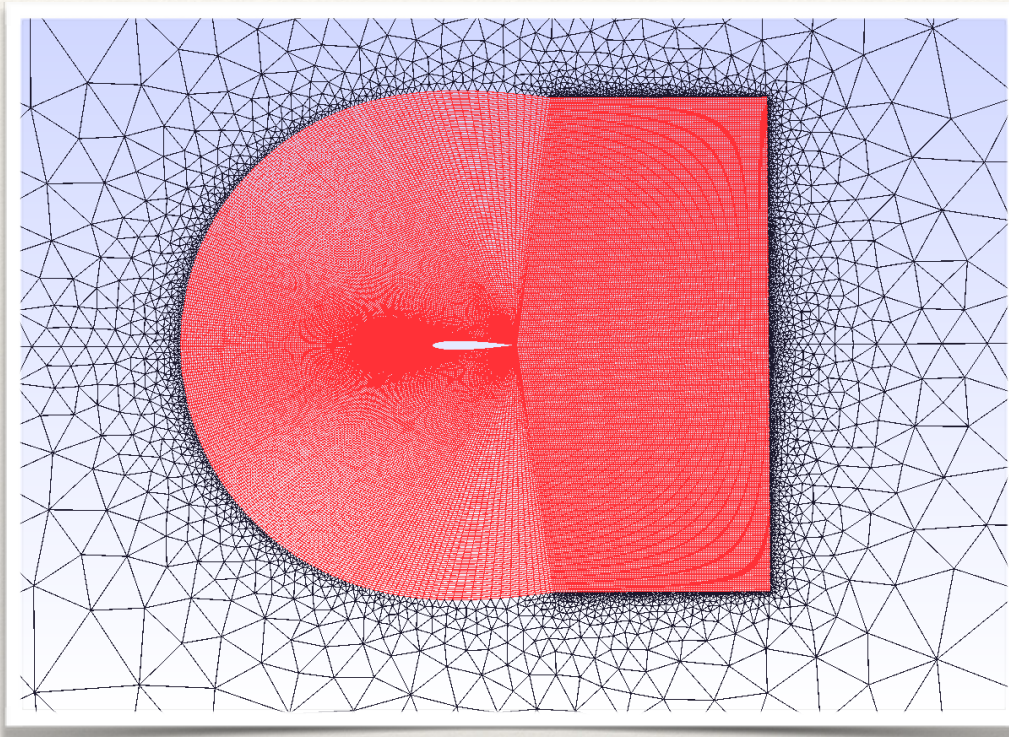
2D Transonic Flow: Triangles



2D Transonic Flow: Triangles



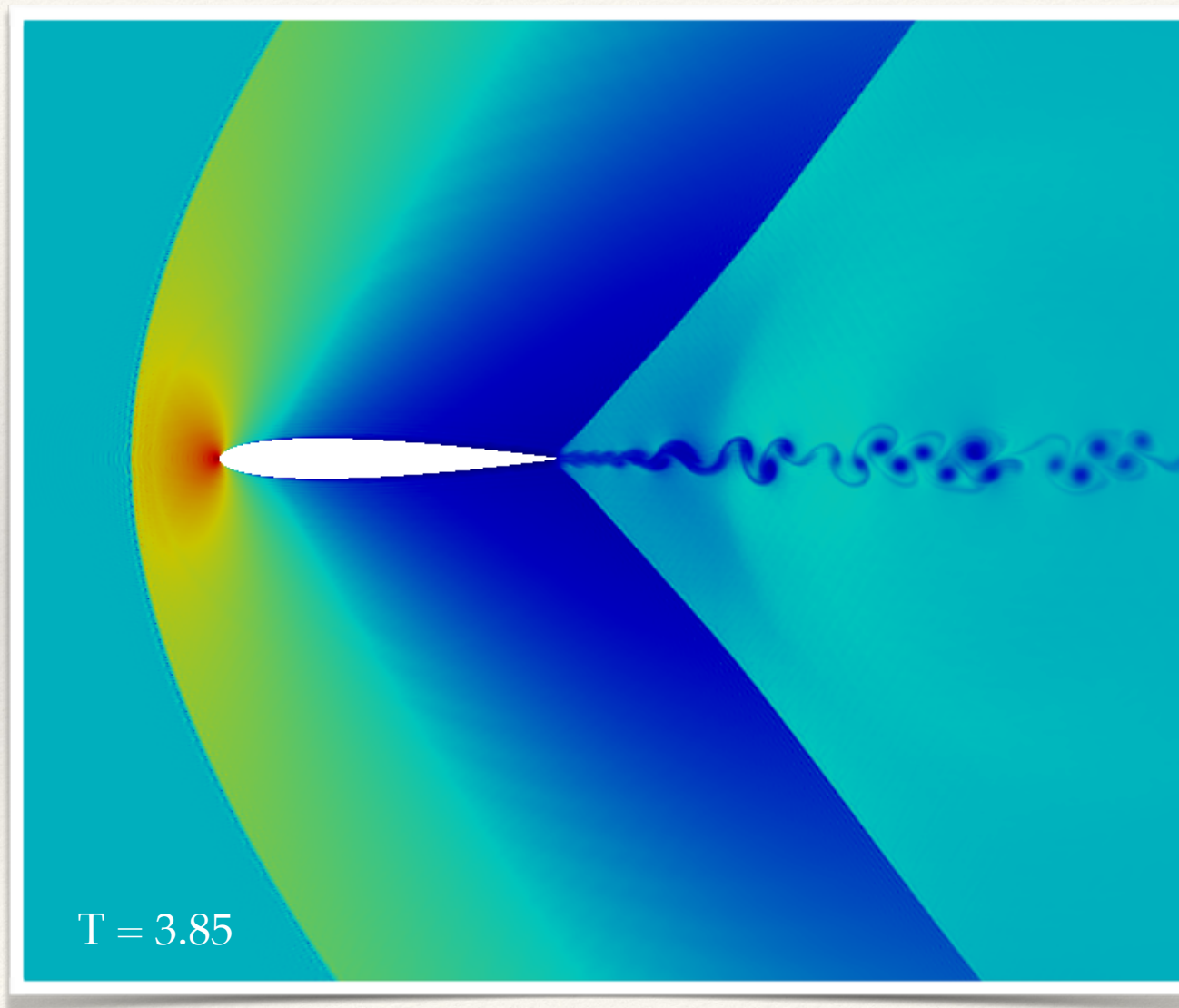
2D Supersonic Viscous Flow



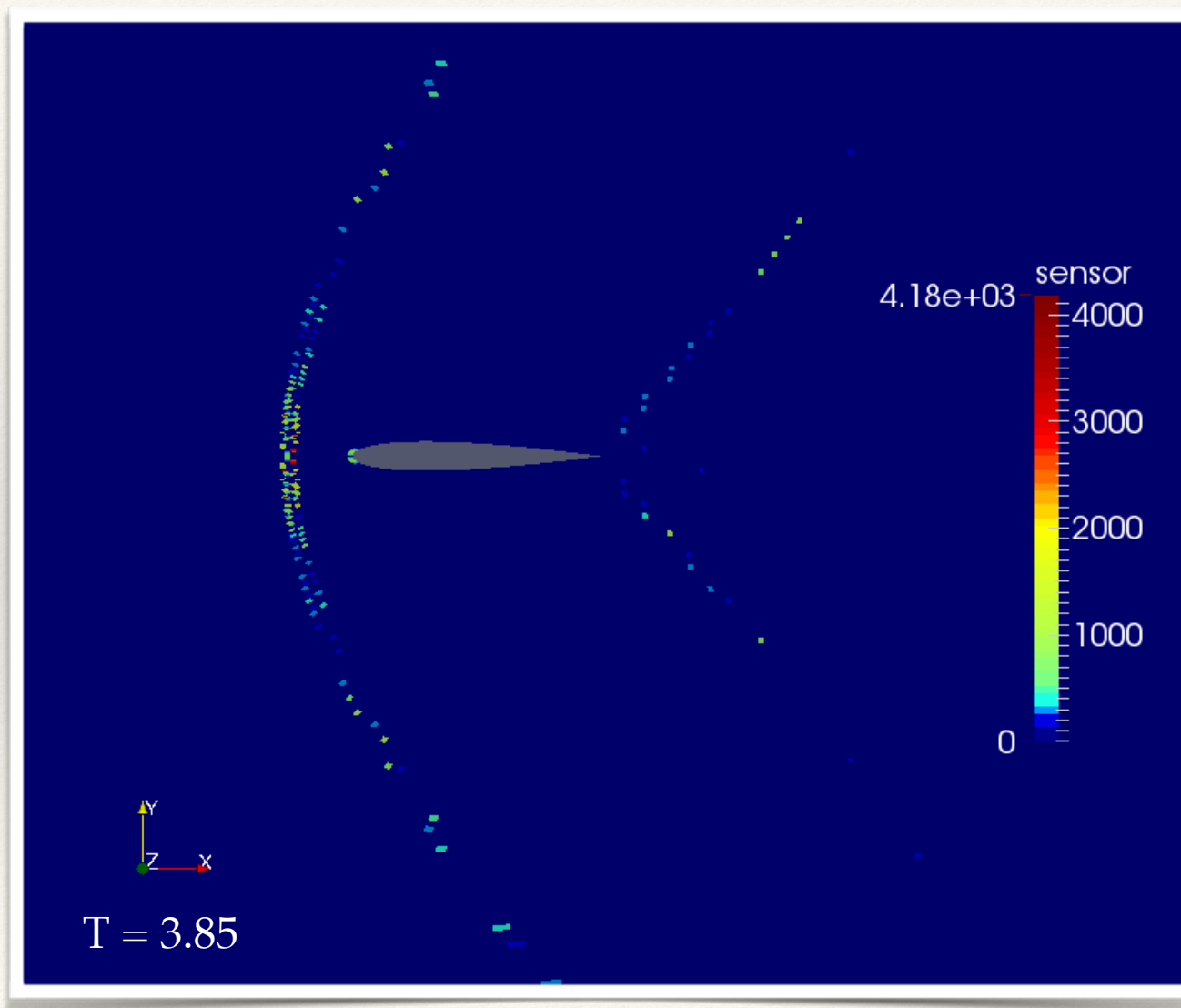
- ❖ Navier-Stokes Equations
- ❖ NACA 0012 airfoil
- ❖ Hybrid Mesh
- ❖ Adiabatic no-slip wall

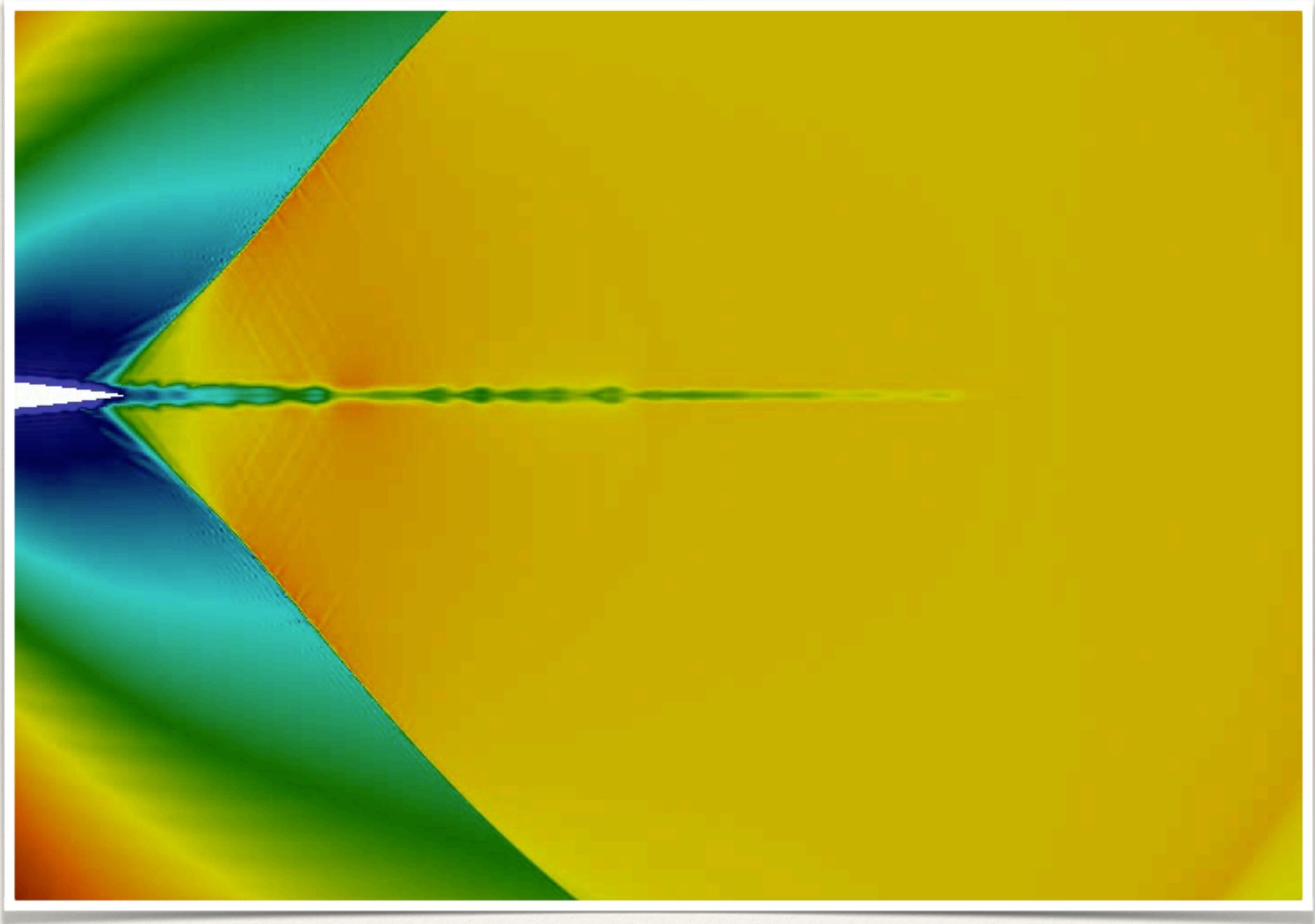
Mach	AoA	Re	Num Elem	Order	Filter Order	Filt Strength
1.2	2°	60,000	72,790	4	6*	1

2D Supersonic Viscous Flow

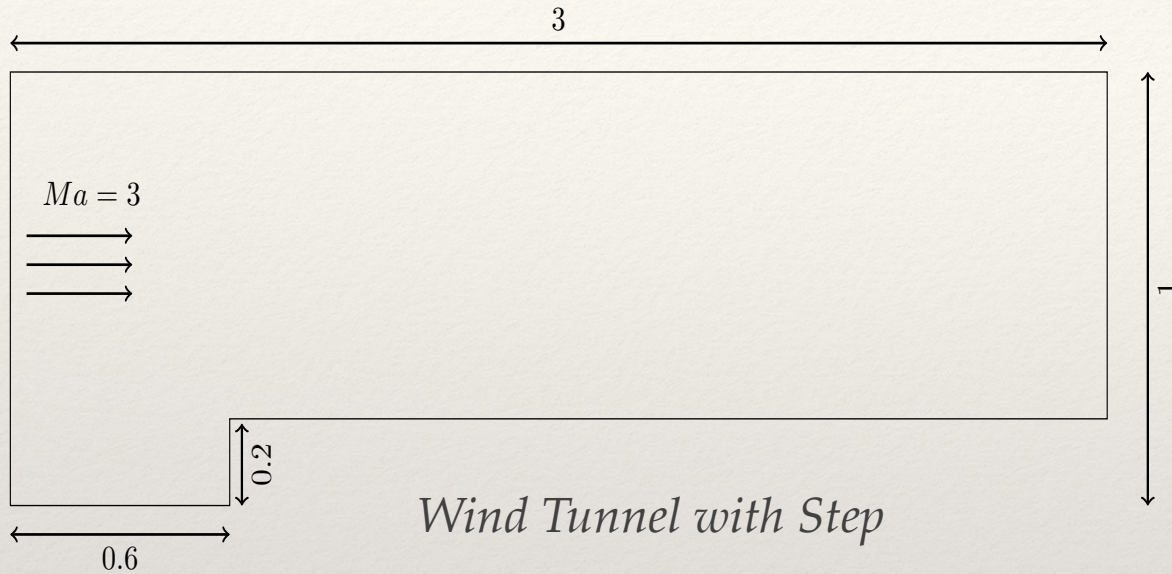


2D Supersonic Viscous Flow





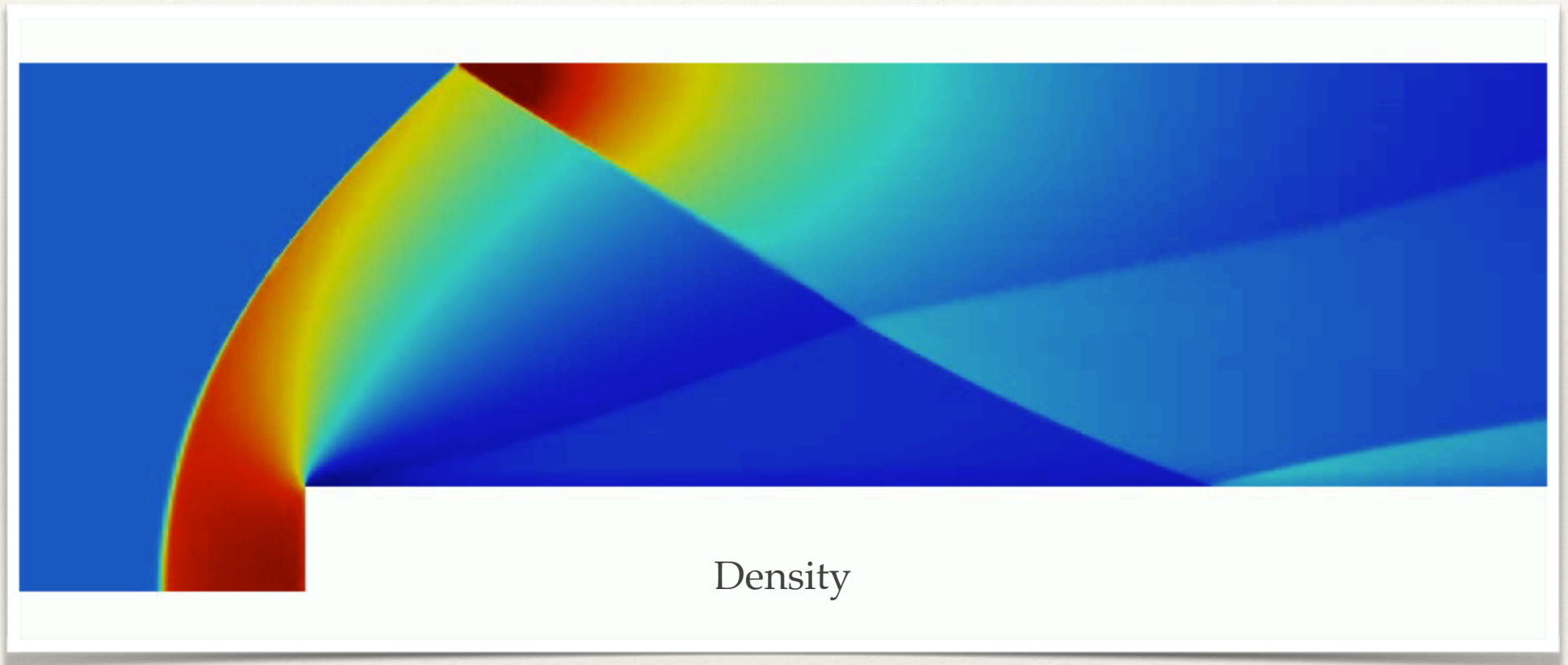
Supersonic flow over a step

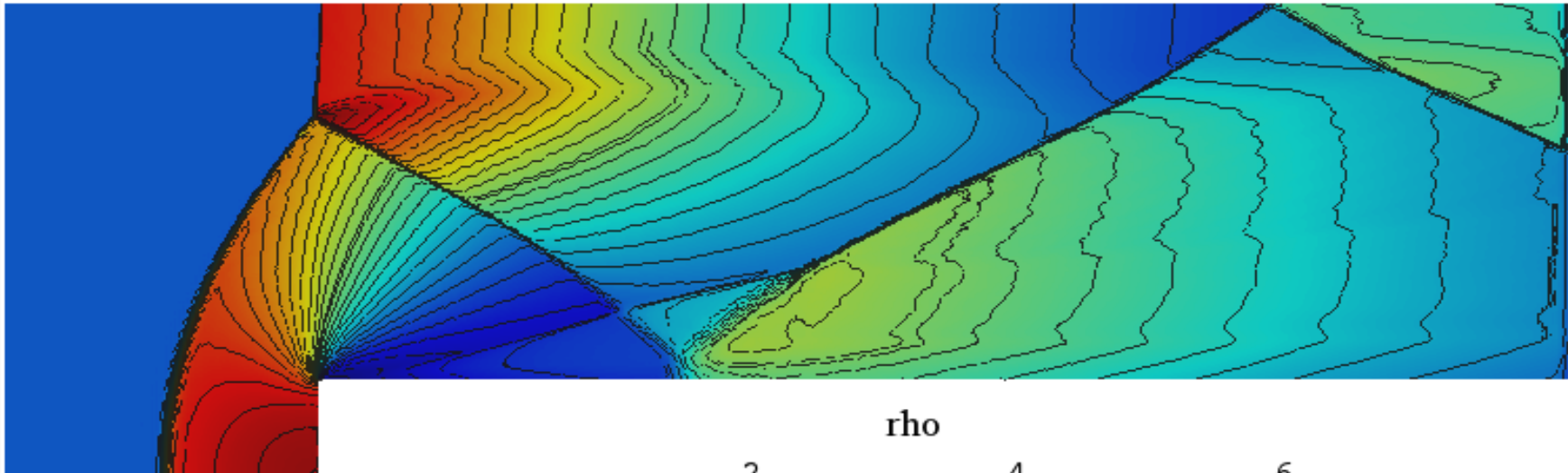


- ❖ Euler Equations
- ❖ Structured Quad Mesh
- ❖ Sensor at ramp
- ❖ Positivity Limiter

Mach	Flow Angle	Num Elem	Order	Filter Order	Filt Strength
3.0	0°	63,004	3	2	5

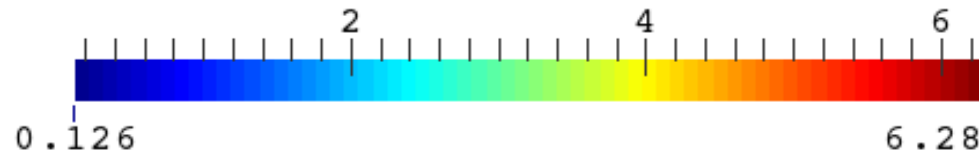
Supersonic flow over a step



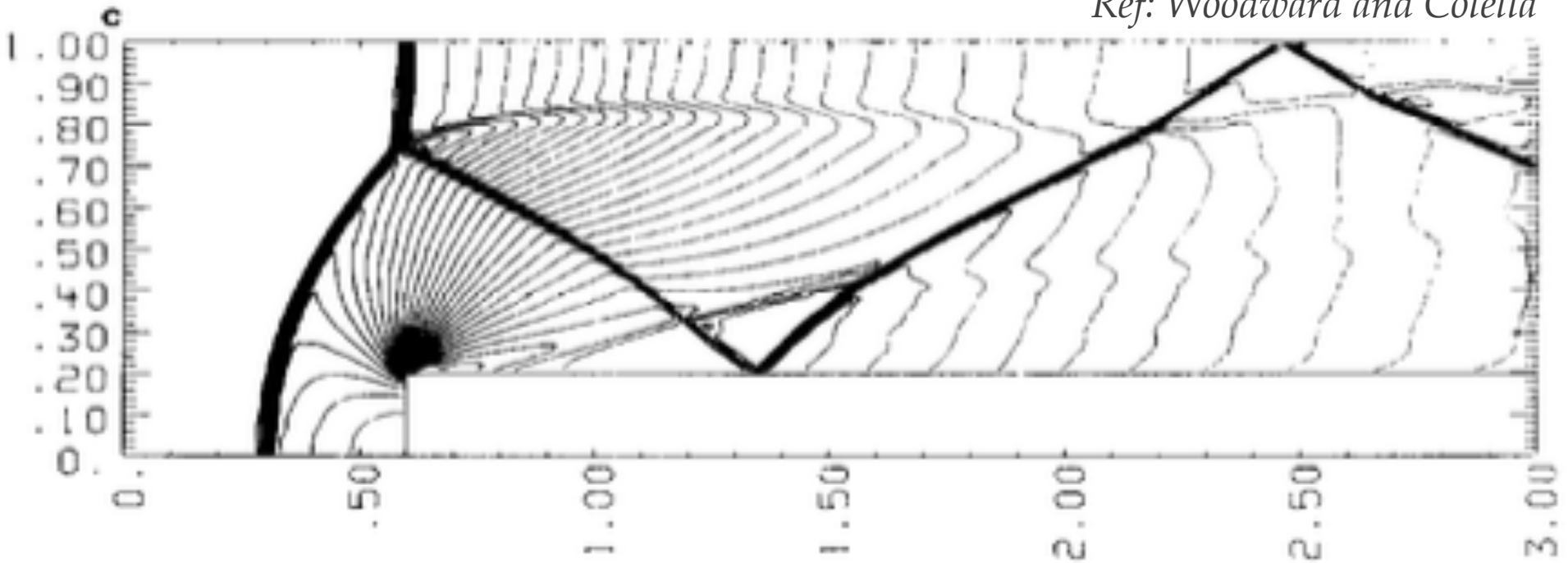


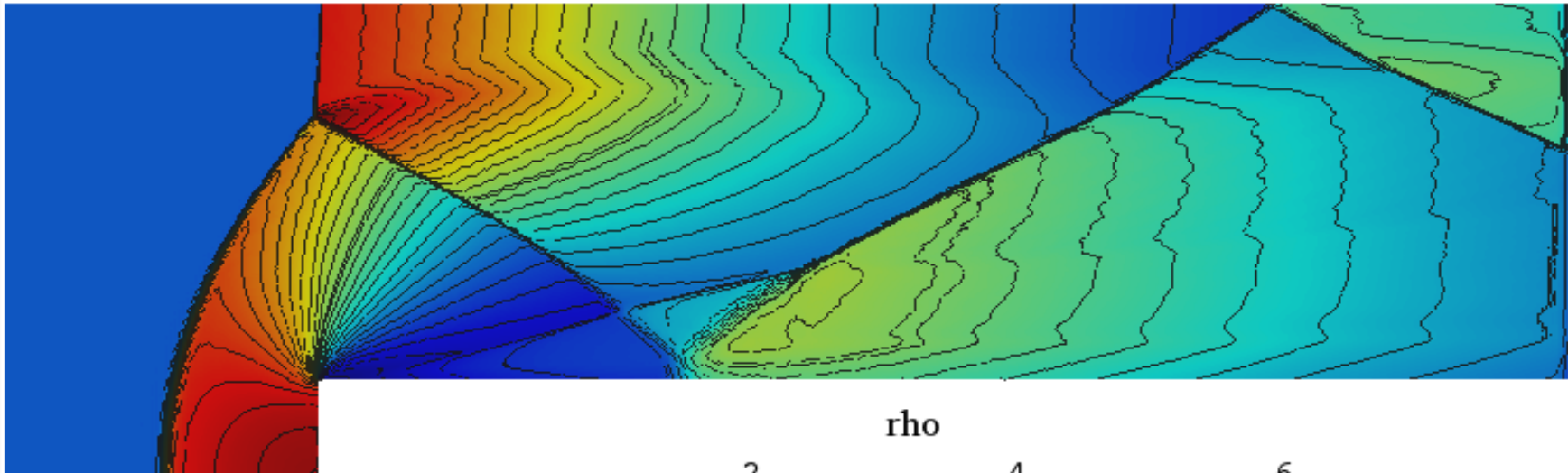
T = 4

rho

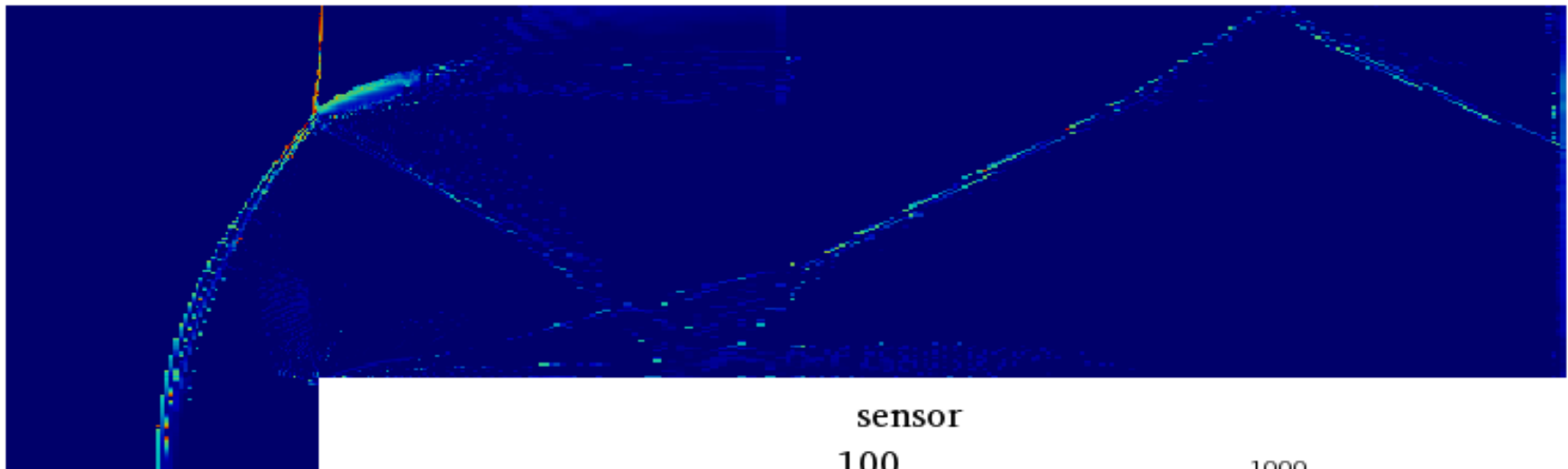
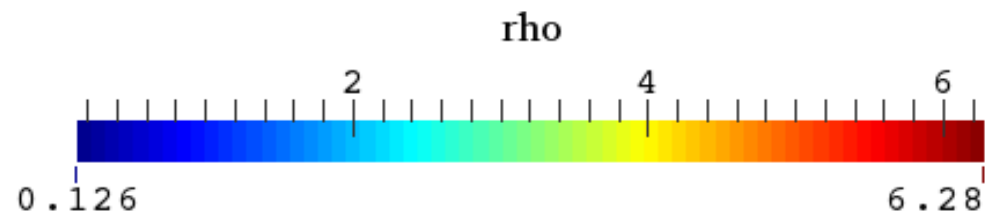


Ref: Woodward and Colella

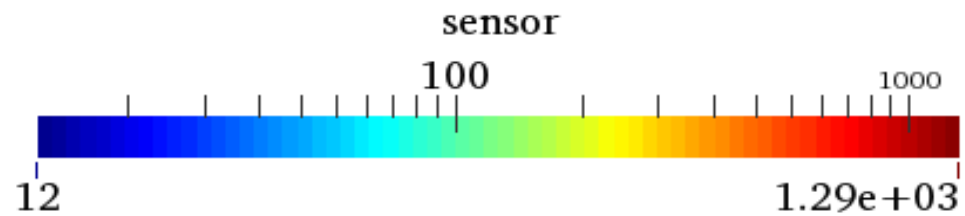




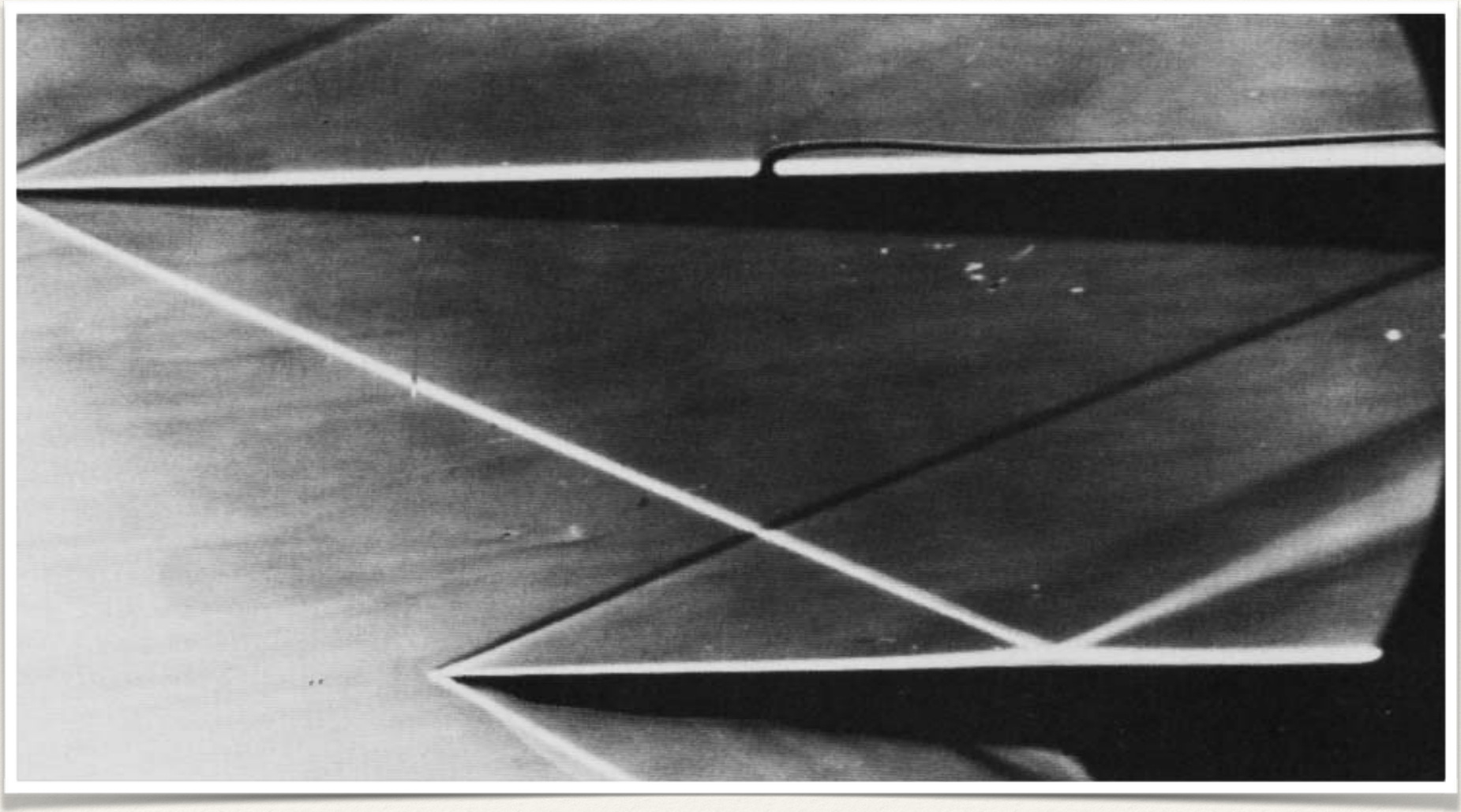
T = 4



T = 4

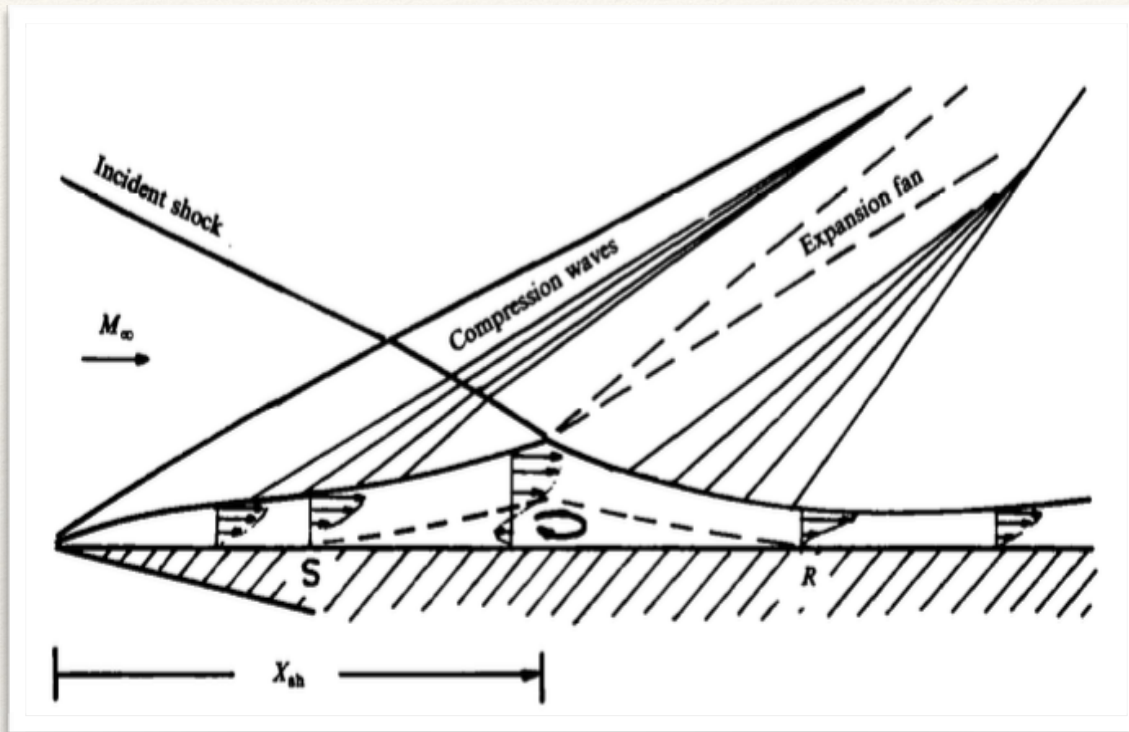


Shock Wave-Boundary Layer Interaction



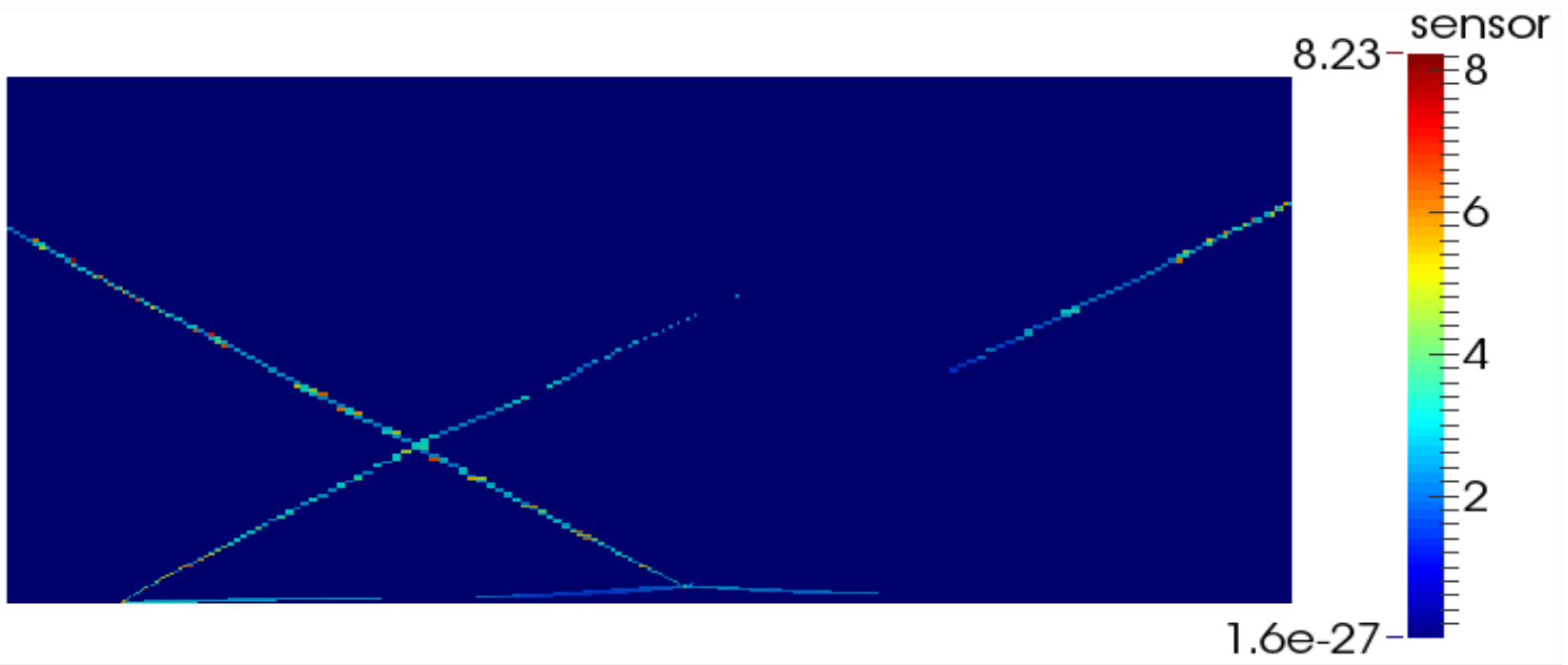
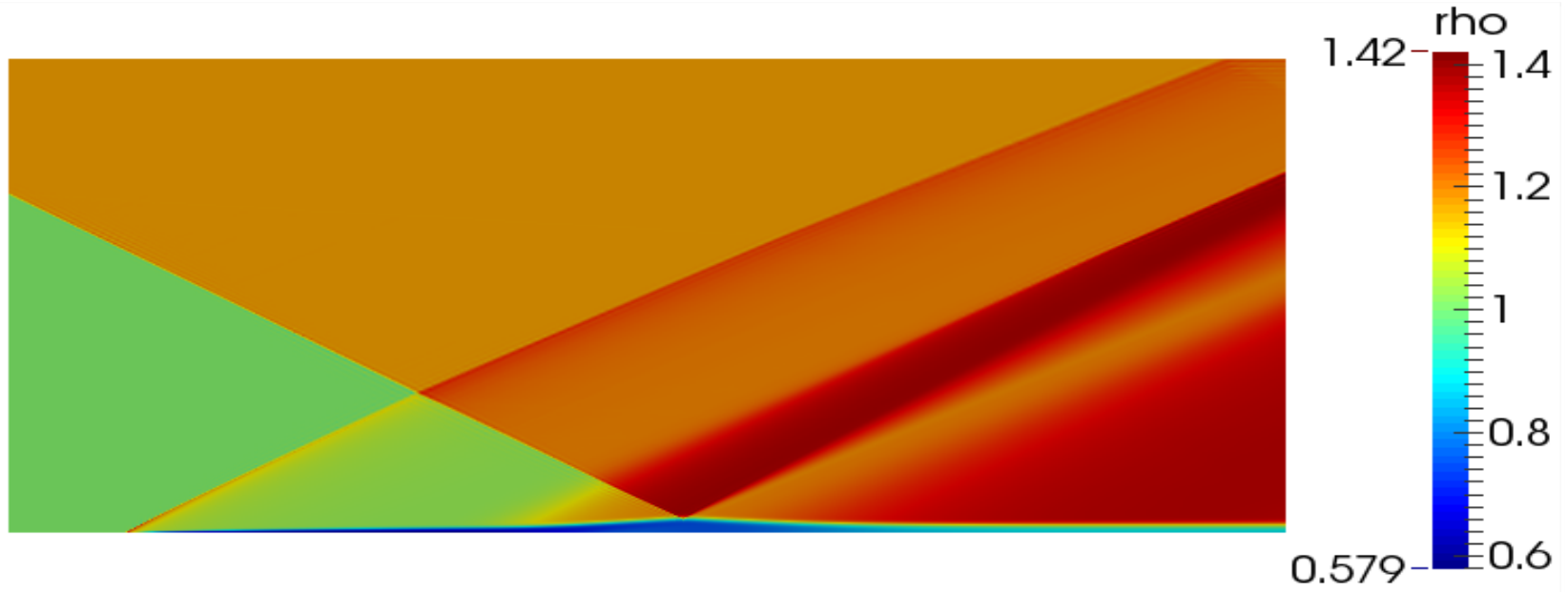
Reference: Degrez et al., JFM, 1987

Shock Wave-Boundary Layer Interaction

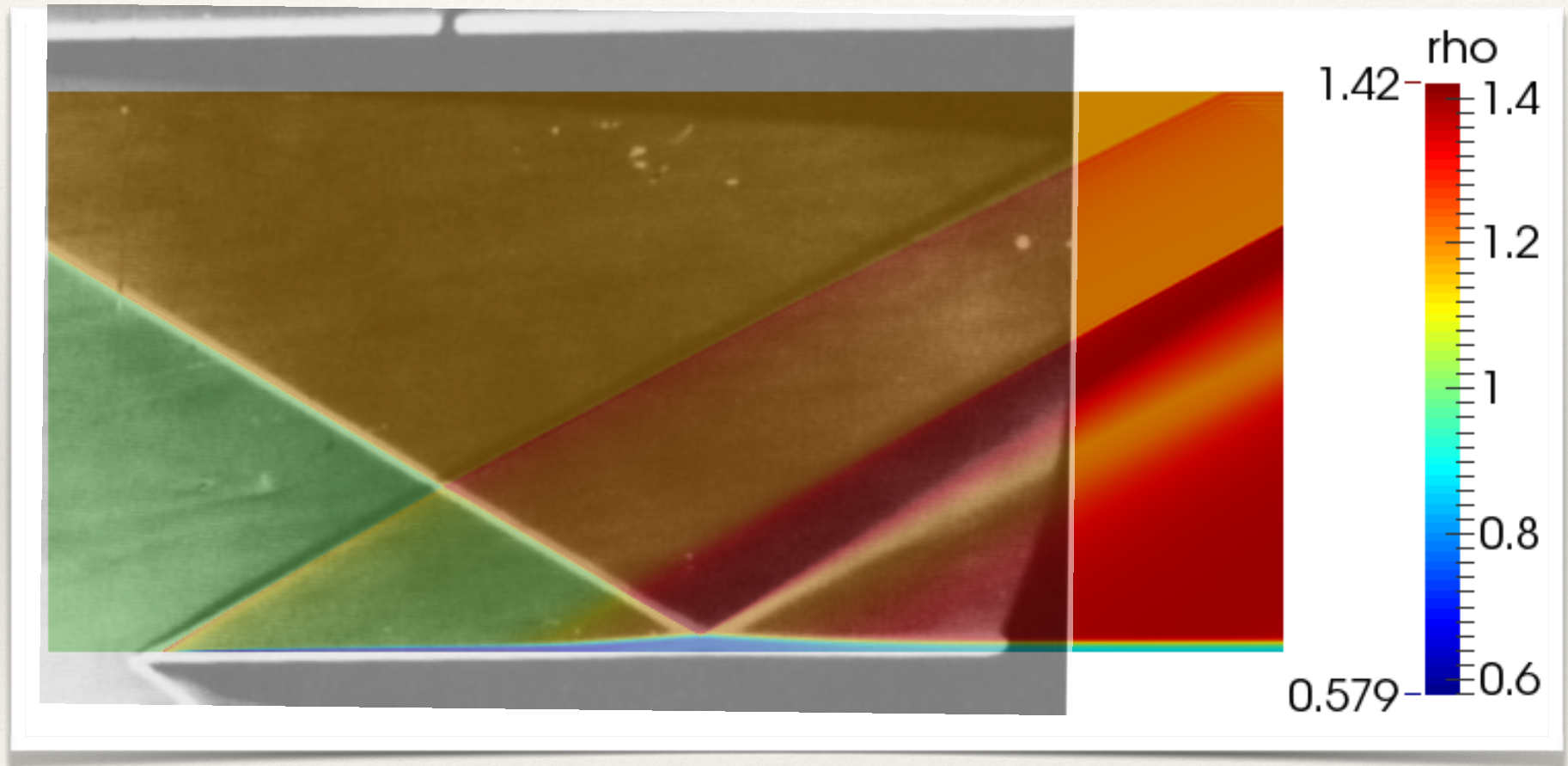


- ❖ Navier Stokes Equations
- ❖ Laminar flow
- ❖ Structured Quad Mesh

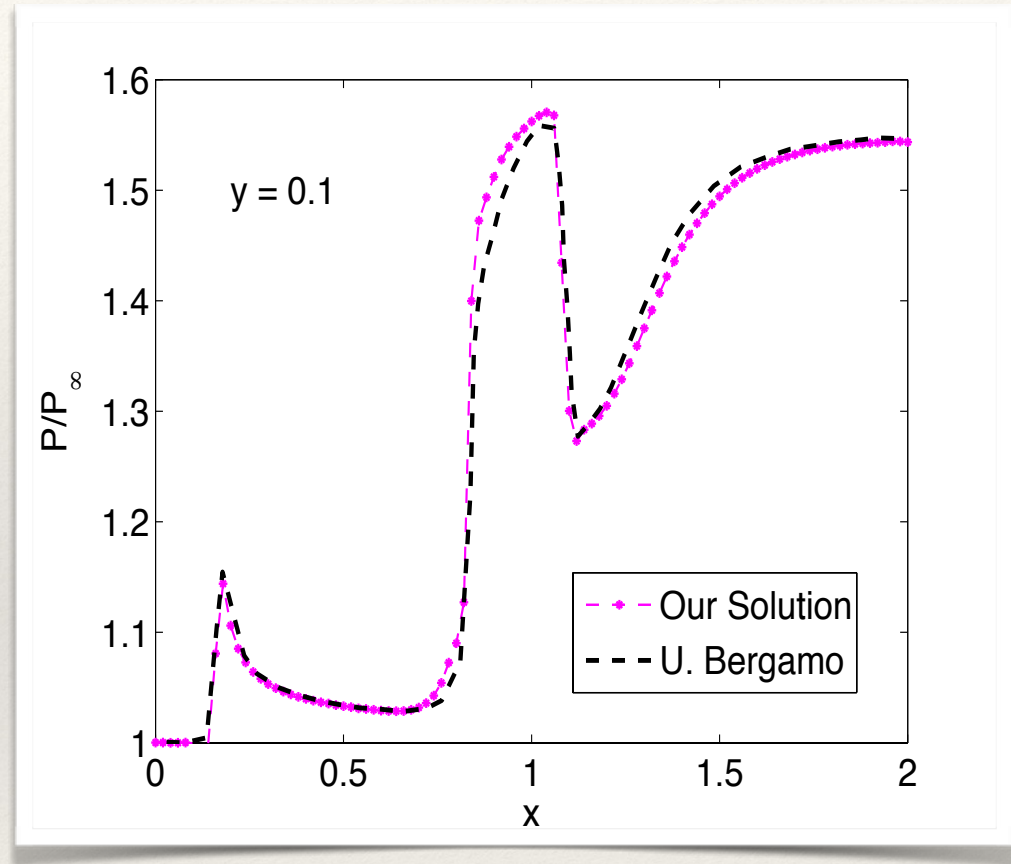
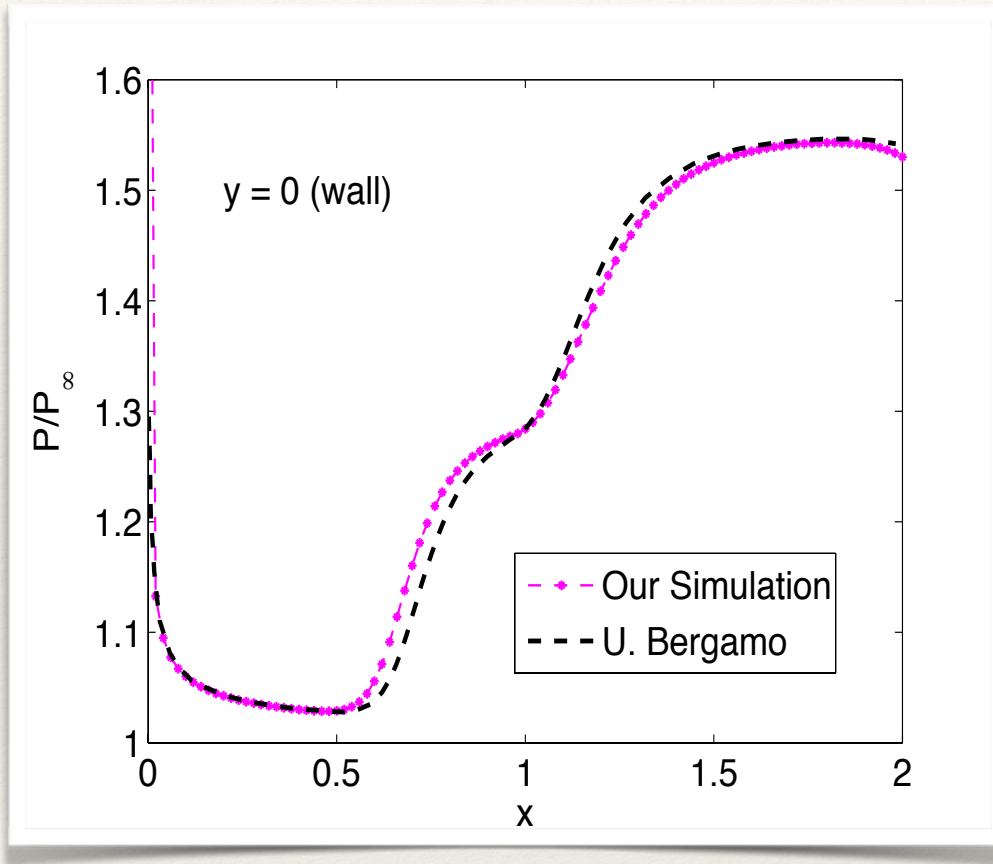
Mach	AoA	Re	Num Elem	Order	Filter Order	Filt Strength
2.15	30.8°	100,000	19,000	3	2	1



Shock Wave-Boundary Layer Interaction

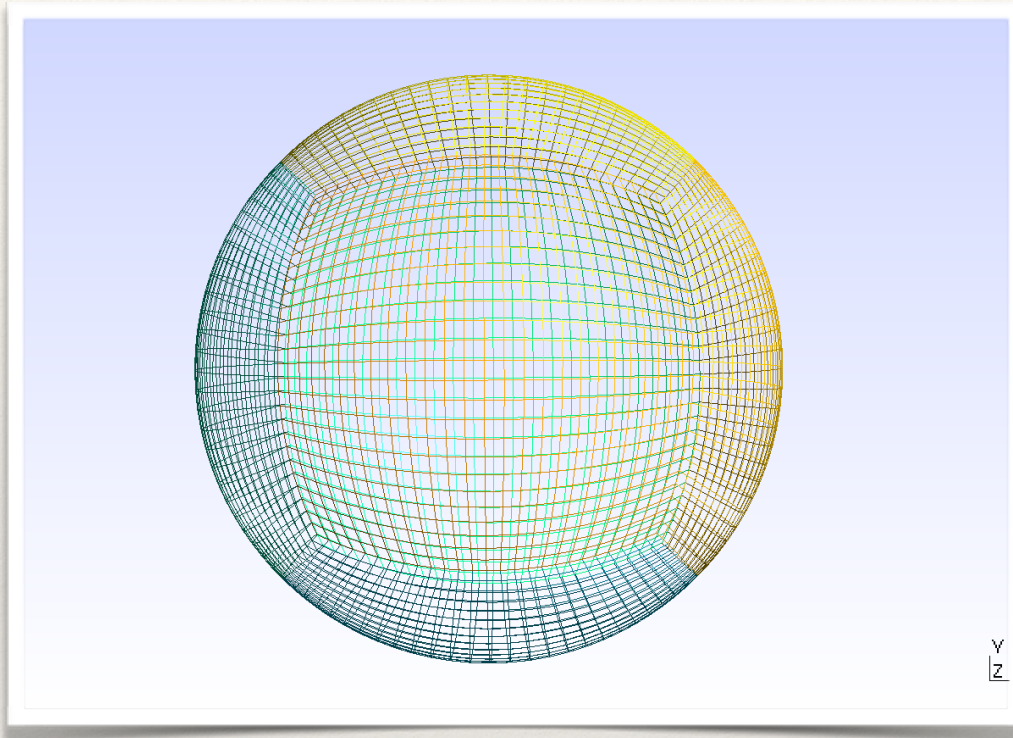


Shock Wave-Boundary Layer Interaction



Reference: 4th Int'l Workshop on High-Order Methods in CFD

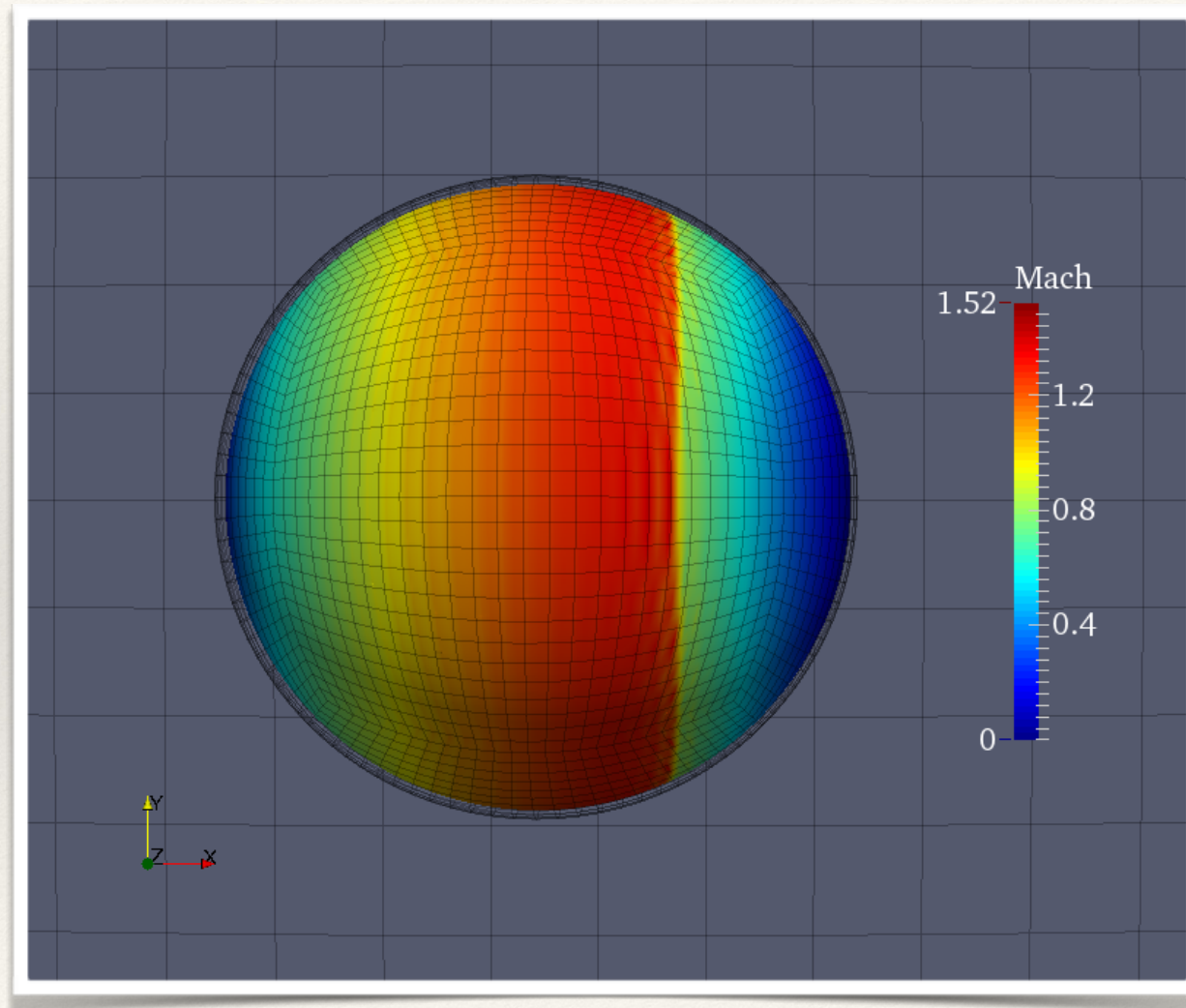
3D Transonic Flow over a sphere



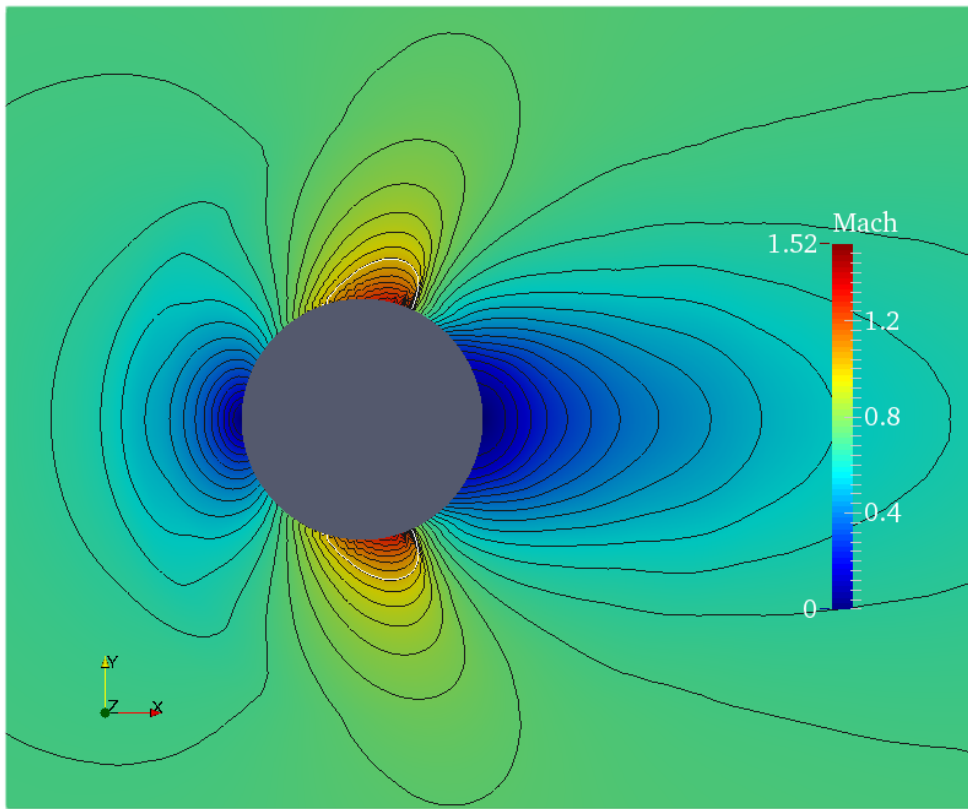
- ❖ Euler Equations
- ❖ Steady State
- ❖ Spherical Domain

Mach	AoA	Num Elem	Order	Filter Order	Filt Strength
0.7	0°	~80,000	3	2	1

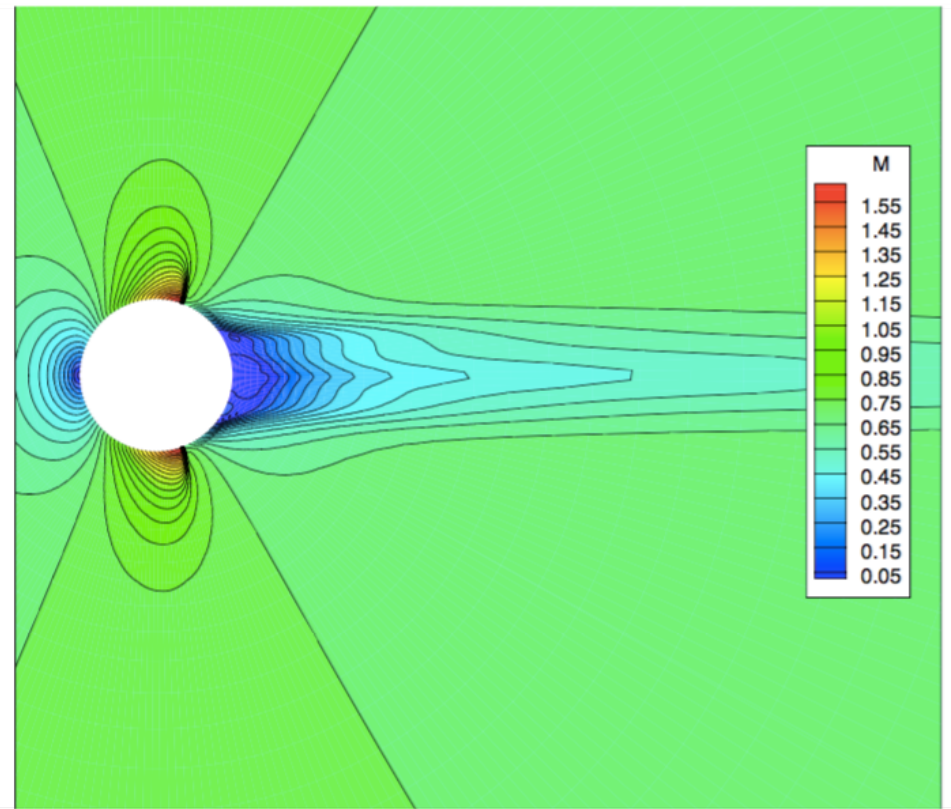
3D Transonic Flow over a sphere



3D Transonic Flow over a sphere



Our Solution



Reference Solution

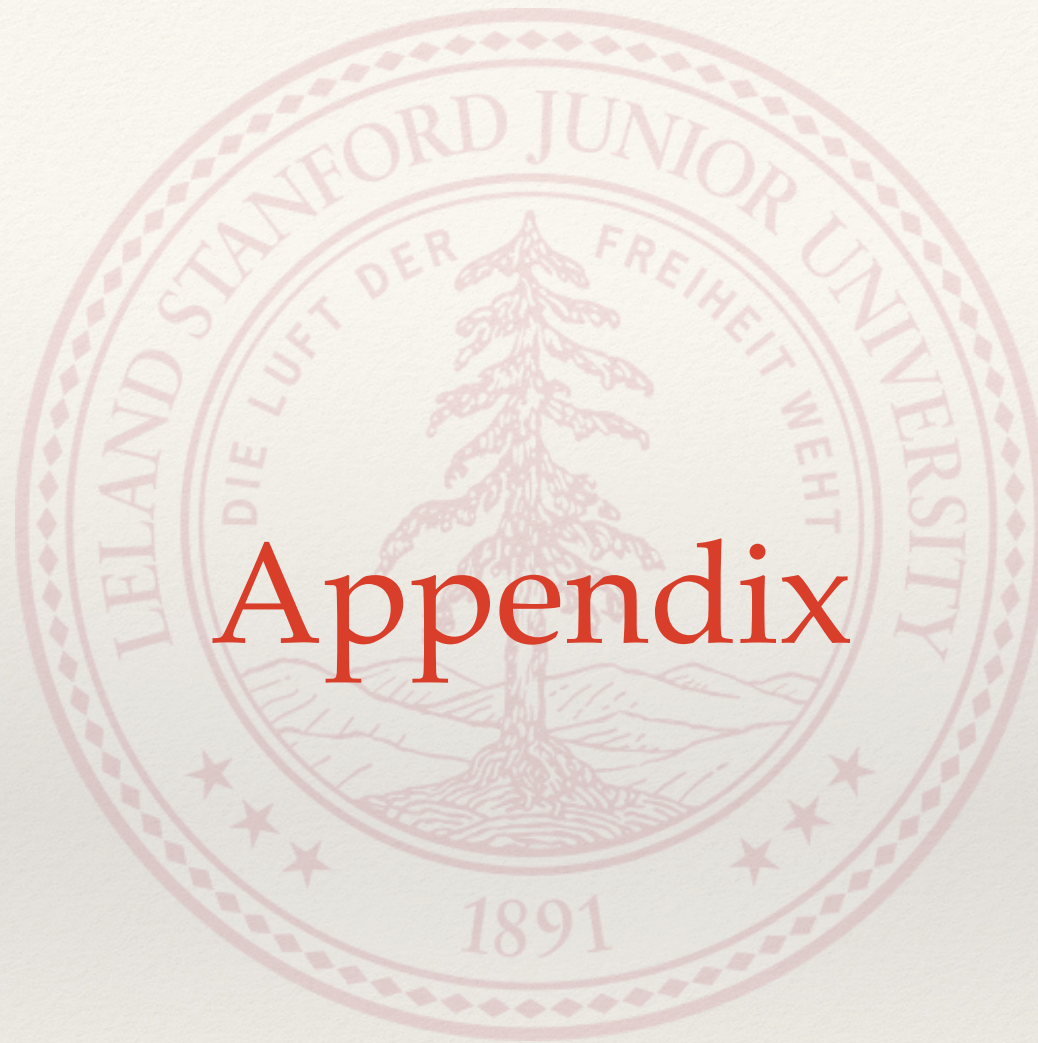
Reference: Karanjkar P, UoF

Summary

- ❖ Novel approach for shock detection
- ❖ Efficient and Robust shock capturing strategy
 - ❖ Minimizes Parameter fine-tuning
 - ❖ Aliasing, Convergence Acceleration, Mesh Adaptation
 - ❖ General - other high-order schemes, PDEs



Thank You
Questions?



Appendix

References

- ❖ F1 image: Pointwise v17 Release picture
- ❖ Lungs: Youbing Yin, U Iowa
 - ❖ http://user.engineering.uiowa.edu/~yoyin/index_files/Research.htm
- ❖ MHD: Vriesema Jess, Uni. of Arizona
 - ❖ Presented at NASA SC14
 - ❖ <http://www.nas.nasa.gov/SC14/demos/demo28.html>

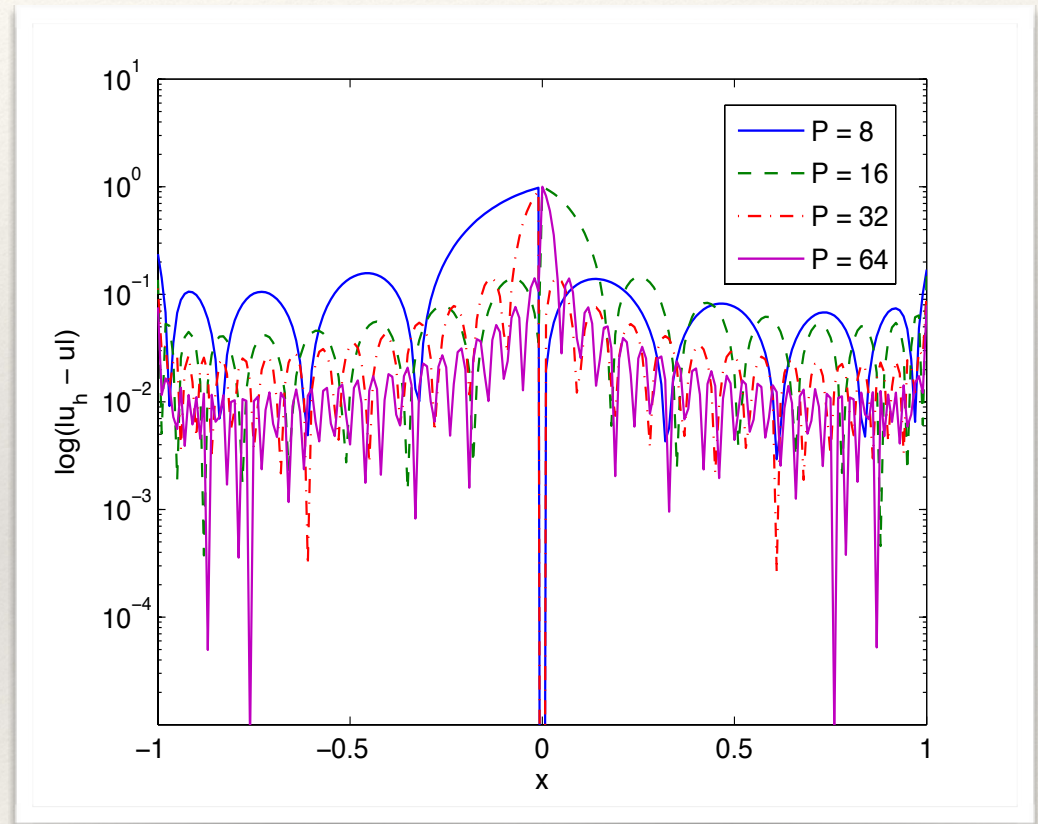
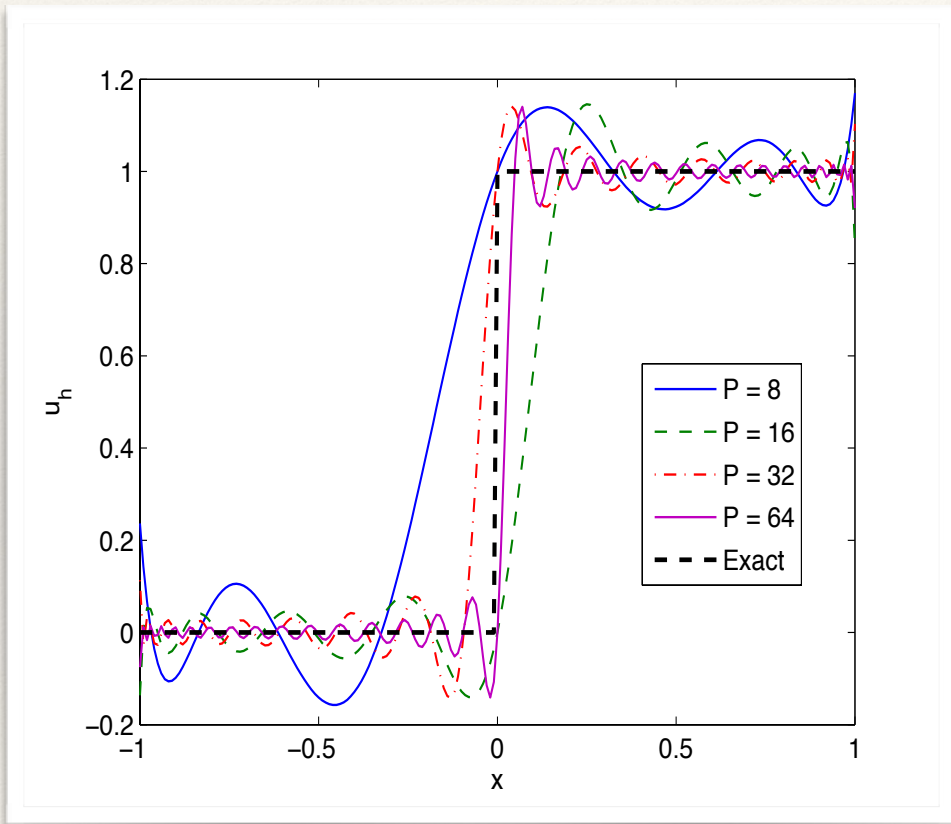
Details of pyFR vs STARCCM+

- ❖ DNS of Taylor Green:
 - ❖ Re 1600, Ma = 0.1, Run until $t = 20t_c$; Figure at $15t_c$
 - ❖ 256^3 hexahedral elements for STARCCM+
 - ❖ Show results are with pyFR P 8 scheme ($29^3 = 261^3$ DOF)
- ❖ Circular Cylinder:
 - ❖ Re 3900, Ma = 0.2
 - ❖ ~ 13.5 million DOFs for both; pyFR used P 4
 - ❖ pyFR - implicit LES; STAR - WALE SGS Subgrid scale model
 - ❖ Similar phases in the vortex shedding cycle

Insights Gained

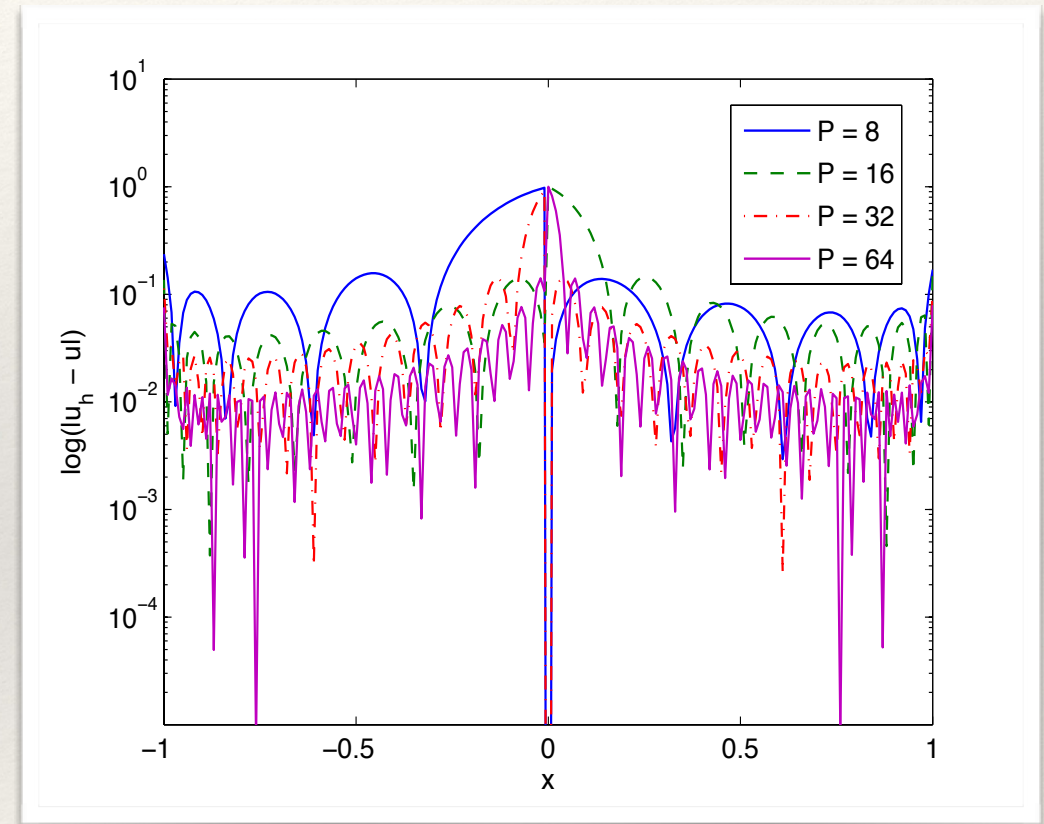
- ❖ Vincent et al. considered a spatially varying flux wherein the DG case develops aliasing instabilities (case from Hesthaven and Warburton).
- ❖ For such a case, with central flux, DG blows up, but c-scheme blows up at an earlier time. SD and G2 don't blow up.

Discontinuous Solutions



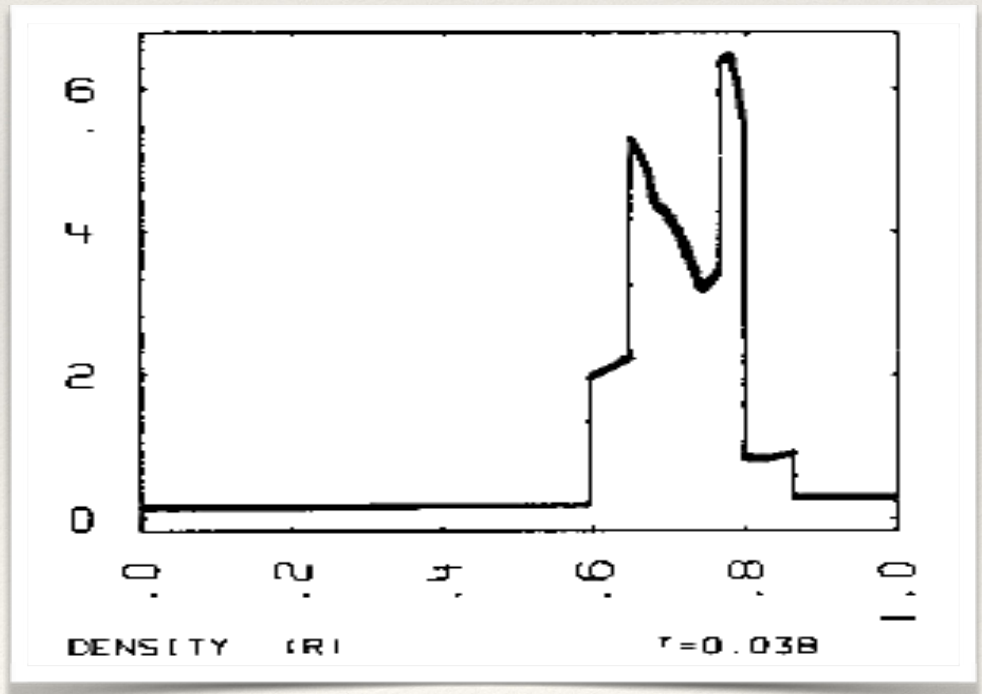
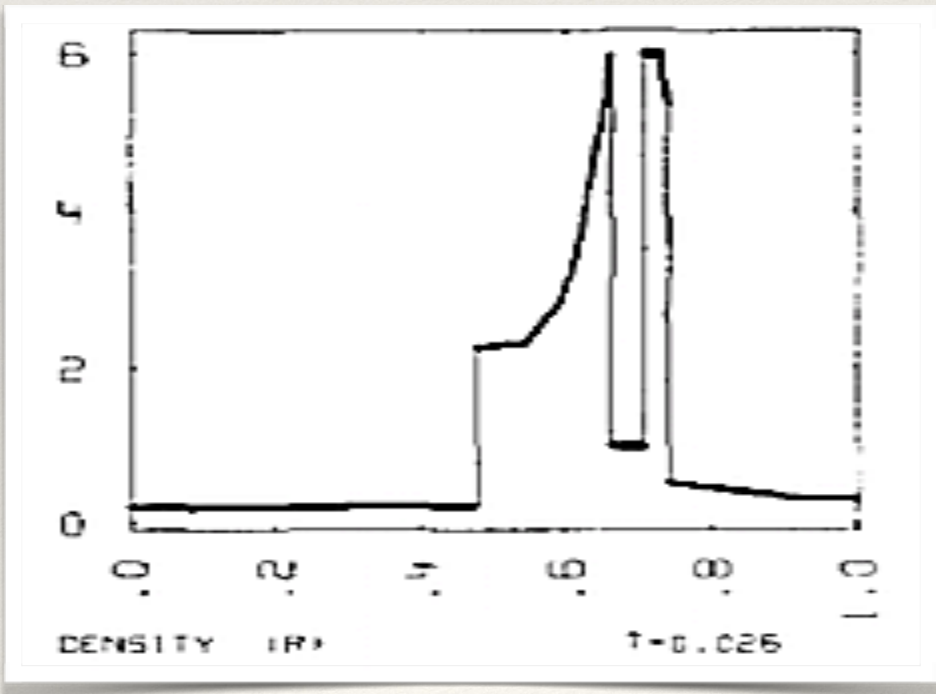
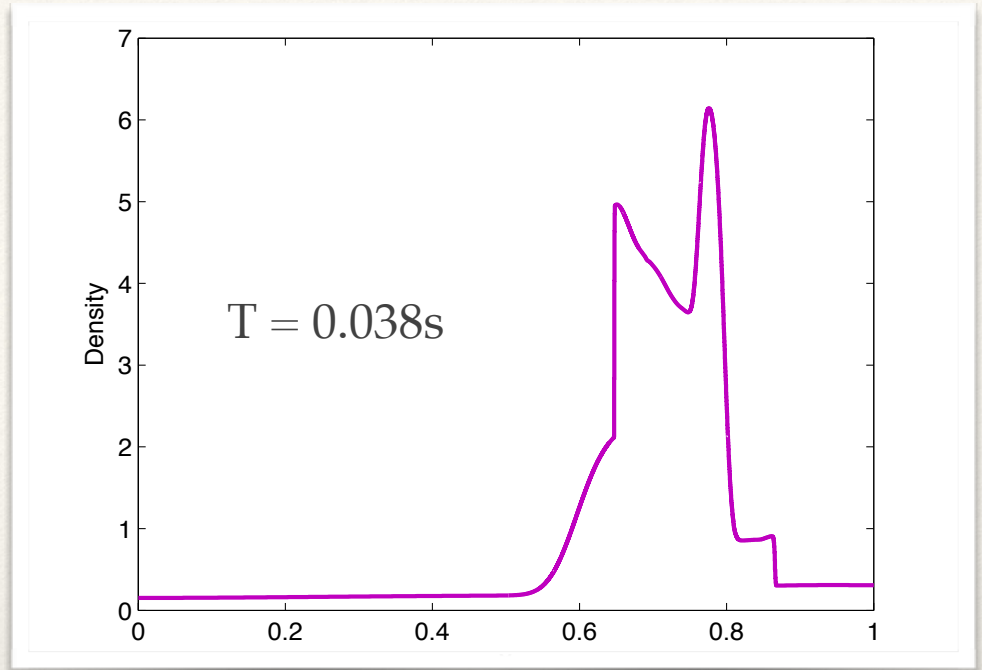
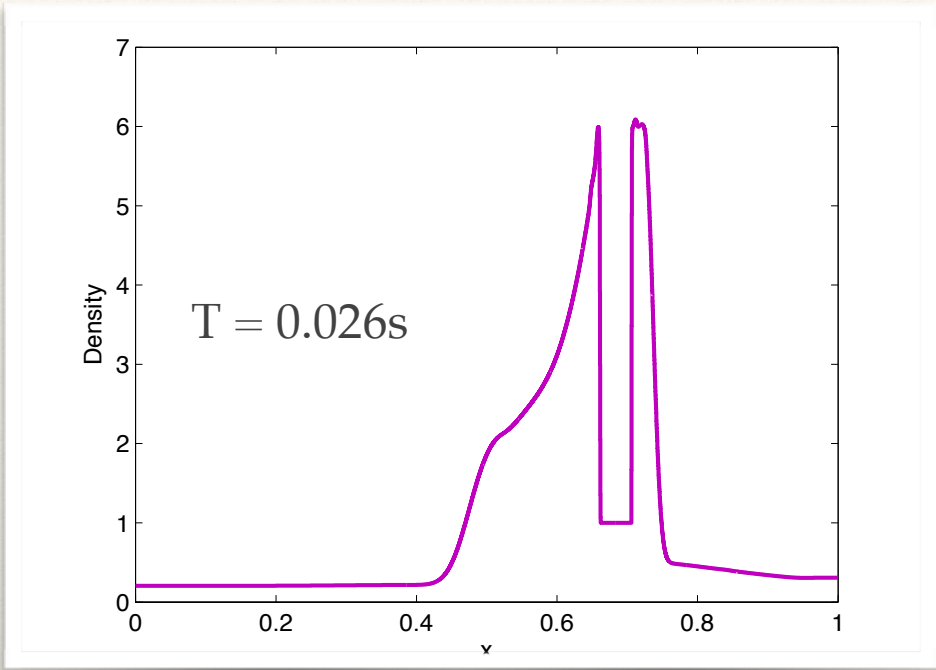
Discontinuous Solutions

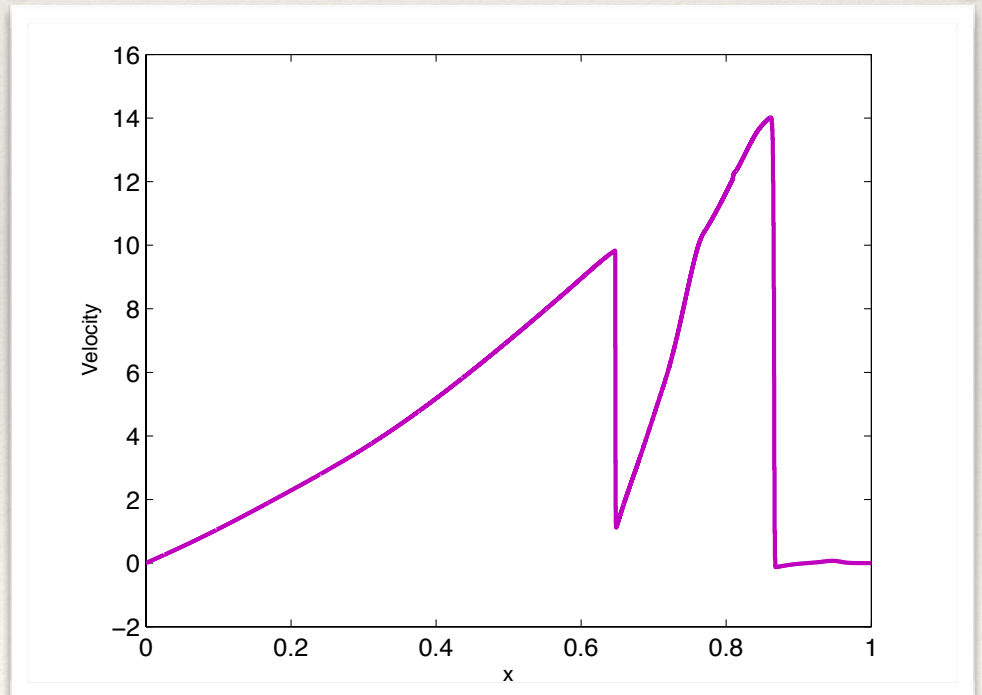
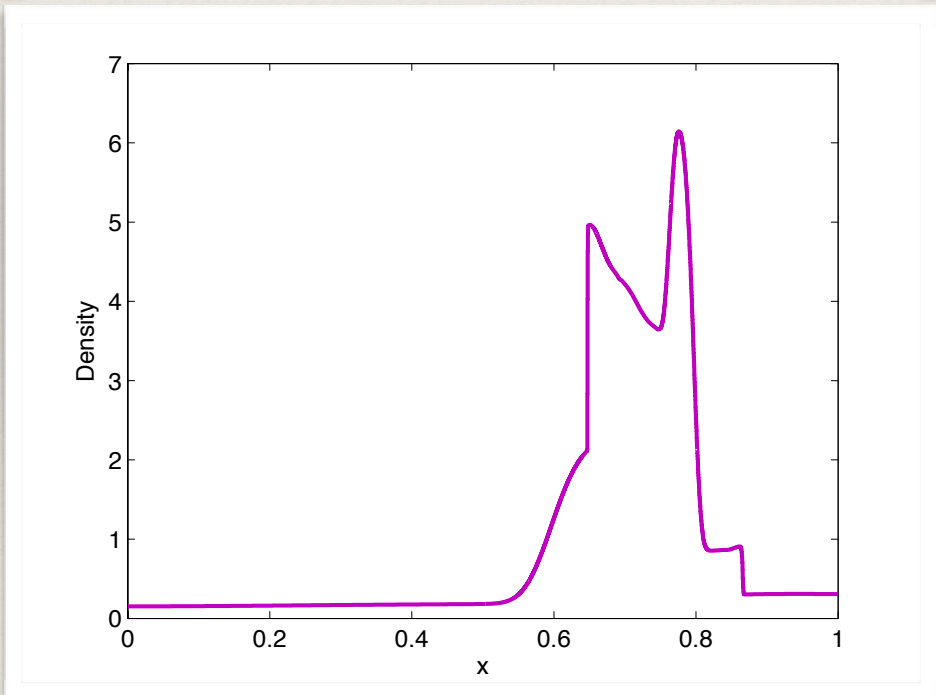
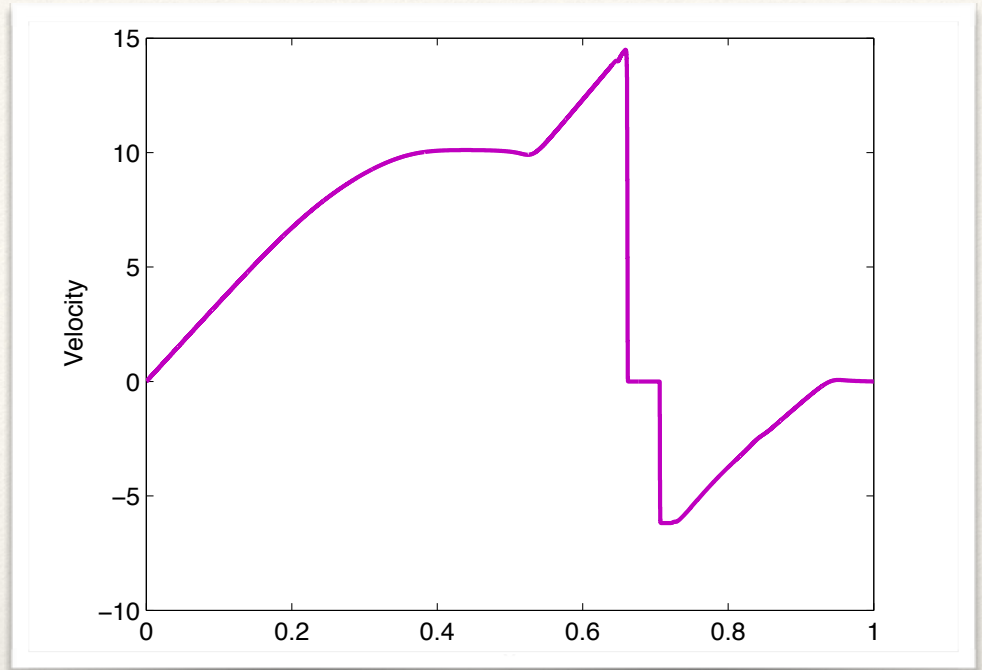
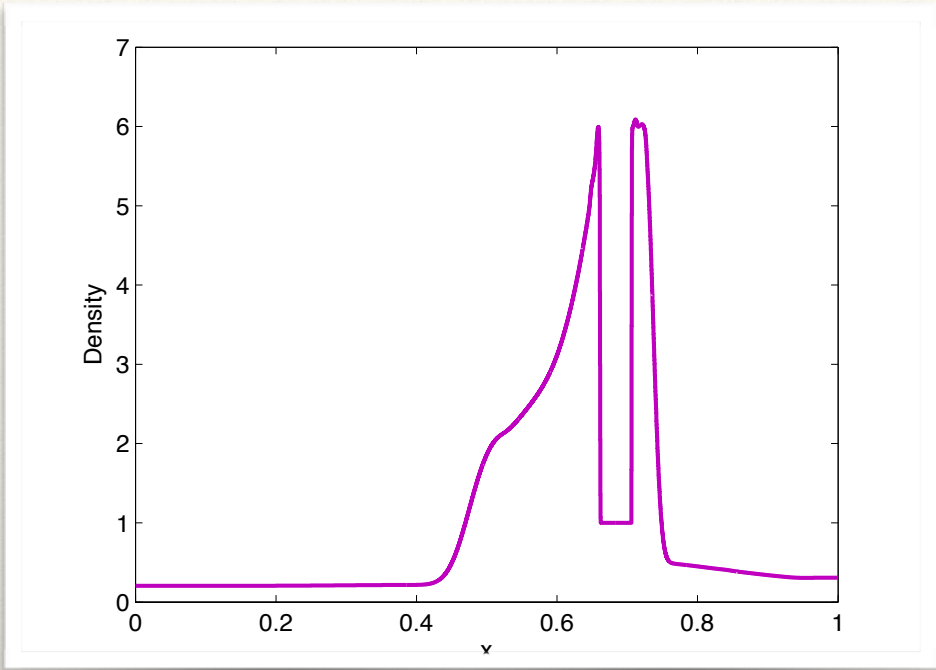
- ❖ Loss of pointwise convergence at the shock
- ❖ Reduction to first order accuracy away from shock
- ❖ Persistent Oscillations

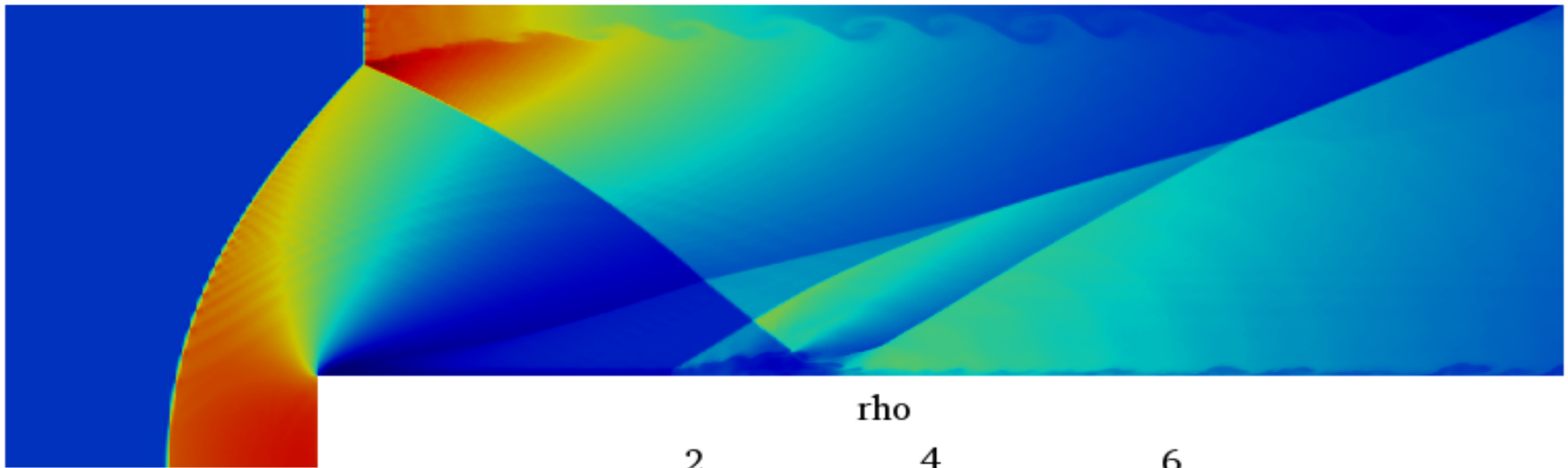


Notes on DFT / Fourier coeffs

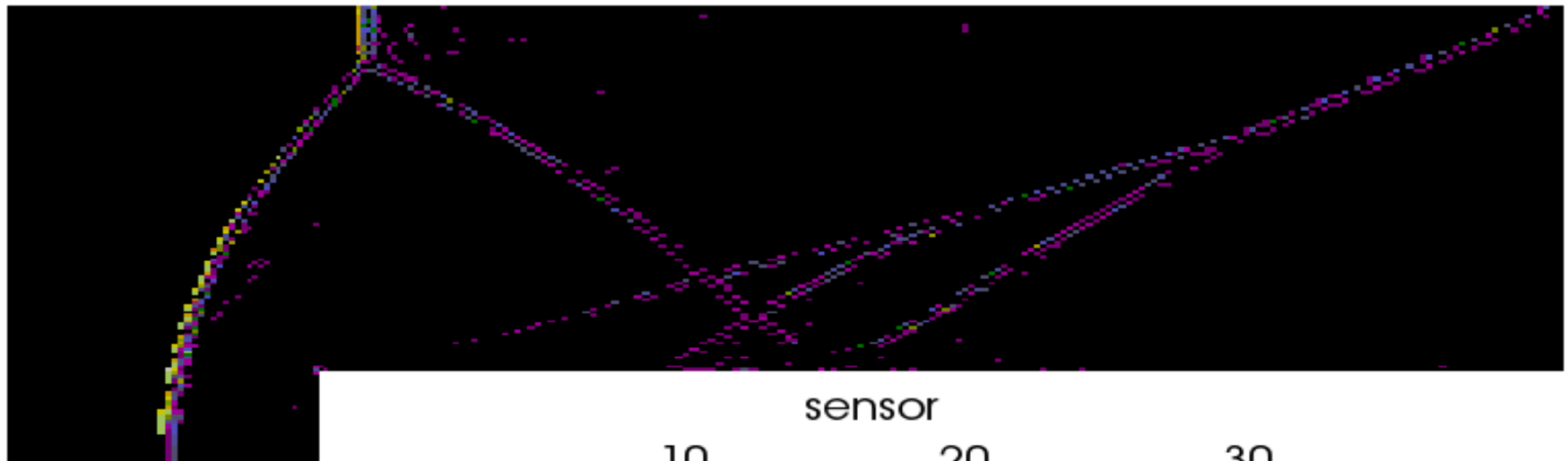
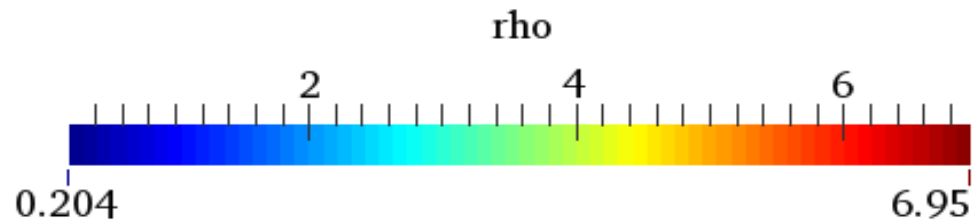
- ❖ DFT can be applied on any non-periodic function - The DFT will be equivalent to the Fourier coefficients of the N -periodic continuation of the non-periodic function.
- ❖ Non-uniform DFT (NDFT) also uses some polynomial interpolation (Lagrange or Newton), so it is more natural to just use the polynomial version
- ❖ If f is C^k , the decay rate is $1/n^k$. But if the $k+1$ derivative is piecewise continuous, the decay rate is $1/n^{k+1}$



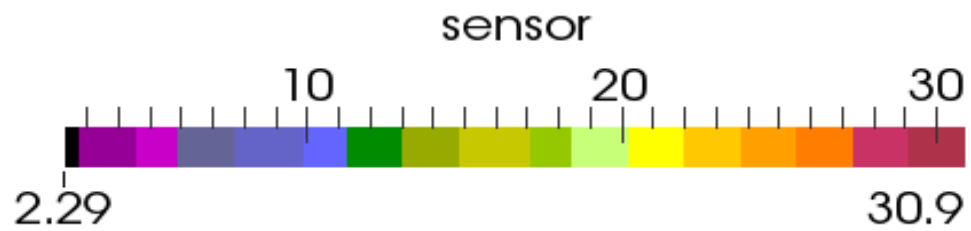




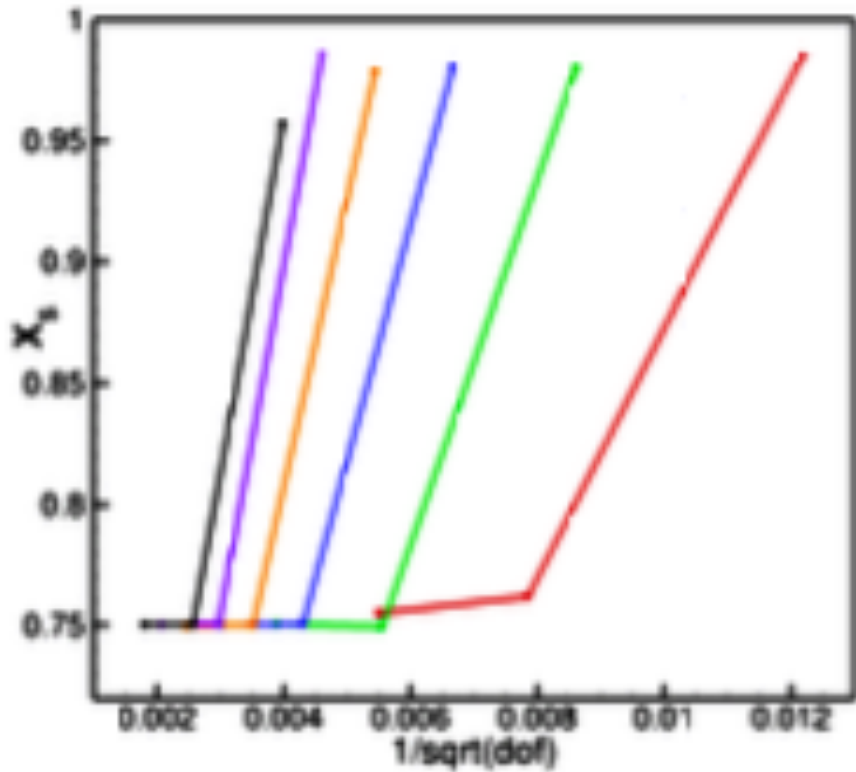
T = 2.5



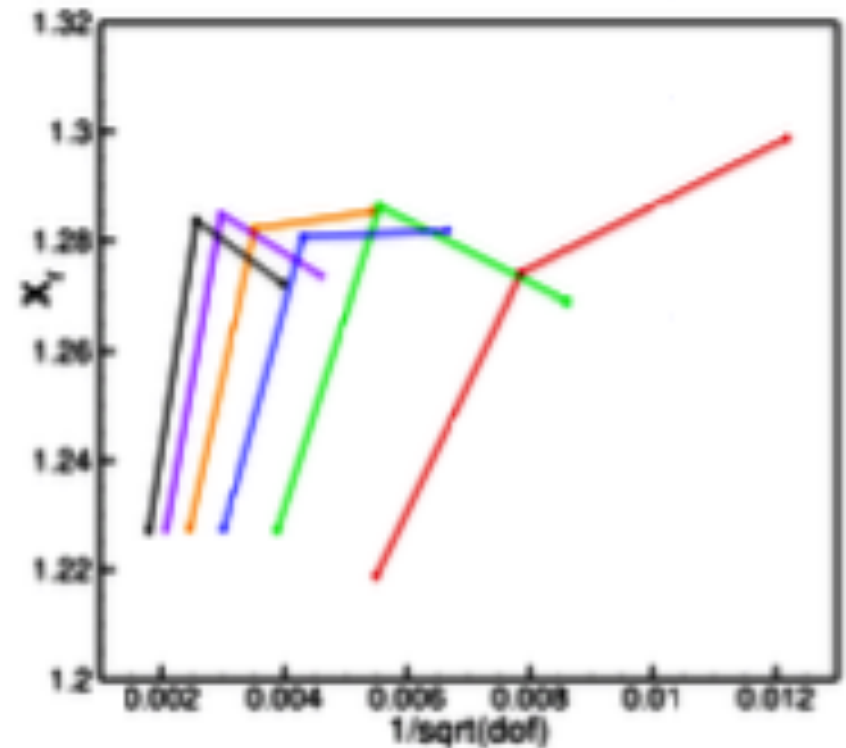
T = 2.5



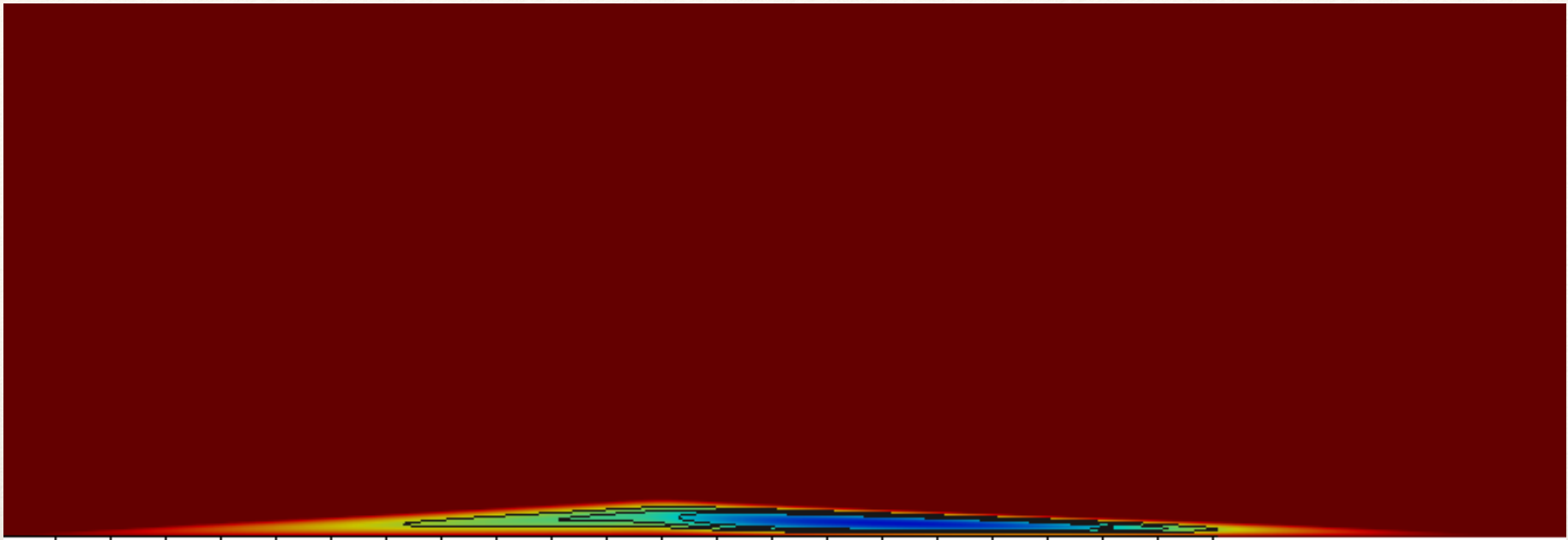
Shock Wave-Boundary Layer Interaction



Separation Point

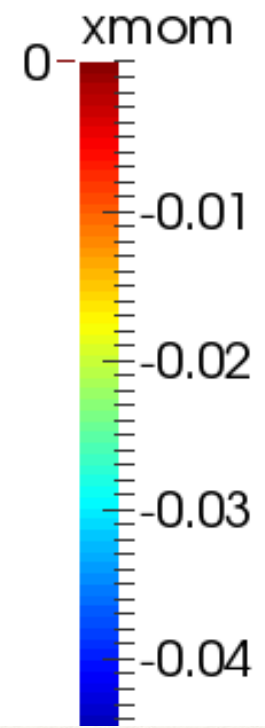


Reattachment Point

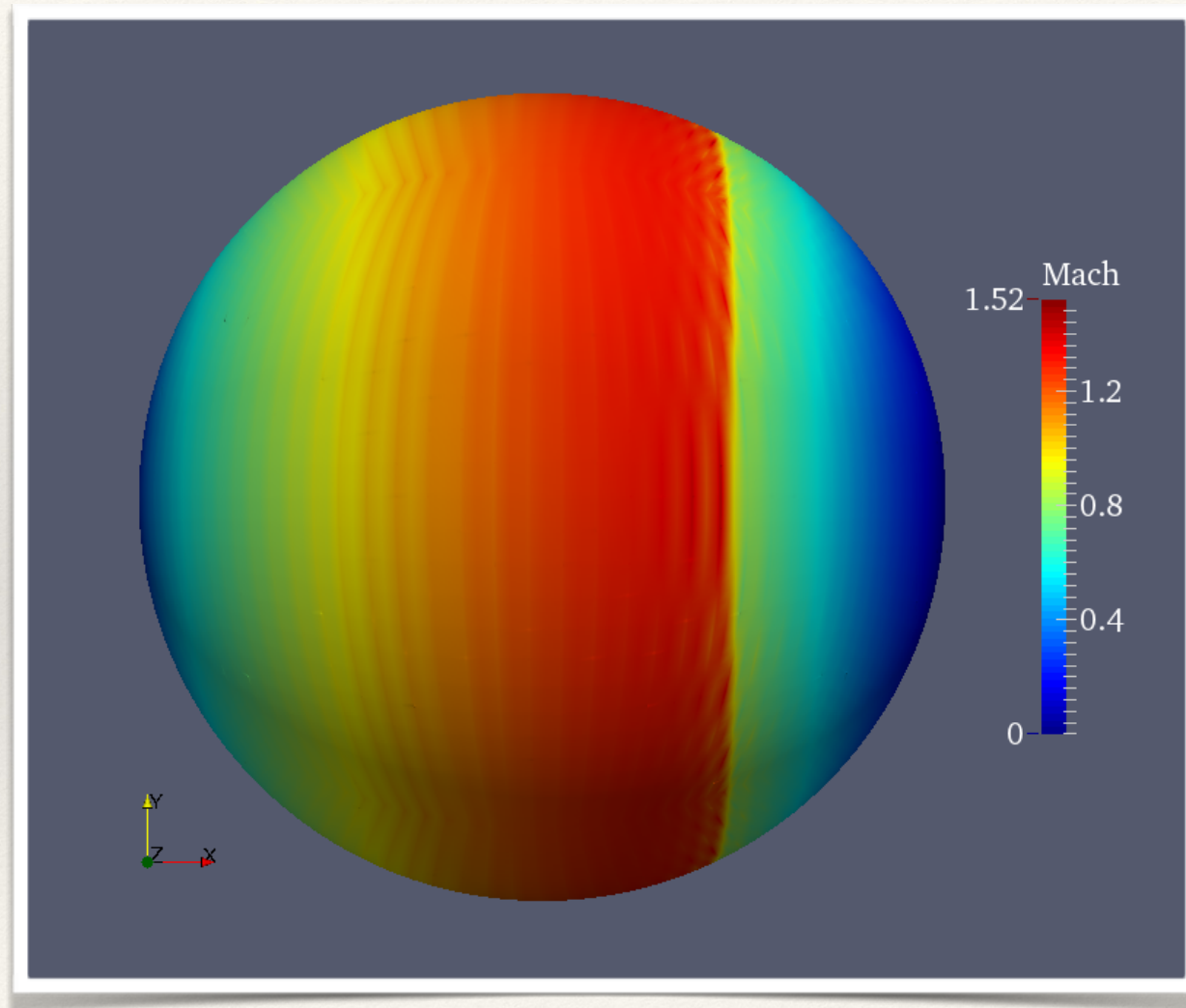


0.8

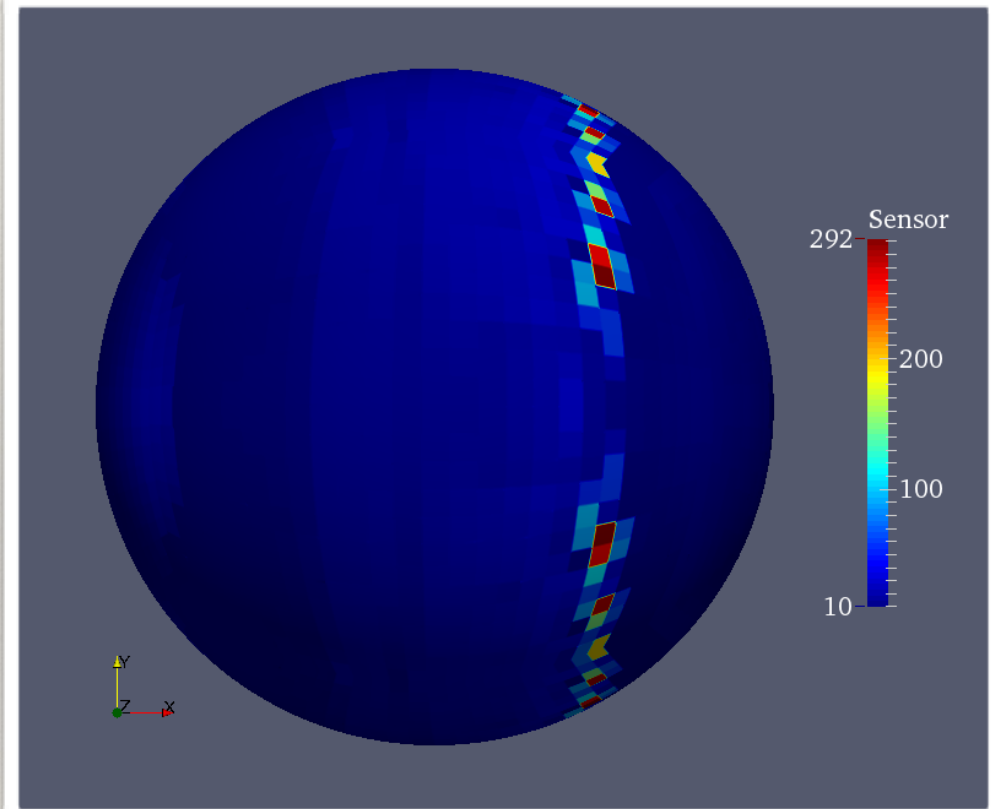
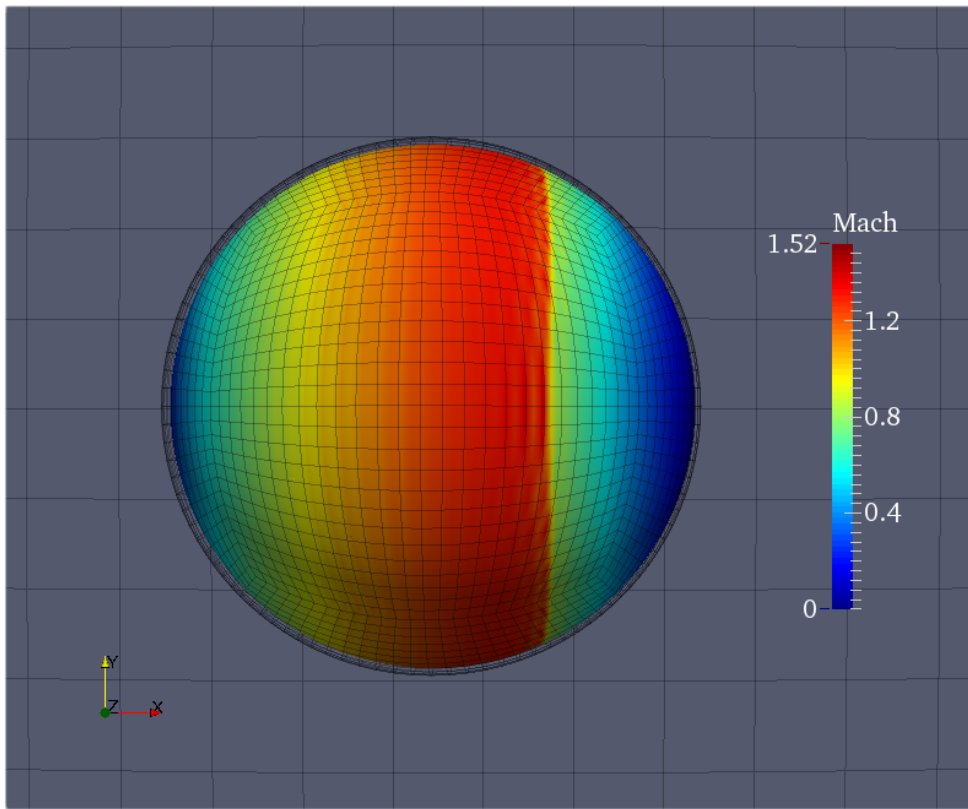
1.0



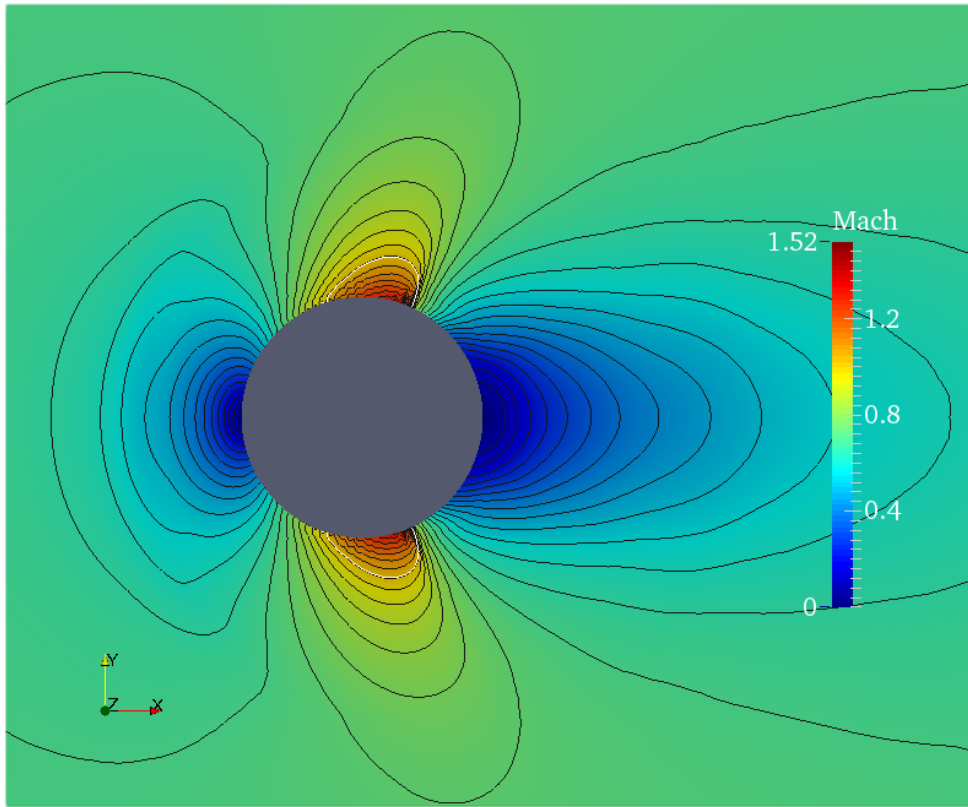
3D Transonic Flow over a sphere



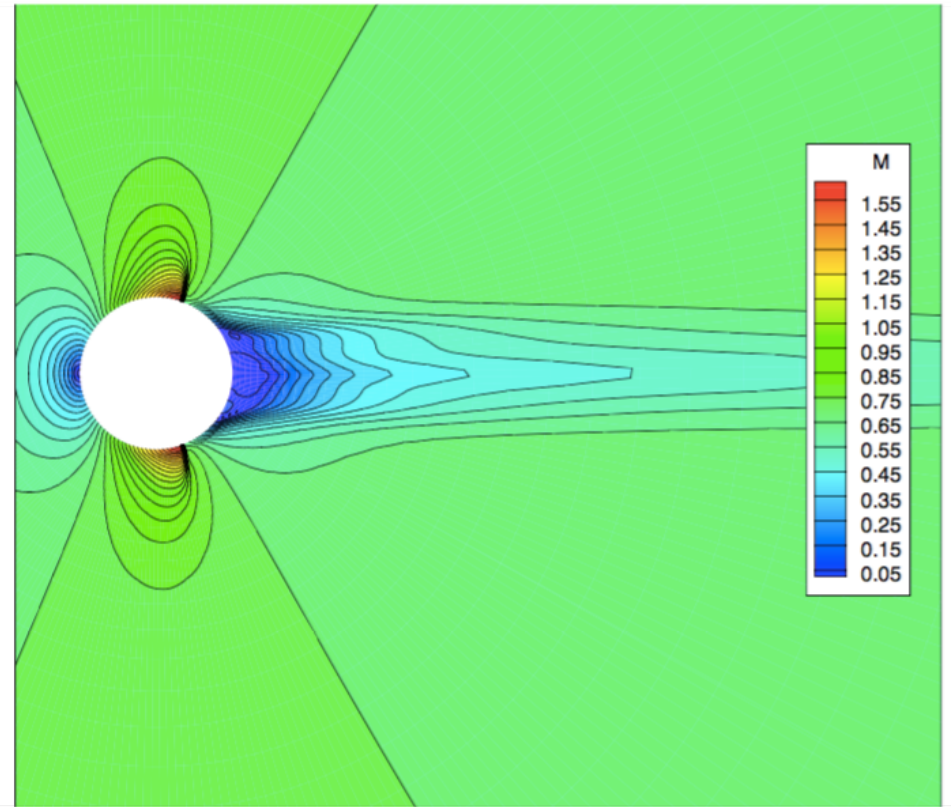
3D Transonic Flow over a sphere



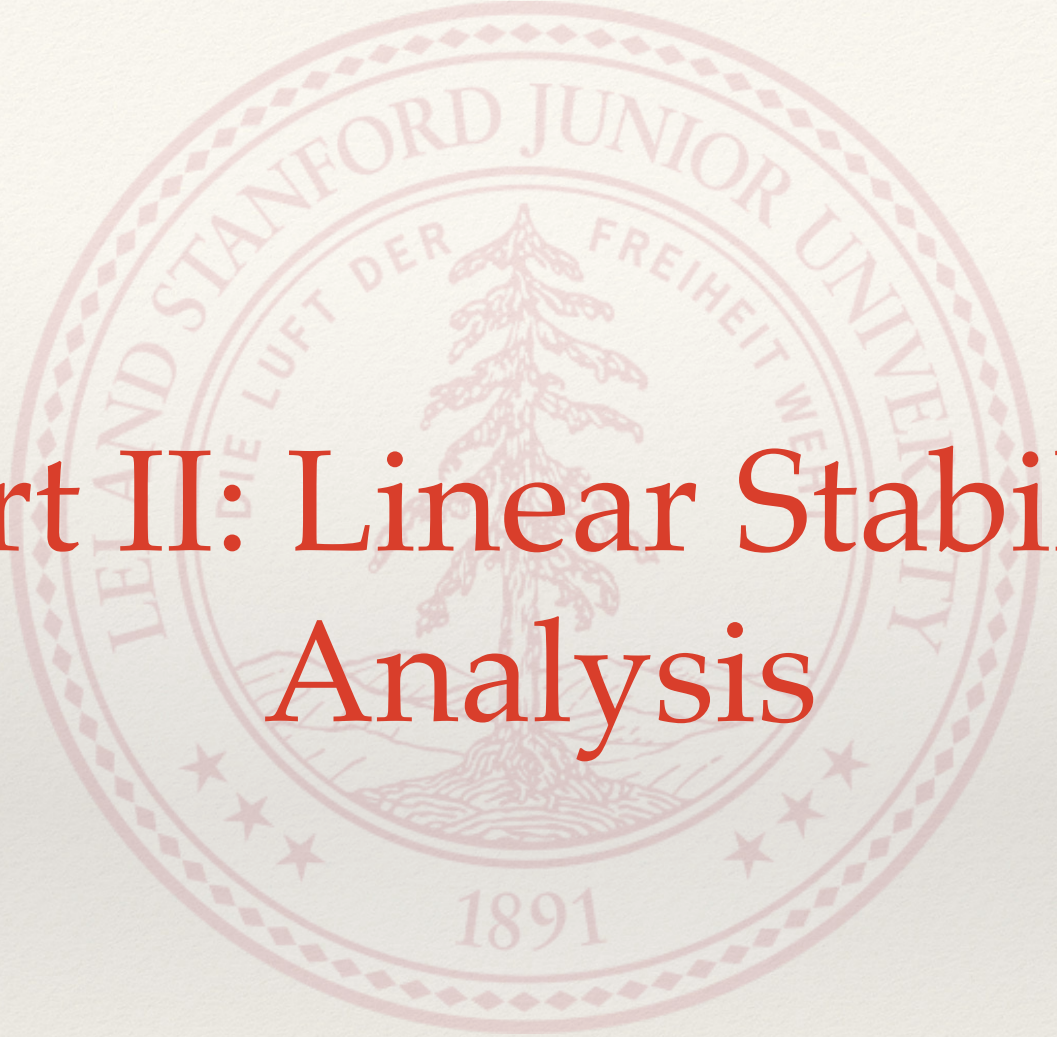
3D Transonic Flow over a sphere



Angle 114 degrees



Angle 111.7 degrees

The background features a large, faint watermark of the Stanford University seal. The seal is circular and contains the text "LELAND STANFORD JUNIOR UNIVERSITY" around the top edge. Inside the seal, there is a tree and the motto "DIE LUFT DER FREIHEIT WEHT". The year "1891" is at the bottom of the seal.

Part II: Linear Stability Analysis

Background

- ❖ FR approach - proposed by Huynh in 2007 & 2009
- ❖ VCJH correction functions - stable family of FR schemes in 1D
- ❖ Extended to triangles and tetrahedra

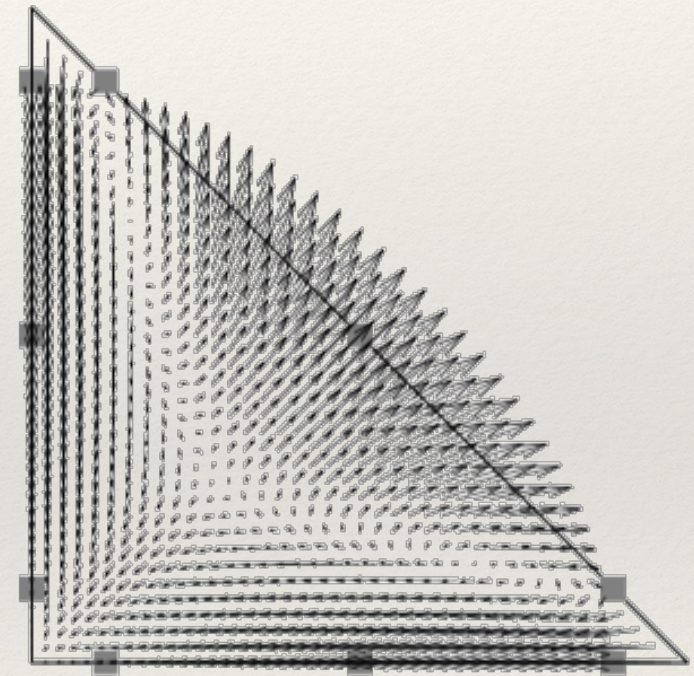


Image Courtesy: PhD Thesis, Williams D. M.

Tensor Product Elements

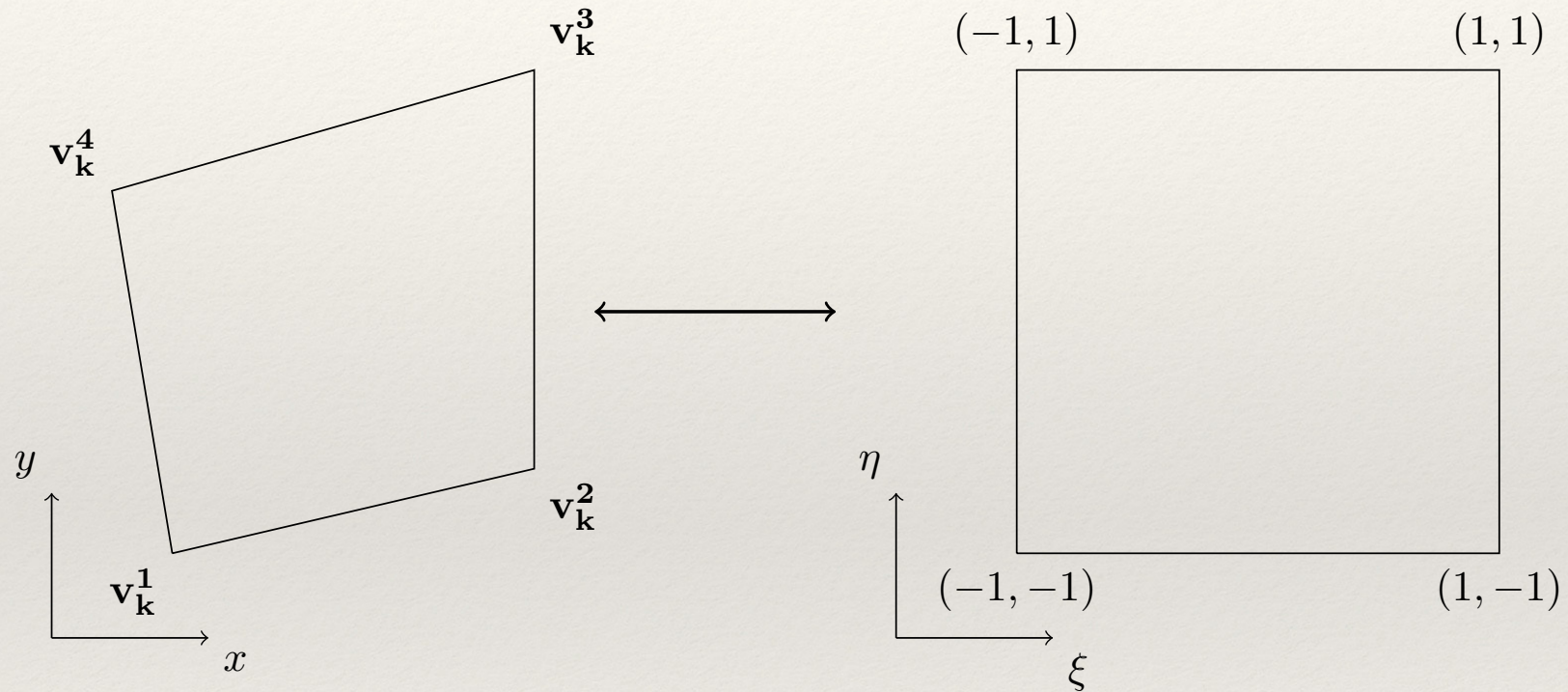
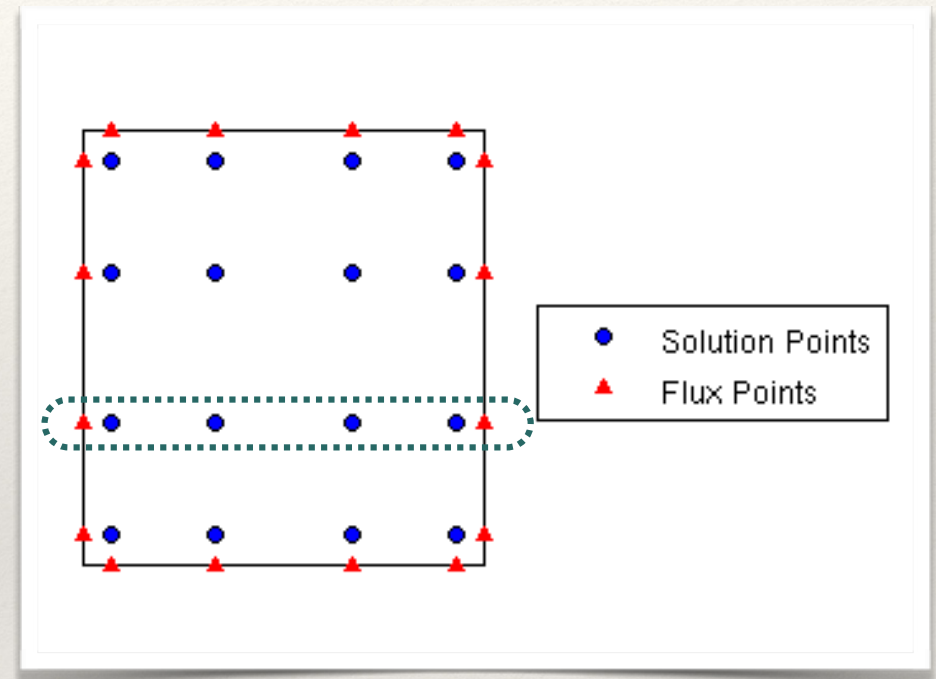


Figure 1: Transformation from physical to reference domain

Tensor Product Elements

- ❖ Simple Extension of 1D
- ❖ Normal continuity



But is this stable?

1st Difficulty

- Consider flux representation in 1D vs 2D:

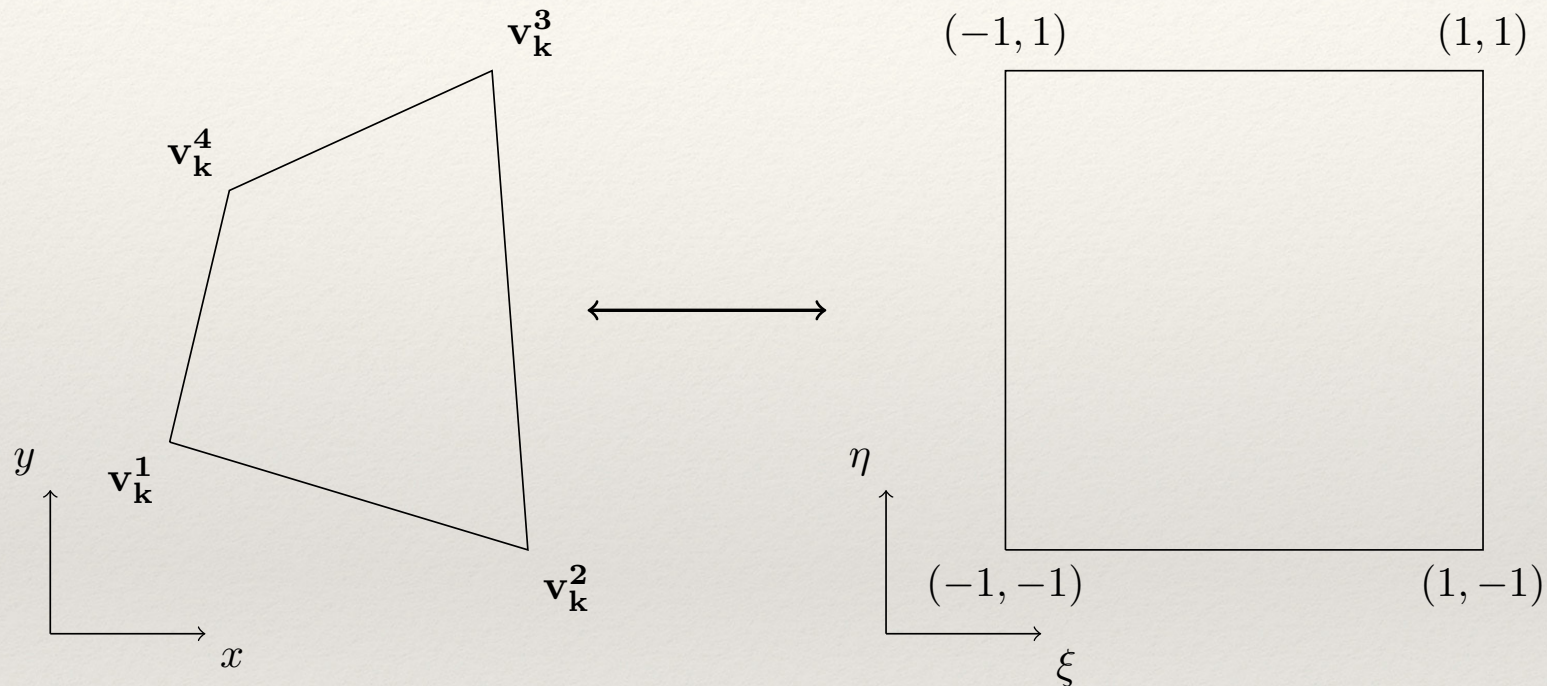
$$\hat{f}^D = \sum_{i=0}^P l_i(\xi) \hat{f}_i^D \quad vs. \quad \hat{\mathbf{f}}^D = \sum_{i=0}^p \sum_{j=0}^p l_i(\xi) l_j(\eta) \hat{\mathbf{f}}_{ij}^D$$

- Now consider taking p^{th} derivative of the conservation law:

$$\frac{\partial \hat{u}_k^D}{\partial t} = \left[-\hat{\nabla} \cdot \hat{\mathbf{f}}_k^D \right] - \hat{\nabla} \cdot \hat{\mathbf{f}}_k^C$$

Does not vanish :(

2nd Difficulty



Jacobian not constant inside an element, even for straight-sided elements

2D Linear Advection Equation

- Consider the 2D conservation law on a periodic domain

$$\frac{\partial u}{\partial t} + \nabla \cdot \mathbf{f} = 0 \quad \text{in } \Omega ,$$

- \mathbf{f} is a linear flux of the form

$$\mathbf{f} = \mathbf{a}u \quad \text{with} \quad \mathbf{f} = \begin{pmatrix} F \\ G \end{pmatrix} \quad \text{and} \quad \mathbf{a} = \begin{pmatrix} a \\ b \end{pmatrix} .$$

- We want to show that a certain suitable norm of the solution is non-increasing

Proof of Stability

Lemma 1.

$$\begin{aligned}
 \frac{1}{2} \frac{d}{dt} \int_{\Omega_k} J_k (u_k^D)^2 d\Omega_k &= - \int_{\Omega_S} \hat{u}^D (\hat{\nabla} \cdot \hat{\mathbf{f}}^D) d\Omega_S - \int_{\Gamma_S} \hat{u}^D (\hat{\mathbf{f}}^C \cdot \hat{\mathbf{n}}) d\Gamma_S \\
 &\quad - c \underbrace{\int_{-1}^1 \frac{d^{p+1} h_L(\xi)}{d\xi^{p+1}} \frac{\partial^p \hat{u}^D}{\partial \xi^p} \left(\sum_{j=0}^p \Delta_{L_j} l_j(\eta) \right) d\eta}_{A_1} + c \underbrace{\int_{-1}^1 \frac{d^{p+1} h_R(\xi)}{d\xi^{p+1}} \frac{\partial^p \hat{u}^D}{\partial \xi^p} \left(\sum_{j=0}^p \Delta_{R_j} l_j(\eta) \right) d\eta}_{A_2} \\
 &\quad - c \underbrace{\int_{-1}^1 \frac{d^{p+1} h_L(\eta)}{d\eta^{p+1}} \frac{\partial^p \hat{u}^D}{d\eta^p} \left(\sum_{j=0}^p \Delta_{B_j} l_j(\xi) \right) d\xi}_{A_3} + c \underbrace{\int_{-1}^1 \frac{d^{p+1} h_R(\eta)}{d\eta^{p+1}} \frac{\partial^p \hat{u}^D}{d\eta^p} \left(\sum_{j=0}^p \Delta_{T_j} l_j(\xi) \right) d\xi}_{A_4}
 \end{aligned}$$

Proof of Stability

Lemma 2.

$$\begin{aligned}
 \frac{1}{2} \left(\frac{1}{2}\right) \frac{\partial}{\partial t} \int_{\Omega_k} J_k \left(\frac{\partial^p u_k^D}{\partial \xi^p} \right)^2 d\Omega_k &= - \int_{-1}^1 \frac{\partial^p \hat{u}^D}{\partial \xi^p} \frac{\partial^p}{\partial \xi^p} \left(\frac{\partial \hat{G}^D}{\partial \eta} \right) d\eta \\
 &+ \underbrace{\int_{-1}^1 \frac{\partial^p \hat{u}^D}{\partial \xi^p} \frac{d^{p+1} h_L(\xi)}{d\xi^{p+1}} \left(\sum_{j=0}^p \Delta_{L_j} l_j(\eta) \right) d\eta}_{A_1} - \underbrace{\int_{-1}^1 \frac{\partial^p \hat{u}^D}{\partial \xi^p} \frac{d^{p+1} h_R(\xi)}{d\xi^{p+1}} \left(\sum_{j=0}^p \Delta_{R_j} l_j(\eta) \right) d\eta}_{A_2} \\
 &+ \left(\sum_{j=0}^p \Delta_{B_j} \frac{\partial^p l_j(\xi)}{\partial \xi^p} \right) \left(- \frac{\partial^p \hat{u}^D}{\partial \xi^p} \Big|_{\eta=-1} - \underbrace{c \frac{d^{p+1} h_L(\eta)}{d\eta^{p+1}} \frac{\partial^{2p} \hat{u}^D}{\partial \xi^p \partial \eta^p}}_{B_3} \right) \\
 &- \left(\sum_{j=0}^p \Delta_{T_j} \frac{\partial^p l_j(\xi)}{\partial \xi^p} \right) \left(\frac{\partial^p \hat{u}^D}{\partial \xi^p} \Big|_{\eta=1} - \underbrace{c \frac{d^{p+1} h_R(\eta)}{d\eta^{p+1}} \frac{\partial^{2p} \hat{u}^D}{\partial \xi^p \partial \eta^p}}_{B_4} \right)
 \end{aligned}$$

Proof of Stability

Lemma 3.

$$\begin{aligned}
 & \frac{1}{2} \left(\frac{1}{2} \right) \frac{\partial}{\partial t} \int_{\Omega_k} J_k \left(\frac{\partial^p u_k^D}{\partial \eta^p} \right)^2 d\Omega_k = - \int_{-1}^1 \frac{\partial^p \hat{u}^D}{\partial \eta^p} \frac{\partial^p}{\partial \eta^p} \left(\frac{\partial \hat{F}^D}{\partial \xi} \right) d\xi \\
 & + \underbrace{\int_{-1}^1 \frac{\partial^p \hat{u}^D}{\partial \eta^p} \frac{d^{p+1} h_L(\eta)}{d\eta^{p+1}} \left(\sum_{j=0}^p \Delta_{B_j} l_j(\xi) \right) d\xi}_{A_3} - \underbrace{\int_{-1}^1 \frac{\partial^p \hat{u}^D}{\partial \eta^p} \frac{d^{p+1} h_R(\eta)}{d\eta^{p+1}} \left(\sum_{j=0}^p \Delta_{T_j} l_j(\xi) \right) d\xi}_{A_4} \\
 & + \left(\sum_{j=0}^p \Delta_{L_j} \frac{\partial^p l_j(\eta)}{\partial \eta^p} \right) \left(- \frac{\partial^p \hat{u}^D}{\partial \eta^p} \Big|_{\xi=-1} - \underbrace{c \frac{d^{p+1} h_L(\xi)}{d\xi^{p+1}} \frac{\partial^{2p} \hat{u}^D}{\partial \xi^p \partial \eta^p}}_{B_1} \right) \\
 & - \left(\sum_{j=0}^p \Delta_{R_j} \frac{\partial^p l_j(\eta)}{\partial \eta^p} \right) \left(\frac{\partial^p \hat{u}^D}{\partial \eta^p} \Big|_{\xi=1} - \underbrace{c \frac{d^{p+1} h_R(\xi)}{d\xi^{p+1}} \frac{\partial^{2p} \hat{u}^D}{\partial \xi^p \partial \eta^p}}_{B_2} \right)
 \end{aligned}$$

Proof of Stability

Lemma 4.

$$\begin{aligned}
 & \frac{1}{2} \left(\frac{1}{4}\right) \frac{\partial}{\partial t} \int_{\Omega_k} J_k \left(\frac{\partial^{2p} u_k^D}{\partial \xi^p \partial \eta^p} \right)^2 d\Omega_k = \\
 & \underbrace{+ \frac{\partial^{2p} \hat{u}^D}{\partial \xi^p \partial \eta^p} \frac{d^{p+1} h_L(\xi)}{d\xi^{p+1}} \left(\sum_{j=0}^p \Delta_{L_j} \frac{\partial^p l_j(\eta)}{\partial \eta^p} \right)}_{B_1} - \underbrace{\frac{\partial^{2p} \hat{u}^D}{\partial \xi^p \partial \eta^p} \frac{d^{p+1} h_R(\xi)}{d\xi^{p+1}} \left(\sum_{j=0}^p \Delta_{R_j} \frac{\partial^p l_j(\eta)}{\partial \eta^p} \right)}_{B_2} \\
 & \underbrace{+ \frac{\partial^{2p} \hat{u}^D}{\partial \xi^p \partial \eta^p} \frac{d^{p+1} h_L(\eta)}{d\eta^{p+1}} \left(\sum_{j=0}^p \Delta_{B_j} \frac{\partial^p l_j(\xi)}{\partial \xi^p} \right)}_{B_3} - \underbrace{\frac{\partial^{2p} \hat{u}^D}{\partial \xi^p \partial \eta^p} \frac{d^{p+1} h_R(\eta)}{d\eta^{p+1}} \left(\sum_{j=0}^p \Delta_{T_j} \frac{\partial^p l_j(\xi)}{\partial \xi^p} \right)}_{B_4}
 \end{aligned}$$

Proof of Stability

- Combining the lemmas, we get

$$\frac{d}{dt} \|u^D\|_{W_\delta^{2p,2}}^2 = \Theta_{adv} + c\Theta_{extra}$$

- The norm is a broken Sobolev norm defined as

$$\|u^D\|_{W_\delta^{2p,2}}^2 = \sum_{k=1}^N \left(\int_{\Omega_k} \left[(u_k^D)^2 + \frac{c}{2} \left(\left(\frac{\partial^p u_k^D}{\partial \xi^p} \right)^2 + \left(\frac{\partial^p u_k^D}{\partial \eta^p} \right)^2 \right) + \frac{c^2}{4} \left(\frac{\partial^{2p} u_k^D}{\partial \xi^p \partial \eta^p} \right)^2 \right] d\Omega_k \right)$$

Proof of Stability

$$\Theta_{adv} = \sum_{k=1}^N \left(-\frac{1}{2} \int_{\Gamma_k} u^D (\mathbf{f}^D \cdot \mathbf{n}) d\Gamma_k - \int_{\Gamma_k} u^D (\mathbf{f}^C \cdot \mathbf{n}) d\Gamma_k \right)$$

$$\begin{aligned} \Theta_{extra} = & \sum_{k=1}^N \left(J_{y_k}^{2p+1} \left[\frac{1}{2} \frac{\partial^p u_R^D}{\partial y^p} \frac{\partial^p F_R^D}{\partial y^p} - \frac{\partial^p u_R^D}{\partial y^p} \frac{\partial^p (\mathbf{f} \cdot \mathbf{n})_R^*}{\partial y^p} \right]_k \right. \\ & + J_{y_k}^{2p+1} \left[-\frac{1}{2} \frac{\partial^p u_L^D}{\partial y^p} \frac{\partial^p F_L^D}{\partial y^p} - \frac{\partial^p u_L^D}{\partial y^p} \frac{\partial^p (\mathbf{f} \cdot \mathbf{n})_L^*}{\partial y^p} \right] \\ & + J_{x_k}^{2p+1} \left[\frac{1}{2} \frac{\partial^p u_T^D}{\partial x^p} \frac{\partial^p G_T^D}{\partial x^p} - \frac{\partial^p u_T^D}{\partial x^p} \frac{\partial^p (\mathbf{f} \cdot \mathbf{n})_T^*}{\partial x^p} \right] \\ & \left. + J_{x_k}^{2p+1} \left[-\frac{1}{2} \frac{\partial^p u_B^D}{\partial x^p} \frac{\partial^p G_B^D}{\partial x^p} - \frac{\partial^p u_B^D}{\partial x^p} \frac{\partial^p (\mathbf{f} \cdot \mathbf{n})_B^*}{\partial x^p} \right] \right) \end{aligned}$$

Main Result

Theorem 1. *If the FR scheme for a 2D conservation law with periodic boundary conditions is used in conjunction with the Lax-Friedrichs formulation for the common interface flux with $0 \leq \lambda \leq 1$, then it can be shown that for a linear advective flux and any Cartesian mesh, the following holds:*

$$\frac{d}{dt} \|u^D\|^2 = \Theta_{adv} + c\Theta_{extra} \leq 0 \quad \text{if} \quad c \geq 0$$

Insights Gained

- ❖ The VCJH parameter shows up explicitly, unlike 1D
- ❖ As c increases, dissipation increases
- ❖ Negative values of c make the scheme less stable, but could provide lesser dissipation

Linear Advection-Diffusion

- Consider the 2D Advection-Diffusion Equation

$$\frac{\partial u}{\partial t} + \nabla \cdot \mathbf{f}(u, \nabla u) = 0 \quad \text{in } \Omega$$

- We solve this by splitting it into a system of first order PDEs:

$$\begin{aligned} \frac{\partial u}{\partial t} + \nabla \cdot \mathbf{f}(u, \mathbf{q}) &= 0 \\ \mathbf{q} - \nabla u &= 0 \end{aligned}$$

Main Result

- Six Lemmas later ...

$$\frac{d}{dt} \|u^D\|_{W_\delta^{2p,2}}^2 \leq 0 \quad \text{when } c \geq 0$$